Intermediate Statistics in Two-Dimensional Quantum Gases

Joar Bølstad

Thesis submitted for the degree of
Master in Physics
(Master of Science)

Department of Physics
University of Oslo

June 2009

Alt for å finne det sannes mysterium,
- det er den ekte forskers kriterium.
(Henrik Ibsen, 1828-1906)

Acknowledgments

The title of the song "You'll never walk alone", the anthem of the British football club Liverpool FC, is as true in scientific life as it is on the soccer pitch. I could never have written this thesis without the extensive help and encouragement, both scientifically and personally, from a number of people.

First of all, I would like to extend my deep gratitude for having the opportunity to work with my supervisors Susanne Viefers and Jon Magne Leinaas. They accepted to supervise me, and have introduced me to the wonderful physics of anyons. I have on numerous occasions stood in awe of their deep physical insight and their command of the numbers. They have patiently considered my questions and suggestions, giving invaluable guidance along the road. It has been a privilege to work with you both. Whatsmore, I would like to thank Johan Engquist for revealing to me his current research in the three-anyon problem.

I would also like to thank Hanne-Torill Mevik, whom I have learned to know during these last two years. Besides being a great friend, you have helped out with numerous LaTeX related questions. You have certainly made writing this thesis a lot more enjoyable than it would have been without you on the other side of the book shelf. In addition, I would like to thank Jan Øye Lindroos, Johannes Rekkedal, and Marit Sandstad for good company at the occasional lunch and other social activities.

Outside the theory group, Øystein Engedal has been my closest friend during these last years, and I am grateful for all the good times we have spent together. I'm looking forward to spending more time with you. Moreover, I thank Kjell Olav Hove for our continuing friendship. Although we have not had much time to see each other in the past years, the wind is about to turn. I am grateful of our friendship. Furthermore, I would like to thank the great guys and girls of Radio Nova. Meeting you all has considerable enriched my life. There are many more that should have been acknowledged here. However, naming a few is a slippery slope, and so I trust that you know who you are.

At last, I am in dept to my family. My parents, Are and Tua, my sisters Ingerid and Kjersti, step-parents Astrid and Jan, step-siblings Anders and Marte, grand-parents Arnljot and Johanna and Eva, and aunt Else-Marie. I thank you all for your continuing support and belief in me.

Finally, I would like to extend my deepest appreciation and thanks to my girlfriend and "partnerka" Pola Slabon. You have put up with my mood swings, the late nights, and given me a place to come home to. I could not have done this without you.

Oslo, June 1. 2009
Joar Bølstad

Contents

Chapter 1

Introduction

The concept of anyons is currently more than thirty years old, yet, its many-body nature is still elusive. Anyons, which roughly speaking are particles confined to two spatial dimensions, are particles obeying intermediate or fractional statistics (see chapter 2 for details). The two-anyon problem consists of determining the two-anyon energy spectrum through solving the appropriate Schrödinger equation. This is the only fully solved N-anyon case. The inherently harder three-anyon problem has effectively terminated any naive attempts of determining the many-anyon description. In order to appreciate the severity of this problem, we first have to understand anyons themselves. Chapter 2 is entirely devoted to the fundamental ideas that lead to anyons - from the identification of identical configurations to the path-integral formalism that eventually yield the anyon Lagrangian. The chapter is concluded with a qualitative treatment of the assumed anyonic manifestation in the fractional quantum Hall effect.

It is hard to prove that something is difficult. Such notions are best experienced first hand. This is why we will assert the complexity of the three-anyon problem[1]. Apparently, the many-body description is not soluble through a systematic treatment of increasing number of particles. A different approach is to examine the quantum statistical mechanics of anyonic systems. As a preparation to this, the two-dimensional ideal Bose-Einstein and Fermi-Dirac gases are studied in chapter 3. This is not only important as limiting cases of the anyon and similar intermediate statistical gases, it also illustrates methods of particular importance in a familiar setting. Specifically, some asymmetrical results concerning the thermodynamics of the before mentioned gases are examined. Finally, the combined expression of a Bose-Einstein and Fermi-Dirac gas is formulated, and its virial expansion is found.

The route to a full understanding of the N-anyon system through the

[1] A sort of proof is the lack of progress among some of the finest minds of the condensed-matter community.

means of a statistical approach is also affected by our inability to solve the N-anyon problem. This is the motivation for examining a different approach to particles exhibiting intermediate statistics. In contrast to anyons, the so-called fractional exclusion statistics are particles which are by construction susceptible to carry fractional statistics. This will be explored in chapter 4. Although we will not explore this connection, there is another, more subtle feature connecting the two systems in addition to their fractional nature. Anyons, as conjectured to be the elementary excitations in the fractional quantum Hall system, obey fractional exclusion statistics (see [39]). The chapter is rounded up with a derivation of the virial expansion fractional exclusion gas.

It is then, in chapter 5, time to close the circle and meet the anyons again. First of all, some preliminary results are established, before we tackle the fully soluble problem of finding the second virial coefficient of an ideal anyon gas. The problem of determining the third virial coefficient is elaborated to some extent. Finally, some results regarding the higher virial coefficients are examined.

Chapter 2

An Introduction to Anyons

2.1 Introduction

Leinaas and Myrheim [24] gave the first argument opening for fractional statistics of systems confined to two dimensions. However, this novel idea did not attract much attention before Wilczek introduced his flux-tube model. In addition, he coined the term anyons [36, 37]. We will not take the chronological route to anyons, rather we will find the mathematical apparatus needed using the path-integral formalism. In the end, we will explore an example of a possible anyonic manifestation. The current chapter focuses on content which is quite foreign to the standard text books of quantum mechanics. Yet, it could have been extended considerably by including more common topics. To keep things clean, however, we have omitted the most standard results. For two good reviews of anyon-related physics, see [18, 25].

2.2 The Emergence of Fractional Statistics

The possiblity of fractional particle statistics arose as a quantum mechanical consequence of a detailed analysis of the classical configuration space. In the mid '70s, about 50 years after the conception of quantum mechanics, the foundation of quantum mechanical system was properly established. All material particles where either classified as bosons, with integer spin, or fermions, with half-integer spin. From the beginning of quantum mechanics, it was clear that a collection of identical particles exhibit different behavior, depending on their particle classification. In terms of wave functions, it was found that a collection of identical fermions would, under a particle exchange, end up with a wave function which was anti symmetric. For a collection of identical bosons, it was found that their wave function turned up symmetric under such exchanges. This had great implications for the statistical mechanics of large systems of identical particles. In addition, the symmetry properties is a mathematical manifestation of Pauli's exclusion

principle. In other words, it is hard to think of a more profound property of nature.

Despite the physical importance of this phenomena, it seemed hard to prove that bosons have symmetric wave functions, while fermions have anti symmetric wave functions. It can be proved using quite technical arguments in quantum field theory - a proof which go by the name of the spin-statistics theorem. In ordinary quantum mechanics, however, this relationship was postulated by the so-called symmetrization postulate. In [24], Leinaas and Myrheim set out to explore the symmetrization postulate - a widely accepted "truth" they found questionable. They considered the requirement of symmetric or anti symmetric wave functions artificial. Although an empirical fact, a more satisfying approach would be to deduce it from first principles. A sketch of their reasoning is as follows.

- Instead of imposing requirements on the wave functions themselves, take the idea of absolute indistinguishability to its natural conclusion. This turns out to have a fundamental impact on the classical configuration space.

- When quantizing such systems it is deduced that, in three- and higher-dimensional systems, the symmetrization postulate is valid. However, in two and one dimension(s) there is a possibility of particles with fractional statistics, i.e. particles that do not behave as either bosons or fermions in a statistical context.

We will limit ourselves to a review of the analysis of the classical configuration space, as this is a logical stepping stone to our later derivation of the N-anyon Hamiltonian.

2.2.1 Particle Identity and Configuration Spaces

As an initiation to the formal discussion of the configuration space, we will have a closer look at the two- and three-dimensional (classical) configuration space. We will take the single-particle position space to be an Euclidean d-space. Consider a system of N identical particles. Let the configuration space for this system be M_N^d. One of the insights in [24] was that the concept of absolute indistinguishability imposes some serious constraints on the configuration space M_N^d. More precisely, the situation is this.

Assume a system of two identical particles. A certain configuration of this system is represented by a point in M_N^d. However, since the particles are indistinuishable, points in M_N^d which differ only by the ordering of the coordinates (and not the set of coordinates themselves) must constitute the same physical configuration. Thus, two such points must be identified as the same configuration, and hence *as the same point* in M_N^d. See figure 2.1 for an illustration.

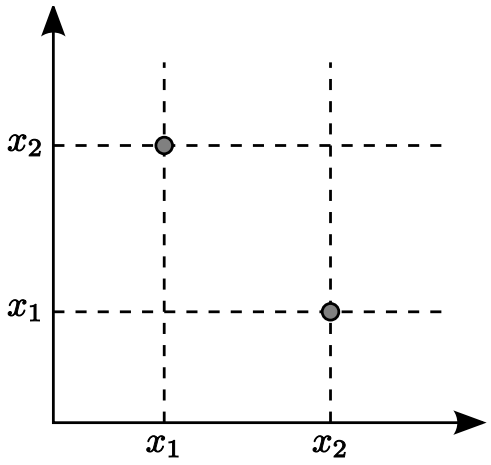

Figure 2.1: The configuration of a system is represented by a point in configuration space. Configurations whose coordinates (in configuration space) which differ only by a permutation, must be identified as the same configuration.

We may consider the configuration space to be a product of the center-of-mass space C_N^d and the relative space r_N^d. In other words, we may write

$$M_N^d \quad = \quad C_N^d \times r_N^d. \tag{2.1}$$

It is not the motion through configuration space that will concern us, rather it is the topological properties of this space that are important to us. C_N^d will, given the conditions above, be equivalent with Euclidean d-space. At the moment, we are examining the interchange of particles. In this respect, the COM space will bear no relevance to us. Let us therefore turn our attention to the relative space r_N^d, which has a slightly more elaborate structure. Note that it represents $d\,(N-1)$ degrees of freedom. This follows from the fact that our system has a total of dN degrees of freedom. The COM motion will account for d degrees of freedom, and so the relative motion will have to account for the remaning $d\,(N-1)$.

For simplicity, we will limit the discussion to a two-particle system, i.e. $N = 2$. In this case, we will see that the relative space may be expressed as a product space between the real line and the real projective space.[1] The real projective space $\mathbb{R}\mathrm{P}^d$ is the space of lines through the origin of $\mathbb{R}^{d+1}$. See figure 2.2 for an illustration. What this means is that every point in $\mathbb{R}\mathrm{P}^d$ corresponds to a single line through that point in $\mathbb{R}\mathrm{P}^d$ and the origin in $\mathbb{R}^{d+1}$. This line has no direction - in other words, the points in $\mathbb{R}\mathrm{P}^d$ describe all possible undirected lines in $\mathbb{R}^{d+1}$. As we will see, this is of fundamental interest to us. In particular, let's consider the two particle

[1] For $N > 2$, the situation is more complicated.

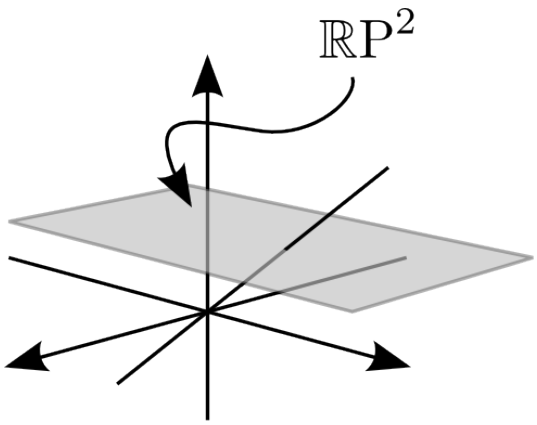

Figure 2.2: The real projective plane $\mathbb{R}\mathrm{P}^2$ is visualized as the plane traced out by all possible lines through the origin in $\mathbb{R}\mathrm{P}^3$. Figure adapted from [8].

system in d dimensions. The relative motion between the two particles may be described by two considerations, namely

- the inter-particle distance, and
- the direction of a line connecting the two particles, relative to some coordinate system.

We emphasize that it is not the equations of motions themselves that we will investigate, rather it is the space of their domains that interests us. The distance between the two particles may take on any positive, real value, and hence the space we are looking for capturing this is the real line $(0, \infty)$. The direction $\pm\mathbf{x}/|\mathbf{x}|$, on the other hand, is described by a point in $\mathbb{R}\mathrm{P}^{d-1}$. It is fairly easy to convince oneself that it must be so. Consider the space r_N^d for $d = 2$ and $N = 2$. All in all, we have four degrees of freedom. Two of these are accounted for by the COM. The two degrees of freedom left for us to investigate are the inter-particle distance and the angle between some coordinate axis and the line connecting the two particles. We find that the angle is given as a point in $\mathbb{R}\mathrm{P}^1$, also known as the real projective line. Similarly, for $d = 3$ and $N = 2$, the direction is described by two angles, and hence as a point in $\mathbb{R}\mathrm{P}^2$ - the real projective plane.

There is one point that must be excluded from the configuration space - the point where two (or more) particles occupy the same position. In terms of a relative space, this is equivalent to removing the origin $\{0\}$ from consideration. This was taken care of by only considering the real line $(0, \infty)$ when describing the distance between the two particles. Combined with the above remarks, this leaves us with the result

$$r_2^d - \{0\} \quad = \quad (0, \infty) \times \mathbb{R}\mathrm{P}^{d-1}. \tag{2.2}$$

In the current context, what matters to us is the physical interchange of two particles. In this respect, it is clear that the inter-particle distance is irrelevant. Thus, all the important information about the interchange of two particles in d-dimensions is encoded by the topological properties of $\mathbb{R}\mathrm{P}^{d-1}$. We will examine the two-particle system in two and three spatial dimensions. However, before we do this, we will need to address the concept of homotopy.

2.2.2 Homotopy and Homotopy Classes

A central concept in topology is that of homotopy and homotopy classes. What is a homotopy? Consider a space X. Loosely speaking, a homotopy is the relationship between two functions where one can be deformed continuously into the other. In terms of paths, we say that two paths in X are "equivalent" or homotopic, if one can be continuously transformed[2] into the other. A homotopy class is the collection of all paths homotopic to each other. Thus any path in a homotopy class may be obtained from any other of the paths in the same class by continuous deformation. If we pick a base point x_0 in X and restrict our attention to closed paths (i.e. loops), we find that the set of all such homotopy classes is encoded by the so-called fundamental group $\pi_1(X, x_0)$. In other words, the fundamental group π_1 is taken to be the set of all homotopy classes of loops on X [21]. It follows that one element in π_1 corresponds to one homotopy class. On the other hand, paths belonging to different elements in π_1 (i.e. to different homotopy classes) may not be continuously transformed into each other.

2.2.3 Topology of the Three Dimensional Configuration Space

To ease the analysis of (the interesting part of) our relative space, we will make the following observation. We know that $\mathbb{R}\mathrm{P}^2$ may be concieved as a plane. However, we can just as well construct $\mathbb{R}\mathrm{P}^2$ from the unit sphere in $\mathbb{R}^3$, i.e. S^2. A point on S^2 may be uniquely identified by a unit vector $|v| = 1$ from the origin to the point in question. The quotient space (also known as an identification space) $S^2/(v \sim -v)$ can informally be thought of as "dividing out" the equivalence relations of S^2; that is removing the redundancy in the space caused by the equivalence relation. An equivalence relation is a concept from set theory.[3] In topological terms, an equivalence relation enable us to glue together different parts of the topological space.

In our case this identification constitutes the removal of antipodal points; that is for example the removal of the southern hemisphere. We see that there

[2] Continuously transform (or deform) means no cutting or gluing, only stretching, twisting and bending.

[3] Informally, we may think of it as a relation between the elements of a set so that it uniquely assign these elements to subsets known as equivalence classes. These equivalence classes are either disjoint or equal, and the elements in a certain equivalence class are equivalent to each other.

is no direction anymore - only lines through the origin. This is exactly the space $\mathbb{R}\mathrm{P}^2$. At this point, we are free to remove the redundancy. Thus it follows that we may think of $\mathbb{R}\mathrm{P}^2$ as the (northern) hemisphere of S^2, with antipodal points on the equator identified. Technically, we say that $\mathbb{R}\mathrm{P}^2$ is homeomorphic to $S^2/(v \sim -v)$.

A closed curve, or loop, is a curve with both ends meeting at the same point. Since $\mathbb{R}\mathrm{P}^2$ is (a part of) the configuration space, tracing a curve in this space represents the physical act of changing the configuration of the system. Consequently, loops constitute physical interchanges of particles in the system - in this case the two particles making up the system switch places.

In figure 2.4 it can be clearly seen how there are two classes of loops in $\mathbb{R}\mathrm{P}^2$ - the ones that may be contracted to a point, represented by α and γ, and the ones who may not, represented by β. The reader might argue that the loop β is an open path and not a loop, but this is merely an artifact of the figure depicted. The antipodal points q are identified as one and the same point in configuration space. Any way we twist, stretch and turn the loop β, it can not be shrunk to on point (the endpoints stay fixed).

We have to take a closer look in order to see that γ is also a contractible loop. In the second figure we see the product of β and β, that is $\gamma = \beta \bullet \beta$. One way to look at this is simply traversing the path β twice, or we can think of the end point of the first β as connected to the starting point of the second β. After all, these two points are identified. Thus, we may think of this as any other point on the entire loop γ. The dotted curve in figure (2.4(c)) indicates this - however it must not be taken too literally (as it moves outside the space available). Consequently, we are permitted to move the end point of the first loop, if we at the same time move the starting point of the second loop, keeping these points antipodal to each other at all times. The end result are the two loops which may be contracted to a point and hence are homotopic to α. We see that there are only two homotopy classes for this space - represented by the trivial loop and the single exchange loop. Thus, the fundamental group consists of only two elements.

In terms of interchange of identical particles in $d = 3$, we identify the path α with no exchange, β with a single exchange, and γ with a double exchange. The double exchange is homotopic to no exchange (because both may be continuously deformed to a point), and so the allowed exchanges in this configuration space is no exchange (α and γ), or a single exchange (β). Now, the single exchange may impose a non-trivial phase on the wave function, but the double exchange may not as it is identical to no exchange. And this is, if not proof of, at least a strong argument for the symmetrization postulate in $d = 3$. Not much new has come out of this - the wave function is either symmetric or anti symmetric under exchange in $d = 3$. However, things are quite differently in $d = 2$.

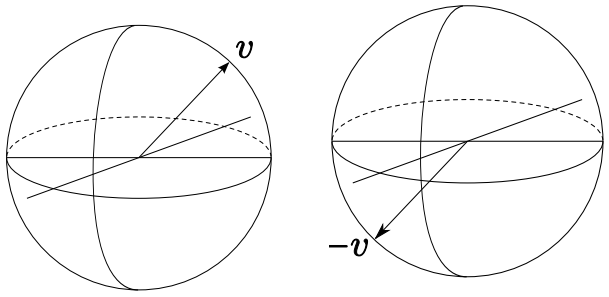

(a) The arbitrary positive vector v is uniquely mapped to every point on the northern hemisphere.

(b) The arbitrary negative vector $-v$ is uniquely mapped to every point on the southern hemisphere.

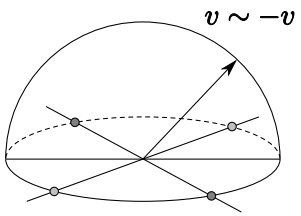

(c) Identical points are indicated by being antipodal on the equator of the hemisphere.

Figure 2.3: Construction of $\mathbb{R}\mathrm{P}^2$ may be achieved through different procedures. Figure 2.3(a) and 2.3(b) depicts the positive and negative vector v and $-v$ on S^2 respectively. As argued in the text, we may construct $\mathbb{R}\mathrm{P}^2$ from a sphere S^2 by the identification $v \sim -v$. This identification renders one half of the sphere redundant, and consequently it may be removed without any loss of information. Here, we have removed the southern hemisphere. Note that antipodal points on the equator is still identified, even though any point outside the equator is uniquely determined on the hemisphere.

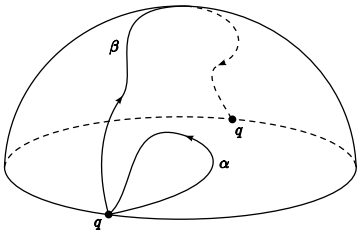

(a) The loop α is trivially shrunk to a point, while β is not.

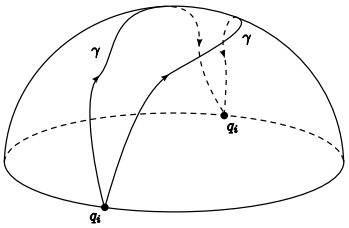

(b) The loop $\gamma = \beta \bullet \beta$ is the loop β traversed twice, which is physically equivalent to a double exchange.

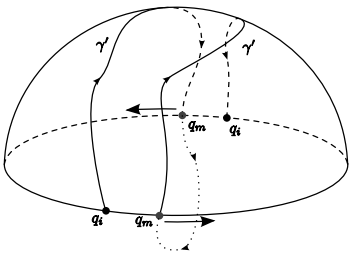

(c) We realize that the path $\gamma = \beta \bullet \beta$ may be looked upon as one single loop. First from q_i to q_m, then (since antipodal points are identified) from q_m to q_i.

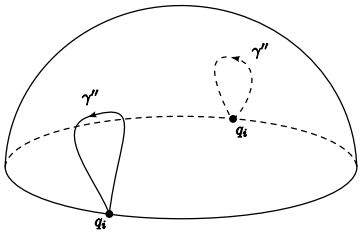

(d) The path γ shrunk to two points, which are identified. Thus, the physical effect is no exchange at all.

Figure 2.4: Possible loops in the real projective plane, and how they may, and may not be continuously deformed to a point.

2.2.4 Topology of the Two Dimensional Configuration Space

What is the topology of the configuration space for two identical particles confined to two dimensions? One subtlety we did not have to take into account in $\mathbb{R}\mathrm{P}^2$ was the removal of the origin. It was already removed by only considering the real line, and removing the origin from $\mathbb{R}\mathrm{P}^2$ would be an error - the origin is not part of $\mathbb{R}\mathrm{P}^2$. Of course, the point at zero inclination angle (the "north pole", that is, the point straight above the origin) must not be excluded. After all, we have to allow for the particles to be on a line with any angle relative to some fixed coordinate system.

In the case of two particles in two dimensions, we wish to broaden our view and consider the entire relative space, simply on aesthetical grounds, and in order to conform with the original literature.[4] There is no problem in considering

$$r_2^2 - \{0\} \quad = \quad (0,\infty) \times \mathbb{R}\mathrm{P}^1 \tag{2.3}$$

instead of merely $\mathbb{R}\mathrm{P}^1$, as long as we are mindful of the singular point at the origin. Once again we impose the equivalence relation $v \sim -v$ due to the identification of $\mathbf{x} = \mathbf{x}_1 - \mathbf{x}_2$ and $-\mathbf{x} = \mathbf{x}_2 - \mathbf{x}_1$. The (interesting part of the) configuration space becomes a punctured plane with antipodal points identified. This identification may be attained by cutting the plane by a straight line segment l from the origin to any point on the circle, and fold the plane into a circular cone with half angle 30°. What was $\mathbf{x}$ and $-\mathbf{x}$ effectively becomes the same point on the new cone.[5] See figure (2.5).

Examining the possible exchanges in this configuration space gives some surprising results. The loop of no exchange may be shrunk to a point - reflecting that no exchange can not give rise to any phase. The single exchange may not be shrunk to a point, and may give rise to a phase. The double exchange is the new and exciting operation. The loop representing a double exchange is embracing the singular point at the origin twice, and hence may not be shrunk to a point. Because the double exchange and the no exchange are not homotopic, the double exchange may give rise to a non-trivial phase in two dimensions - in contrast to three dimensions. This is the source of the possibility for fractional statistics.

Just as $\mathbb{R}\mathrm{P}^2$ is homeomorphic to $S^2/(v \sim -v)$, so is $\mathbb{R}\mathrm{P}^1$ to $S^1/(v \sim -v)$. A little consideration should convince us that there are an infinitude of dif-

[4] Recall, how it is only $\mathbb{R}\mathrm{P}^d$ that really matters when we are analyzing interchanges for two particles in $\mathbb{R}^{d+1}$.

[5] To see that this half angle becomes 30°, we cut the unit circle as suggested along the line l. The circumference of this circle is $O_{disk} = 2\pi r = 2\pi$ where we have chosen $r = 1$. This very same circumference has to circumvent the origin exactly twice in the cone, that is, the circumference of the cone is half of the circumference of the original circle. This circumference is thus $O_{cone} = \pi$, making the radius $r = 1/2$. The side of the cone is now of unit length, and according to the law of sines we get $\sin\alpha = 1/2$ that is $\alpha = \pi/6$ or $\alpha = 30°$.

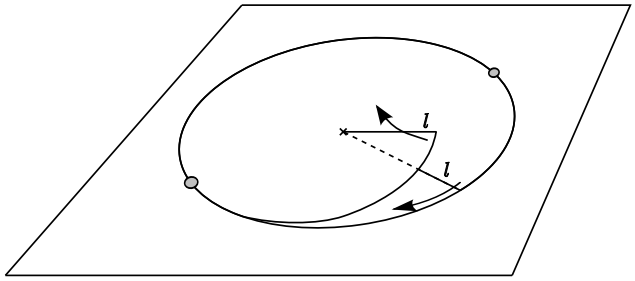

(a) The initial cut of the punctured disk, with antipodal points identified as indicated.

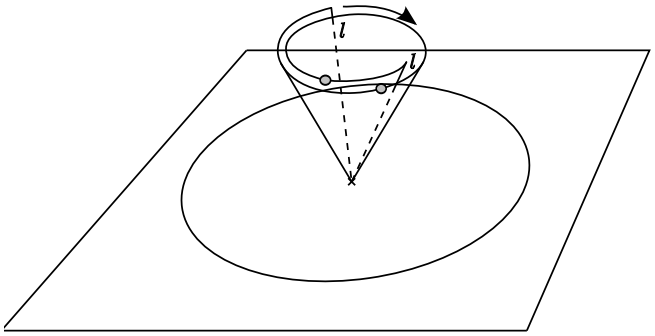

(b) The curling of the punctured and cut disk, in order to form the tip-less cone. Note how the identical points will match up once l and l lines up.

Figure 2.5: The cut and subsequent curling up of a disk to form a cone.

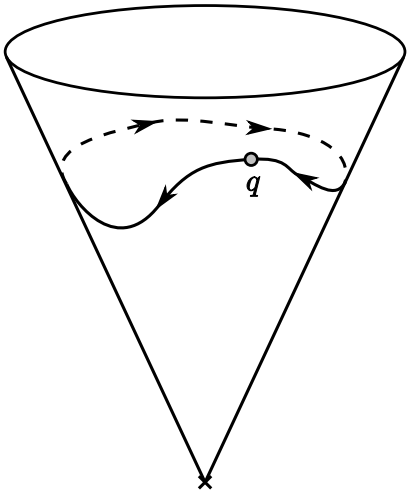

Figure 2.6: One possible loop representing a particle interchange in the relative configuration space of $d = 2$. Note the singular point at the tip of the cone. This ensures an infinitude of homotopy classes on this space, or in other words that this is an infinitely connected space. The consequences for the quantum mechanics of a system, whose classical relative space is a product of the real, positive line and this space, is that we must allow for the possibility of any statistics.

ferent loops in the case of $S^1/(v \sim -v)$; one for each number of times the loop winds about the origin. In effect, the winding number becomes unique and countable, and every such non-homotopic loop give rise to a non-trivial phase factor on the wave function.

Formally, this kind of space is called an infinitely connected space. Had we not excluded the singular point at the origin, any path on the cone would have been homotopic to a point, and correspondingly we would have only one homotopy class on this space. However, since the singular point *is* removed, we are faced with a fundamental group of infinitely many elements. An infinitely connected space is a space whose fundamental group has an infinite number of elements, i.e. homotopy classes. In relation to the wave function, this infinite connectivity will have the effect that a double exchange of two identical particles does not return the system to the original state.

2.2.5 The Classical Configuration Space of Identical Particles

In principle, the structure of M_N^d could be almost anything. We will now examine a certain subset of possible configuration spaces. As mentioned above, indistinguishability impies an identification of points in M_N^d which differ only by a permutation in coordinates. This identification may be achieved by a division of S_N - the permutation group. To keep things simple, we will assume that the single-particle position spaces are $\mathbb{R}^d$, the Euclidean d-space. Just as in the previous sections, we will deny particles to occupy the same physical position, which implies that we have to remove the diagonal points

$$D = \left\{ \mathbf{x}_1, \cdots, \mathbf{x}_N \in \mathbb{R}^{dN} \ : \ \mathbf{x}_i = \mathbf{x}_j \text{ for all } i \neq j \right\}. \tag{2.4}$$

It follows that the configuration space for the entire system is

$$M_N^d = \frac{\mathbb{R}^{dN} - D}{S_N}. \tag{2.5}$$

It can be shown that the fundamental group associated with this configuration space, is identical to either the braid group B_N or the permutation group S_N, depending on the dimensionality of the configuration space

$$\pi_1\left(M_N^d\right) = \begin{cases} S_N & d \geq 3 \\ B_N & d = 2 \end{cases}. \tag{2.6}$$

This is a very important statement. It is not only a verification of the essential result obtained in [24][6], but also provides us with a clear idea of the dynamics, as well as it is a mature mathematical theory in its own right.

[6] The result referred to being the connectedness of the space in question as a function of spatial dimensionality.

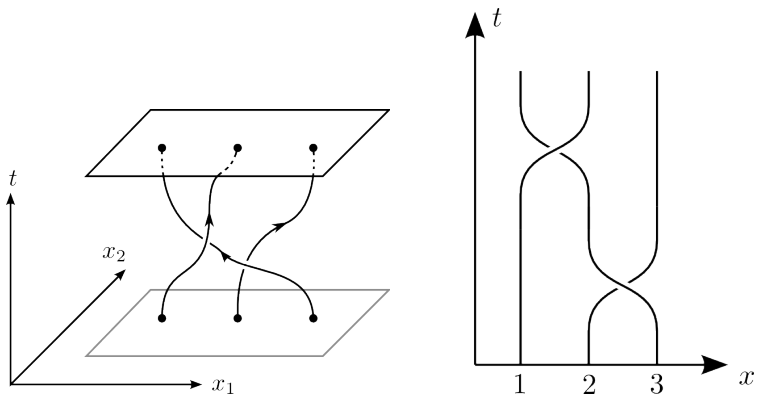

(a) World lines of a three particle system.

(b) The projection of the three particle system into a $1+1$ plane.

Figure 2.7: Examples of world lines for interchange of three particles confined to the plane. The world lines of the $2+1$ system to the left are projected down to the $1+1$ plane to the right. Illustrations are adapted from [7].

2.3 The Formalism of Anyons

In the following section we will develop a formal theory from which the quantum mechanics of anyons may be calculated. First, we will deal with the theory of braid groups. This will turn out to be of great importance in our derivation of the anyon quantum mechanics.

2.3.1 The Braid Group

An important tool in developing the anyon dynamics are the so-called braid groups. These arise naturally from considering interchanges of particles in the plane. Let the interchange of two particles, confined to the plane, trace out a world line in $2+1$ dimensional space as time passes by. An example is shown in figure (2.7(a)). We project these world lines onto a $1+1$ dimensional space, with the result shown in figure (2.7(b)). Although we lose some information by doing this, the projection captures the essential physics of the system. The projected graph is in turn readily analyzed using the braid group. The elements of the braid group are the braids, i.e. arrangements of interweaving strands. These arrangements of strands are constructed by the basic operations σ_i where $i = 1, 2, \ldots, N-1$, see figure 2.8. The operations σ_i are the group generators, and for an N-braid system there are $N-1$ generators. In relation to the projection of world lines we realize that N braids implies an N-particle system.

As indicated above, some information is lost in the process of projecting the world lines. An elementary braid generator does not encode any infor-

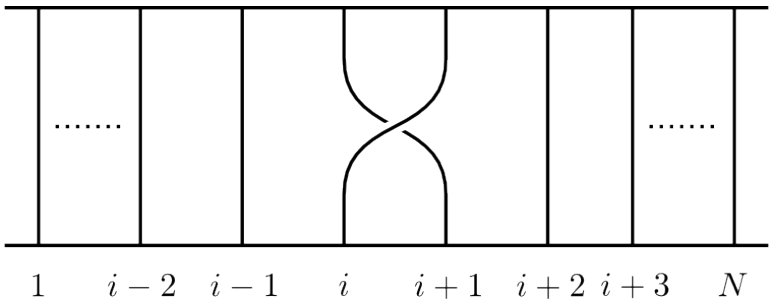

Figure 2.8: A single braid operation among a system of N strings. Clearly, the operation σ_i is only defined for $1 \leq i \leq N-1$.

mation of "how much" it should act, i.e. either you let it act on a strand or you don't. Thus, the generators can only describe an *interchange of particles*. Physically, a braid generator corresponds to a full interchange of two particles by rotating the two particles about their center of mass. The intital and final positions must be the same, since the braid operation does not carry any information regarding translations. It is when we combine these interchanges in succession, that we get the elements of a braid group.

So far, we have addressed the relation between particle interchange and the braid groups. But as the name imply, there is a mathematical group theoretical structure to these braids as well. Braid groups, as introduced by Artin [17], originally arose in in the study of intertwining strings in 1925.[7] Let's consider an arrangement of N strings. The basic operation is identified by the symbol

$$\sigma_i \tag{2.7}$$

which in words says that "take string number i and let it pass above string number $i+1$ while simultaneously letting string $i+1$ pass under string I so that these two strings exchange positions". This group operation is better understood graphically, as shown in figure 2.9. So much for the basic operations. The really interesting part is when we start combining these in sequence. First of all, we have the braid relations

$$\sigma_i \sigma_j \quad = \quad \sigma_j \sigma_i \tag{2.8}$$

for all $i, j = 1, 2, \ldots, N-1$ where $|i-j| \geq 2$ and

$$\sigma_i \sigma_{i+1} \sigma_i \quad = \quad \sigma_{i+1} \sigma_i \sigma_{i+1} \tag{2.9}$$

for $i = 1, 2, \ldots, N-2$. A note is in order; by convention, the series of operations are read from the right to the left. The first relation is clearly seen to be true by comparing figure 2.10(a) and figure 2.10(b).

[7] Hurwitz reportedly did some earlier work, however in a covert fashion.

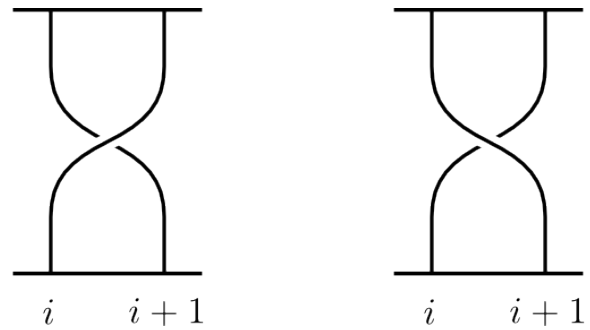

(a) The basic braid operation σ_i.

(b) The braid operation inverse σ_i^{-1}.

Figure 2.9: The basic generators of any braidgroup.

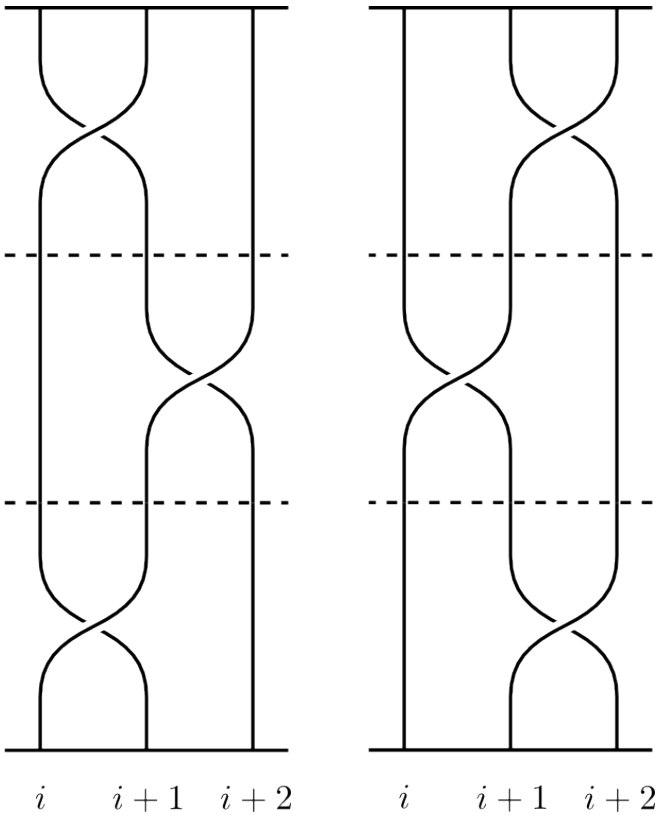

(a) The $\sigma_i\sigma_{i+1}\sigma_i$ series of operations.

(b) The $\sigma_{i+1}\sigma_i\sigma_{i+1}$ series of operations.

Figure 2.10: A graphical proof of the relation $\sigma_i\sigma_{i+1}\sigma_i = \sigma_{i+1}\sigma_i\sigma_{i+1}$. Note that, although not clear from this illustration, the series of operations are read from right to left.

The important thing to look for in these diagrams is if a string connecting two points passes over or under the neighboring strings. We see that in figure 2.10(a), the string starting out in position j ends up in position $j+2$, and by doing so, it passes over both the other strings in question. The string starting out in position $j+1$ ends up in $j+1$. To get there, it passes under the string starting out in j, and over the string starting out in $j+2$. It follows that the last string passes under the two others. The exact same picture emerges in figure 2.10(b). The order of how this happens is not the same. However, this is insignificant as it is the way we get from the initial to final ordering that matters. Hence, we conclude that

$$\sigma_i\sigma_{i+1}\sigma_i \quad = \quad \sigma_{i+1}\sigma_i\sigma_{i+1} \tag{2.10}$$

is correct. From an exchange perspective, the braid group reduces to the permutation group in three dimensions.

2.3.2 Path Integrals and the Representation of Braid Groups

Having motivated how the possibility of fractional statistics emerges in two spatial dimensions, the natural next question is "How can we describe such systems mathematically?". E.g. what is the Lagrangian of a N-anyon system? Perhaps the easiest way to aquire such a Lagrangian is by using the path-integral formalism of Feynman. Wu [38] was the first to derive this result which is reviewed in [7, 25]. The path integral of multiply connected spaces was studied in [21] which proves the symmetrization postulate.

In the path integral formalism, the probability amplitude for a system which start out in the configuration q_i at time t_i to end up in q_f at time t_f is given by

$$\begin{aligned} K\left(q_f,t_f;q_i,t_i\right) &= \langle q_f,t_f|q_i,t_i\rangle \\ &= \int_{q(t)} e^{(i/\hbar)S[q(t)]}\,\mathcal{D}q \\ &= \int_{q(t)} e^{(i/\hbar)\int_{t_i}^{t_f} L[q(t),\dot{q}(t)]\,dt}\,\mathcal{D}q \end{aligned} \tag{2.11}$$

The integral $\int_{q(t)}\mathcal{D}q$ is taken to be a sum over all paths $q\left(t\right)$ connecting the initial and final configuration q_i and q_f . As pointed out in section 2.2, the classical configuration space M_N^d of N identical particles in d dimensions must be a multiply connected space due to the identification of equivalent configurations. As the configuration space is multiply connected, closed paths in this space are naturally assigned to different homotopy classes, or in other words to different elements of the fundamental group π_1 (which was introduced in section 2.2.2). Furthermore, composition of paths is expressed as the multiplication of group elements [21]. Specifically, let a and b be two paths so that $a,b\in\pi_1\left(M_N^d\right)$. Then $ab\in\pi_1\left(M_N^d\right)$, that is, the product of

the two paths is also an element of the fundamental group. Topologically, we may think of this as the path formed by first taking the path a, then taking the path b.

One particular constructive approach is to let α designate a certain homotopy class, that is $\alpha \in \pi_1\left(M_N^d\right)$. By doing this, we may rewrite the path integral as

$$\begin{aligned} & K\left(q_f, t_f; q_i, t_i\right) && (2.12) \\ = & \sum_{\alpha \in \pi_1\left(M_N^d\right)} \chi(\alpha) K_\alpha\left(q_f, t_f; q_i, t_i\right) \\ = & \sum_{\alpha \in \pi_1\left(M_N^d\right)} \chi(\alpha) \int_{q_\alpha(t)} e^{(i/\hbar) \int_{t_i}^{t_f} L\left[q_\alpha(t), \dot{q}_\alpha(t)\right] dt} \mathcal{D} q_\alpha && (2.13) \end{aligned}$$

As such, we focus on *partial probability amplitudes* $K_\alpha\left(q_f, t_f; q_i, t_i\right)$, rather than all the individual paths. Here, we have introduced the weight $\chi(\alpha)$ associated with different homotopy classes. This is allowed as long as the general rules of probabilities are respected.

We wish to take a closer look at the weights $\chi(\alpha)$. Because $K\left(q_f, t_f; q_i, t_i\right)$ is a probability amplitude, $\chi(\alpha)$ must follow the relationship

$$\chi(\alpha\beta) \quad = \quad \chi(\alpha)\chi(\beta). \tag{2.14}$$

This can be seen if we consider $K\left(q_f, t_f; q_i, t_i\right)$ to be a composition of $K\left(q_m, t_m; q_i, t_i\right)$ and $K\left(q_f, t_f; q_m, t_m\right)$ where q_m is an intermediate configuration at time t_m. Explicitly, we have

$$\begin{aligned} K\left(q_f, t_f; q_i, t_i\right) &= \left\langle q_f, t_f | q_i, t_i \right\rangle \\ &= \int \left\langle q_f, t_f | q_m, t_m \right\rangle \left\langle q_m, t_m | q_i, t_i \right\rangle \, dq_m \\ &= \int K\left(q_f, t_f; q_m, t_m\right) K\left(q_m, t_m; q_i, t_i\right) \, dq_m \end{aligned} \tag{2.15}$$

since we can always insert the identity $\sum_i |q_i\rangle \langle q_i| = 1$ (or in the continuous case $\int |q_i\rangle \langle q_i| \, dq_i$). We have assumed that the set $\{|q_i\rangle\}$ form a complete set of states. By inserting for $K\left(q_f, t_f; q_i, t_i\right) = \sum_{\alpha \in \pi_1\left(M_N^d\right)} \chi(\alpha) K_\alpha\left(q_f, t_f; q_i, t_i\right)$, we get that

$$\sum_{\alpha\beta \in \pi_1\left(M_N^d\right)} \chi(\alpha\beta) K_{\alpha\beta}\left(q_f, t_f; q_i, t_i\right) \tag{2.16}$$

$$\begin{aligned} = & \int \sum_{\alpha \in \pi_1\left(M_N^d\right)} \chi(\alpha) K_\alpha\left(q_f, t_f; q_i, t_i\right) \\ & \times \sum_{\beta \in \pi_1\left(M_N^d\right)} \chi(\beta) K_\beta\left(q_f, t_f; q_i, t_i\right) \, dq \end{aligned} \tag{2.17}$$

It is clear that this must be true for any combination of paths, i.e. compositions $\alpha\beta \in \pi_1\left(M_N^d\right)$. In other words, we can limit ourselves to the case

$$\chi(\alpha\beta)\, K_{\alpha\beta}(q_f, t_f; q_i, t_i) \tag{2.18}$$

$$= \chi(\alpha)\,\chi(\beta) \int K_\alpha(q_f, t_f; q_i, t_i)\, K_\beta(q_f, t_f; q_i, t_i)\, dq \tag{2.19}$$

where we could pull $\chi(\alpha)\,\chi(\beta)$ outside the integral, as this is independent of q. In other words, we have established the proposed relationship (2.14). Furthermore, it can be shown [21] that

$$|\chi(\alpha)| = 1. \tag{2.20}$$

At this point, it is necessary to go through a lightning fast review of the concept of group representations.

Group Representation

Following [16], we define a group representation as follows. "A representation of dimension n of the abstract group G is defined as a homomorphism $D : G \to \mathrm{GL}(n, \mathbb{C})$, the group of non-singular $n \times n$ matrices with complex entries. In other words it is a mapping under which $g \mapsto D(g)$, preserving the group structure:

$$D(g_1 g_2) = D(g_1)\, D(g_2) \tag{2.21}$$

The mapping is necessarily into the set of non-singular matrices, since each matrix must be invertible: $D\left(g^{-1}\right) = (D(g))^{-1}$." A homomorphism is a mapping that preserves the structure between the mapped objects. In plain English, a group representation is a concrete expression of the group structure exhibited by a certain mapping. So, in a sense, working with abstract groups in contrast to working with a group representation is akin to working with coordinate-free vectors in contrast to working with vectors in a specific coordinate system [31].

In the case of $\chi(\alpha)$, we have that

$$\chi(\alpha\beta) = \chi(\alpha)\,\chi(\beta) \tag{2.22}$$

The paths α and β are elements in $\pi_1\left(M_N^d\right)$. We see that eq. (2.22) is the very definition of a group representation. In other words, we realize that $\chi(\alpha)$ is a scalar representation of the fundamental group $\pi_1\left(M_N^d\right)$. To conclude the discussion of a representation, we need to show the form of $\chi(\alpha)$.

Any acceptable representation must necessarily respect the group structure. We have seen that the braid group B_N is generated by the operators

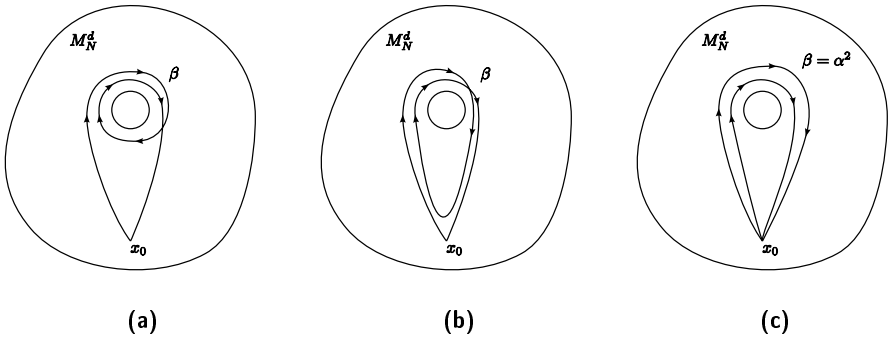

Figure 2.11: A double encirclement of a singularity and its decomposition to the product of two single encirclements. The situation is topologically identical to closed loops on the tip-less cone, which is another example of an infinitely connected space.

$\sigma_1, \sigma_2, \ldots, \sigma_n$. In section 2.3.1 we proved the realtions eq. (2.8) and eq. (2.9) which where found to be

$$\sigma_i \sigma_j \quad = \quad \sigma_j \sigma_i \qquad \text{for } |i-j| \geq 2 \tag{2.23}$$

and

$$\sigma_i \sigma_{i+1} \sigma_i \quad = \quad \sigma_{i+1} \sigma_i \sigma_{i+1}. \tag{2.24}$$

It can be shown that these are the only operations relating different σ_k (see [38] for reference). Moreover, we know that in $d = 2$, the fundamental group $\pi_1\left(M_N^d\right)$ reduces to the braid group B_N. Since a homotopy class $\alpha \in \pi_1\left(M_N^d\right)$, we realize that in $d = 2$, these classes correspond to different braids. We need to break down these elements to their most basic constituents. See figure 2.11 for an example of such a decomposition. Just as loops with an arbitrary winding number can be decomposed to a sequence of single winding number loops, so can the arbitrary braid be decomposed to a sequence of single braid operations σ_i.

As we have seen, the weight $\chi(\alpha)$ associated with a certain homotopy class α is a scalar representation of the fundamental group $\pi_1\left(M_N^d\right)$. Since $\pi_1\left(M_N^d\right)$ reduces to B_N in $d = 2$, the elements $\alpha \in \pi_1\left(M_N^d\right)$ corresponds to elements $a \in B_N$, and so it is clear that χ must also serve as a representation of the braid group. Since homotopy classes α in a sense can be reduced to braids, and using the fact that

$$\chi(\alpha\beta) \quad = \quad \chi(\alpha)\,\chi(\beta) \tag{2.25}$$

we immediatly find

$$\chi(\sigma_i \sigma_j) \quad = \quad \chi(\sigma_i)\,\chi(\sigma_j)\,. \tag{2.26}$$

The last important property we will deduce from the relations among the generators σ is the following. From

$$\sigma_i\sigma_{i+1}\sigma_i = \sigma_{i+1}\sigma_i\sigma_{i+1} \tag{2.27}$$

it follows that

$$\chi(\sigma_i)\chi(\sigma_{i+1})\chi(\sigma_i) = \chi(\sigma_{i+1})\chi(\sigma_i)\chi(\sigma_{i+1}). \tag{2.28}$$

However, the $\chi(\sigma_k)$'s are *scalar* representations, and so we may simply divide by $\chi(\sigma_i)\chi(\sigma_{i+1})$ on both sides. Thus

$$\chi(\sigma_i) = \chi(\sigma_{i+1}). \tag{2.29}$$

It immediatly follows that

$$\chi(\sigma_i) = \chi(\sigma_j) \tag{2.30}$$

which concludes our analysis of the general properties of the representation $\chi()$.

From

$$|\chi(\alpha)| = 1 \tag{2.31}$$

and

$$\chi(\alpha\beta) = \chi(\alpha)\chi(\beta) \tag{2.32}$$

we see that χ may be realized by a phase factor

$$\chi(\alpha) = e^{i\theta}. \tag{2.33}$$

As a matter of convention, we identify the representation of the braid group generator a phase

$$\chi(\sigma_i) = e^{-i\theta} \tag{2.34}$$

and the generator inverse

$$\chi\left(\sigma_i^{-1}\right) = e^{i\theta}. \tag{2.35}$$

The parameter θ will be identified with the statistics of the particle species in question.

The goal of this section is to derive the N-anyon Lagrangian. In hindsight, it is found that this may easily be done once we are able to relate the phase factor $\chi\left(\sigma_i^{\pm 1}\right)$ to the action of the path-integral. In particular, we will identify the change in relative angles $\Delta\varphi_{ij}$ between particle i and j as a statistical interaction term in the Lagrangian. Keeping this in mind, the

following line of reasoning will (hopefully) be appreciated once the desired results are obtained.

For a general braid, which is constructed by a finite number of compositions of the generators σ, the associated phase will be

$$\begin{aligned}\chi\left(\sigma_{i_1}\sigma_{i_2}\cdots\sigma_{i_k}\right) &= \chi\left(\sigma_{i_1}\right)\chi\left(\sigma_{i_2}\right)\cdots\chi\left(\sigma_{i_k}\right) \\ &= \exp\left(-i\theta\sum_{i=1}^{k}\epsilon_i\right)\end{aligned} \tag{2.36}$$

where $\sigma_{i_k}$is an arbitrary generator σ_j or its inverse σ_j^{-1}. Here, we have introduced the signature ϵ_k of the kth element, which is defined as

$$\epsilon_k = \begin{cases} -1 & \text{if } k\text{th element is } \sigma_k^{-1} \\ +1 & \text{if } k\text{th element is } \sigma_k \end{cases}. \tag{2.37}$$

The real parameter θ encodes the particle statistics, which interpolates between $\theta = 0$ identified as Bose-Einstein and $\theta = 1$ identified as Fermi-Dirac statistics. In the following, the statistical parameter will usually be written as $\alpha \equiv \theta/\pi$, with $\alpha = 0$ and $\alpha = 1$ as the bosonic and fermionic particle species.

As a matter of convention, interchange of particles is carried out exclusively on two particles at a time. We will now briefly address the effect on the relative angles among the particles by such an interchange. When two particles i and j are interchanged, their relative angle changes by $\Delta\varphi_{ij} = \pm\pi$. Clearly, all the relative angles between one of these particles and any other particle in the system will change as well. E.g. say we have an $N = 4$ particle system. By a counterclockwise (relative to some fixed coordinate system) interchange of particles $i = 1$ and $j = 2$ will have the effect that $\Delta\varphi_{ij} = \pi$. Now, φ_{13}, φ_{14}, φ_{23}, and φ_{24} will change as well. The only relative angle that remains fixed is φ_{34}. However, we see that, although the relative angles involving either i or j (or both) will change, *the sum* of relative angles will remain invariant, *except for* an addition from φ_{ij}, which changes by $\Delta\varphi_{ij} = \pm\pi$. For an illustration, see figure 2.12 and the accompanying table 2.1.

As labeling is arbitrary, the net effect is thus equivalent to the change in the relative angle between i and j exclusively.

Due to the braid group picture of interchange, we must have that i and j are related as $j = i + 1$. By introducing

$$\epsilon_i = \Delta\varphi_{ij}/\pi \tag{2.38}$$

as a way to express the signature, we realize that the phase may be written

$$\chi\left(\sigma_k\right) = \exp\left(-i\frac{\theta}{\pi}\sum_{i<j}\Delta\varphi_{ij}\right). \tag{2.39}$$

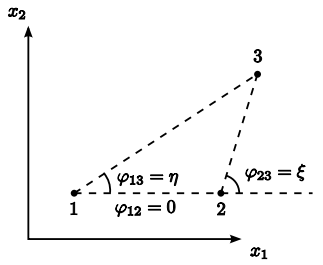

(a) The configuration at $t = t_0$.

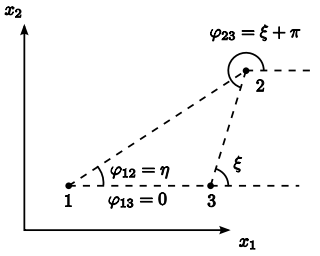

(b) The configuration at $t = t_1$.

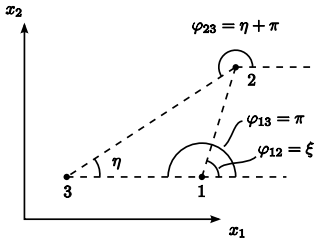

(c) The configuration at $t = t_2$.

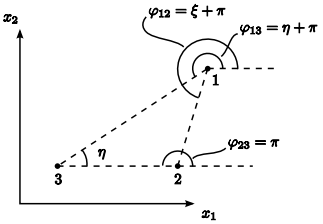

(d) The configuration at $t = t_3$.

Figure 2.12: Four consequtive configurations of a three-particle system.

Time	$\varphi_{12}(t)$	$\varphi_{13}(t)$	$\varphi_{23}(t)$
t_0	0	η	ξ
t_1	η	0	$\xi+\pi$
t_2	ξ	π	$\eta+\pi$
t_3	$\xi+\pi$	$\eta+\pi$	π

Table 2.1: The set of relative angles at different times for the system depicted in 2.12. Note how the sum of relative angles is constant, with the exception of the additional $\pm\pi$ due to particle interchange.

This sum over all pairs is permissible since $\Delta\varphi_{ij}$ is vanishing for all terms except one, whose value is $\pm\pi$. This result may be generalized to

$$\chi(\alpha) = \exp\left(-i\frac{\theta}{\pi}\sum_{i<j}\int_{t_i}^{t_f}\frac{d}{dt}\varphi_{ij}(t)\,dt\right) \tag{2.40}$$

where $\alpha \in \pi_1\left(M_N^d\right)$. This is the most general expression for the path integral weights. Note that the functions $\varphi_{ij}(t)$ are in general highly complicated and one needs to take into the account the full dynamics of the system to determine it.

In order to complete the analysis of our path integral, we substitute this weight into (2.13). This gives

$$K(q_f,t_f;q_i,t_i) \tag{2.41}$$

$$= \sum_{\alpha\in\pi_1\left(M_N^d\right)}\int_{q_\alpha(t)} e^{(i/\hbar)\int_{t_i}^{t_f}\left(L[q_\alpha(t),\dot{q}_\alpha(t)]-\hbar\frac{\theta}{\pi}\sum_{i<j}\frac{d}{dt}\varphi_{ij}(t)\right)dt}\,\mathcal{D}q_\alpha \tag{2.42}$$

from which we extract the Lagrangian

$$L' = L - \hbar\frac{\theta}{\pi}\sum_{i<j}\frac{d}{dt}\varphi_{ij}(t)\,. \tag{2.43}$$

As such, we may consider L' to be bosons with a peculiar interaction term $\hbar\frac{\theta}{\pi}\sum_{i<j}\frac{d}{dt}\varphi_{ij}(t)$, or as non-interacting (free) anyons.

2.4 Anyonic Manifestations

In any conversation between a physicists and a layperson on the nature of anyons, the question is bound to come up: "Where can I find these anyons, anyway?". In this section, we will give a rough guide to the quantum Hall effect, and explore how anyons are believed to be elementary excitations in certain quantum Hall systems. There will be no room for detailed calculations, only a qualitative picture will be presented. There is an abundance of literature for the interested reader [29, 34, 33]. The current treatment has been inspired by [6, 13, 29].

2.4.1 The Quantum Hall Effect

There were two great experimental discoveries in the 1980's; the discovery of the W and Z bosons at CERN in 1983, and the integer and fractional quantum Hall effect (IQHE/FQHE) in 1980 (von Klitzing [19]) and 1982 (Tsui, Störmer, Gossard [35]) respectively. Yet, there was one big difference between them. Whereas the arrival of the W and Z bosons had been expected for a long time, the QHE appeared more or less out of the blue.[8] Which is a fascinating order of events, considering the amount of theoretical work that had been carried out in the field of quantum mechanics. Although the IQHE could be explained using a simple non-interacting picture, it soon became clear that in order to explain the FQHE, a more advanced model was needed.

Recall how the classical Hall effect is understood. Let a longitudinal current pass through a conducting slab. Expose the slab to a magnetic field perpendicular to the plane (and hence the current). This will deflect the moving charge carriers so that they accumulate along one side of the conductor, effectively giving rise to potential difference V_H between the opposite sides of the conductor. Correspondingly, the Hall resistance R_H can be shown to be

$$R_H^{\text{classical}} = \frac{B}{Ne} \tag{2.44}$$

which makes it a great device to measure either the magnetic field strength B or the number of charge carriers per unit area N. As usual, e is identified with the electron charge.[9] Prior to the discovery, the common view was that this linear behavior should be correct for all B and at all temperatures.

In 1980, von Klitzing conducted his studies of the Hall resistance for a two dimensional, high mobility electron gas. At extremely low temperatures $T <$

[8] The effect was not entirely unexpected, as discussed in [29]. In particular there was some work done in [2]. However, it seems that von Klitzing et. al. where unfamiliar with this result, as it is not quoted in the seminal paper [19] (which contains a reference to another paper by one of the authors (Ando)).

[9] Although the Hall coefficient is measured in ohms, it is not equivalent to the resistance of the material.

4 K and strong magnetic fields $B \sim 30$ T, something wonderful happened. The Hall resistance exhibited plateaus as a function of the magnetic field strength - in other words, the Hall effect was quantized, hence the name QHE.

When Tsui and Störmer two years later discovered the FQHE, it was found that both results could be described by the relation

$$R_H^{\mathrm{QHE}} = \left(h/e^2\right) / \left(p/q\right) \tag{2.45}$$

where h is the Planck constant, while p and q are integers. When the fraction p/q itself is an integer, this result coincides with the corresponding expression found by von Klitzing. One of the most marvelous aspects of the QHE is its precision. Von Klitzing found the plateaus to deviate by less than 10^{-7}. As a matter of fact, the inherent precision of the effect opened up new territory to the field of metrology. The calibration of the SI resistance is now based on the QHE. In addition, the fine structure constant may be measured quite accurately, as R_H is proportional to h/e^2.

2.4.2 The Integer Quantum Hall Effect

To understand the IQHE, one has to consider the electron orbits due to the presence of a magnetic field. In classical theory, the charged electrons move in circular paths perpendicular to the magnetic field, paths with arbitrary radius known as cyclotron orbits. In a quantum mechanical setting, these orbits have a quantized radius, i.e. only certain radii are possible. The energy levels associated with these quantized radii are known as Landau levels. As the magnetic field strength B increases, the spacing between consecutive levels will increase with the magnetic field. The low temperature assures us that the electrons won't be excited to a higher level by thermal excitation - in other words, the energy levels are assumed to be filled from the ground up. The number of electrons per Landau level, i.e. the degeneracy, is found to be

$$D = \frac{eB}{h}. \tag{2.46}$$

Combined with

$$R_H = \frac{B}{Ne} \tag{2.47}$$

wee see that the Hall resistance may be written as

$$\begin{aligned} R_H &= \frac{B}{Ne} \\ &= \frac{1}{\nu}\frac{h}{e^2} \end{aligned} \tag{2.48}$$

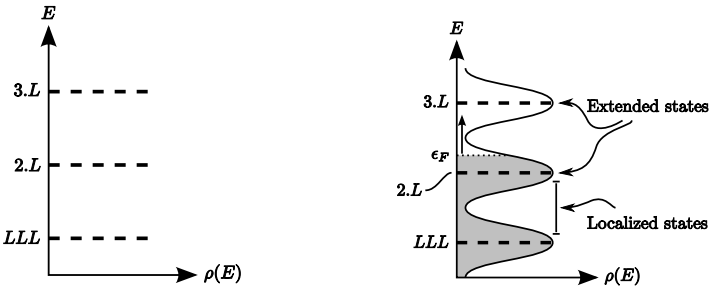

(a) The three first Landau levels, corresponding to an ideal (pure) system with no Coulomb repulsion (electron-electron interaction).

(b) The broadening of Landau levels due to sample impurities, with no Coulomb repulsion assumed. States are filled up from the ground state and the Fermi energy lies at some point between the first and second Landau levels.

Figure 2.13: The integer quantum Hall effect can be explained by a system of electrons subject to a magnetic field, with no inter-particle Coulomb repulsion and certain sample impurity effects.

where we have defined the filling factor $\nu = N/D$. This corresponds to the fraction q/p in (2.45). The filling factor tells us how many Landau levels that are filled up. We see that when the B field is very strong, the degeneracy D will outnumber the number of charge carriers N.

The quantum Hall effect (both fractional and integer) will emerge only under certain conditions. First of all, the sample in question has to be very pure as the effect is a high mobility phenomena. On the other hand, if there are no impurities in the sample, the effect will be absent. The reason is that impurities will broaden the Landau levels. It is this broadening of levels that account for the plateaus, which is the hallmark of the IQHE. (For the details relevant to FQHE, see the subsequent section).

We intuitively understand that there is something wrong with the delta function energy levels as depicted in figure 2.13(a). Such a picture can not possibly represent the true nature of a system as complex as this. Yet, the picture is not entirely removed from reality. Impurities in the sample happen to broaden the possible energies, while the Landau levels are still quite prominent. As the system fills up, the states associated with these intermediate energy levels become trapped by the impurities, or in other words they are localized in space (i.e. the term localized states). As these states represent electrons that are not free to roam throughout the sample, they do not contribute to the charge transport.

On the other hand, states with energy in the vicinity of the Landau levels

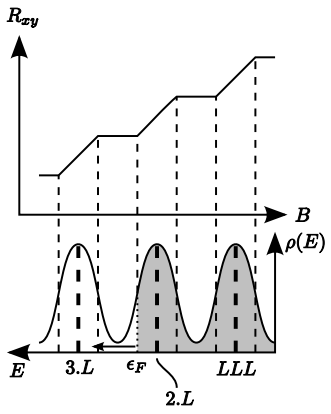

Figure 2.14: For the IQHE, the plateaus correspond to Fermi levels at which the Fermi energy ϵ_F lies between the extended states, that is, lies in the mobility gap. At these energies, the impurities of the sample will trap excess electrons and impair charge transport. This figure, which is only a qualitative picture, must not be taken too literally. Amongst other things, it is not to scale.

happen to be non-localized, or extended states. Consequently, these states contribute to the current through the sample. Experimentally, the filling of states is accomplished by turning the B-dial of our apparatus. As the Landau level degeneracy, as given by eq. (2.46) is directly proportional to the magnetic field strength B, a decrease in field strength will decrease the degeneracy. This in turn, will contribute to plateau formation. To see this, assume we start out in $\nu = 1$. Had the sample been completely pure, the electrons would have been forced up into the first Landau level when the degeneracy decreased. However, since there are unoccupied localized states due to the impurities, it will be energetically favorable for the electrons to fill these states first. The energy interval corresponding to localized states is known as a mobility gap.

To a good approximation, we can understand IQHE in terms of a system of non-interacting electrons subject to a magnetic field and material impurities. However, in FQHE, the filling factor is no longer integral - it is a fraction (thus the name). So how do the arguments above explain the plateau at say $\nu = 1/3$? It doesn't. Because there is no filling of the second Landau level, we need to look elsewhere to account for similar mobility gaps to understand the FQHE.

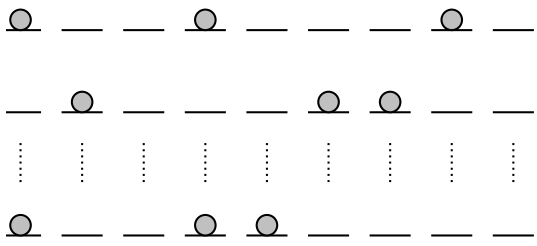

Figure 2.15: The degeneracy of the LLL in a naive model is extremely large. Here depicted by three of the $(9!/3!) = 60480$ equivalent ways of distributing three particles over nine possible states, all with the same energy. The filling factor of the system depicted is $\nu = 1/3$.

2.4.3 The Fractional Quantum Hall Effect

In the $\nu = 1/m$ state, where m is odd[10], positive integer, we will have a situation where all the electrons reside in the lowest Landau level (LLL). Although there are other, more exotic states (e.g. $\nu = 5/2$), we will limit ourselves to the odd denominator states. Let's start out by considering the LLL with degeneracy D for a system of N identical, non-interacting electrons and filling factor $\nu = 1/3$. For realistic N and D, there are stupendously many ways D to order the N particles over the LLL, all of them with equal energy.

At this point, we turn on the Coulomb interaction. What happens is that there will be mutual repulsion between the constituent particles. The interaction will cause the degeneracy of the LLL to break down, and there will be a definite ground state with a minimal energy. More precisely if z_j is the position of the jth particle, the Hamiltonian will be

$$H = \sum_j \left(\frac{1}{2m_e} \left(\frac{\hbar}{i} \nabla_j + \frac{e}{c} \mathbf{A}_j \right)^2 + V(z_j) \right) + \frac{1}{2} \sum_{j<k}^{N} \frac{e^2}{|z_j - z_k|}. \quad (2.49)$$

This beastly looking Hamiltonian has so far, and probably never will be, analytically solved. Thus the problem of finding the true ground state seems impossible. However, Laughlin [23] found the compact expression

$$\psi_m(z_1, \cdots, z_N) = \prod_{j<k}^{N} (z_j - z_k)^m \exp\left(-\frac{1}{4} \sum_{l}^{N} |z_l|^2 \right) \quad (2.50)$$

by minimizing the energy of a more general wave function. This wave function, known as the Laughlin ground state, has an amazing overlap with

[10] When the electron gas becomes sufficiently dilute, it will form a so-called Wigner crystal. This implies that for $\nu = 1/m$ where m is of a certain magnitude, the gas forms a Wigner crystal.

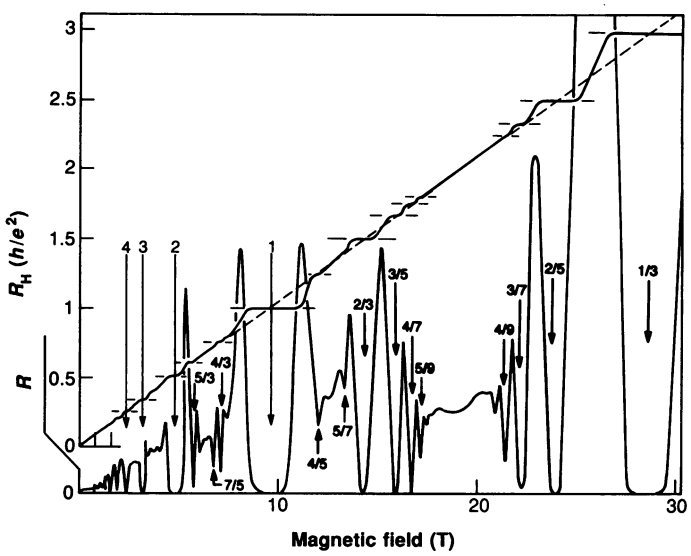

Figure 2.16: One of the most famous plots in contemporary condensed matter physics, this beautiful plot reveals the occurrence of the FQHE. The $\nu = 1/3$ is shown in the upper right, being the effects most prominent exponent. From [6].

the numerical calculation of the true ground state. As Laughlin points out himself: "The near perfect overlap, particularly at large values of m, is non-trivial, and gives one confidence that the physics is right", [29]. And indeed we see that the the wave function must be anti symmetric (due to $(z_j - z_k)^m$ where m is odd). It follows that this ground state is a guarantor that the Pauli principle will be respected. It also captures the repulsive nature in the $(z_j - z_k)$ term (there is a vanishing probability that particles will be in the proximity of each other, and zero probability for being in the same place).

Furthermore, it can be shown (assuming there is no degeneracy) that the elementary excitations of this system are quasi-particles or quasi-holes carrying a fraction $q = e/m$ of the elementary charge e. According to [29], the first argument was given by [22] and later improved by [10]. Reportedly, the fact that these fractionally charged excitations must obey fractional statistics and are understood to be anyons, was first made clear by [11, 12]. These excitations are not what we usually think of as elementary particles (like electrons or quarks), rather they are collective phenomena with the apparent behavior of particles. However, the modern view is that electrons and quarks are no more elementary than the constituents of a condensed matter system. The so-called effective field theories are approximate theories which limit themselves to the relevant degrees of freedom at the energy scale in question. We would never dream of describing a system like e.g. DNA from electrons and quarks - we use the four nucleotides to do this (the nucleotides are

rather complex molecules). The same goes for this condensed matter system, where quasi-particle and quasi-holes are are the elementary constituents at the relevant energies.[11]

Yet, we still have not seen any mobility gap. It turns out that these quasi-particles or quasi-holes will, just like the electrons in the IQHE, will be trapped by the sample impurities. This happens on the expense of further filling of the LLL. However, at some point, the impurities will be saturated and consequently the plateau will break down. This account for the mobility gap in the FQHE $\nu = 1/m$ state.

So do anyons really exist? From an experimental point of view, there are some serious obstacles to surmount, in order to prove the existence of anyons. First of all, there is no such thing as a "phase-o-meter", which could be used to probe what phase is acquired by particle interchanges. Recall, that the wave function is not real, in the sense that we can make a direct measurement of it. Not to mention the problem of penetrating a condensed matter region without destroying the phenomena in question. It should come as no surprise that any experiment aiming at proving the existence of anyons, must necessarily be highly technical. Such an experiment was conducted in 2005 by Goldman et. al. We will not try to explain the experiment itself, simply refer the reader to the original paper [4]. Yet, the chain of reasoning from measurement to prediction is so complex, that there is still no consensus whether the experiments really prove the existence of anyons or not. Although anyons remains to be inconclusively observed in experiment, there is little controversy in the community that anyons exist as elementary excitations in the FQHE system, see e.g. [18].

[11] For an argument supporting this modern view, see the highly readable [1].

Chapter 3

Ideal Quantum Gases

3.1 Introduction

Generalization is one of the finest tools at any physicists disposal. Sometimes a goal in itself, a generalized result can carry new and deeper understanding of seemingly unrelated phenomena. The combination of the Bose-Einstein and Fermi-Dirac distributions into a single mathematical expression is the content we will address here. In particular, we look into the two-dimensional case. Another incentive for the current discussion is the introduction of important techniques frequently encountered in (quantum) statistical mechanics. Familiarity with the counting of states will be important in subsequent sections. Some of the material in the current section is standard. In these cases, the method, rather than the result will be emphasized.

There are primarily two different ways to derive the distribution functions. The first one, which involves counting of microstates and an ensuing process of maximizing entropy, is said to be based on the microcanonical ensemble. The second method involves forming the grand canonical partition functions. When differentiated with respect to the proper thermodynamical variable, these partition functions yields the desired distribution.

3.2 BE/FD Distributions in Microcanonical Ensemble

In the microcanonical ensemble, both the total energy E and the total number of particles N are conserved, i.e. they are not allowed to be exchanged with the heat bath. As we assume that it is possible to count the number of particles n_i in different states i, we may express the total energy and number of particles as

$$E = \sum_{i=1}^{\infty} \epsilon_i n_i \tag{3.1}$$

and

$$N = \sum_{i=1}^{\infty} n_i. \tag{3.2}$$

The number n_i is known as the occupation number of the ith state.

By letting the system grow big, the energy spectrum assumes an almost continuous character. When we are faced with such a near-continuous spectrum, it becomes rather awkward to work with exact energy levels[1]. So instead of looking a single energy levels, we choose to group levels of similar energy into cells, see figure (3.1(a)). Let the ith cell contain $g_i \gg 1$ consecutive energy levels of the full spectrum. The number of particles in the ith cell is then given by n_i. We take ϵ_i to be identified as the average energy in the ith cell. Using this notation, the relations (3.1) and (3.2) still holds. With these concepts established, we are ready to tackle the problem of finding the distribution functions.

3.2.1 Counting States

When we subdivide the energy spectrum into cells as we have here, we quickly realize that the number of microstates has a similar subdivided structure. Let $W\{n_i\}$ be the number ways we we may arrange a certain distribution set $\{n_i\}$. A distribution set constitutes a microstate of the system. The microstate of an energy cell is independent of the other energy cells. An interchange of particles between different cells does not alter the system state. In other words, we may think of each cell as an individual system. It follows that the total number of distributions for the entire set of occupation numbers $\{n_i\}$ is a product over all energy cells, that is

$$W\{n_i\} = \prod_i w(i). \tag{3.3}$$

We point out that the set $\{n_i\}$ is *unique* - however, there are in general many distribution sets which satisfy the constraints. This is eventually due to the absolute indistinguishability of identical quantum particles. All we can say is how many particles which occupy a certain state. They describe the same macrostate, however they have a different distribution set $\{n_i\}$ and (in general) a different statistical weight $W\{n_i\}$. The total number of microstates accesible to a system is

$$\Omega(N,V,E) = {\sum_{\{n_i\}}}' W\{n_i\} \tag{3.4}$$

where the notation $\sum'_{\{n_i\}}$ indicates that we are to sum over every possible distribution set $\{n_i\}$ that conforms to the constraints (3.1) and (3.2).

[1] Not to mention the experimental side of things. When measured, how do we know what energy the system is in? If the resolution of the measuring device is so coarse that two neighboring levels can not be told apart, we have an obvious source of ambiguity.

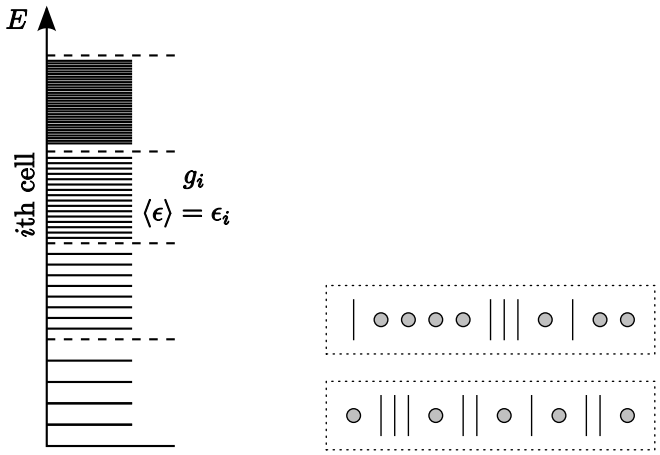

(a) Energy spectrum subdivided into cells of multiplicity g_i for the ith cell. The difference $\Delta\epsilon$ in two neighboring energy levels ϵ within a cell is of the same order. The mean energy of the ith cell is ϵ_i.

(b) Dots representing particles, vertical lines represents partitions. The upper figure represents a bosonic system, while the lower figure represents a fermionic system. Note how there are no "boundary" partitions or lines.

Figure 3.1: Division of energy spectrum into cells and pictorial representation of possible ways to distribute particles within a cell.

3.2.2 The Bose-Einstein Statistical Weight

Let us consider the ith energy cell in more detail. In how many ways can we distribute n_i identical bosons over g_i energy levels? To count this, we need to recall that there is no theoretical limit to the number of identical bosons in the same energy level. In order to work out the number of possible arrangements, it is common to employ a pictorial representation of the situation. Let a dot represent a particle and the space between partitions represent an energy level. An example is shown in figure (3.1(b)) .

There are n_i particles and there are $g_i - 1$ partitions dividing the energy cell into g_i energy levels. In how many ways may we reshuffle this setup?

The total number of *symbols* are $n_i + g_i - 1$. The number of ways to arrange all these symbols are $(n_i + g_i - 1)!$. We are interested in the number of distinct arrangements (not in the way they come about). However, this is an ordered arrangement. To compensate for this, we divide by the possible ways to order the symbols. There are $n_i!$ different ways to order the dots and $(g_i - 1)!$ ways to order the lines, all in all $n_i!\,(g_i - 1)!$ ways to order the entire

set of graphical symbols. Thus, the number of unordered arrangements are[2]

$$w_{\mathrm{BE}}(i) = \frac{[n_i + g_i - 1]!}{(n_i)!\,[g_i - 1]!} \tag{3.5}$$

Since $W\{n_i\}$ is simply the product over all cells, we find in the boson case, the number of distinct microstates given a certain distribution set $\{n_i\}$ is

$$W_{\mathrm{BE}}\{n_i\} = \prod_{i=1}^{\infty} \frac{[g_i + n_i - 1]!}{(n_i)!\,[g_i - 1]!} \tag{3.6}$$

3.2.3 The Fermi-Dirac Statistical Weight

For fermions we are faced with a simpler situation. We are still focusing on a single energy cell. The cell has n_i particles which are to be distributed over g_i energy levels. From the exclusion principle it follows that the number of particles in any one of the g_i levels are either 0 or 1. There are $(g_i)!$ ways to order the levels, regardless of whether they are occupied or not. However, we only care about the unordered selection, and so we correct for this by dividing the ordered set with the ways to order it. This means that in total there are

$$w_{\mathrm{FD}}(i) = \frac{(g_i)!}{(n_i)!\,[g_i - n_i]!} \tag{3.7}$$

ways to distribute the n_i particles over g_i energy levels[3] in a fermionic system. This gives us the result that, for fermions, the statistical weight for the distribution set $\{n_i\}$ is given by

$$W_{\mathrm{FD}}\{n_i\} = \prod_{i=1}^{\infty} \frac{(g_i)!}{(n_i)!\,[g_i - n_i]!} \tag{3.8}$$

3.2.4 The BE and FD Distributions

The most probable distribution of occupation numbers, $\{n_i^*\}$, is the particular set of occupation numbers that maximizes the function $W_{\mathrm{BE}}\{n_i\}$ (or $W_{\mathrm{FD}}\{n_i\}$). Whenever we are faced with the problem of finding the extrema of a certain function subject to a number of constraints, we may invoke the method of Lagrange's undetermined multipliers. To find the relevant distribution functions, we seek to find the equilibrium state by maximizing the entropy $S = k_B \ln W\{n_i\}$.[4]

[2] Note that the notation $\left(\begin{array}{c} n_i + g_i - 1 \\ n_i \end{array} \right) = \frac{(n_i+g_i-1)!}{n_i!(g_i-1)!}$ is frequently used.

[3] A widely used notation is $\left(\begin{array}{c} g_i \\ n_i \end{array} \right) = \frac{g_i!}{n_i!(g_i-n_i)!}$.

[4] Technically, the entropy is $S = k_B \ln \Omega$, however the most probable distribution set will dominate this sum to such an extent that it is permissible to *only* consider $S \approx k_B \ln W\{n_i^*\}$.

Assume we have a function F of several variables $F = F(x_1, x_2, x_3, \ldots)$. This function is to be maximized (or minimized). Given a set of constraints $f_1(x_1, x_2, x_3, \ldots) = 0$, $f_2(x_1, x_2, x_3, \ldots) = 0$, etc., we conveniently rewrite the problem as

$$G(x_1, x_2, x_3, \ldots, \lambda_1, \lambda_2, \lambda_3, \ldots) = F + \lambda_1 f_1 + \lambda_2 f_2 + \cdots . \quad (3.9)$$

This new function G has an extrema when

$$\frac{\partial G}{\partial x_i} = 0 \quad \text{and} \quad \frac{\partial G}{\partial \lambda_i} = 0$$

We wish to apply this method to our particular case. First of all, we need to form the constraints on the problem. The first constraint is that of total number of particles are

$$N - \sum_{i=1}^{\infty} n_i = 0. \quad (3.10)$$

The second constraint is the total energy, which is found to be

$$E - \sum_{i=1}^{\infty} \epsilon_i n_i = 0. \quad (3.11)$$

In relation to the general notation above we let $F = k_B \ln W\{n_i\}$, $f_1 = N - \sum_{i=1}^{\infty} n_i = 0$ and $\lambda_1 = \alpha$ and $f_2 = E - \sum_{i=1}^{\infty} \epsilon_i n_i = 0$ with $\lambda_2 = \beta$. In other words, the factors α and β are the undetermined Lagrange multipliers.

We start out with the case of identical bosons. By Stirling's approximation, we find that

$$\begin{aligned} \ln W_{\mathrm{BE}}\{n_i\} \approx & \sum_{i=1}^{\infty} ([g_i + n_i - 1] \ln [g_i + n_i - 1] \\ & - n_i \ln n_i - [g_i - 1] \ln [g_i - 1]) \end{aligned} \quad (3.12)$$

Inserting this into G gives

$$\begin{aligned} G = & \sum_{i=1}^{\infty} ([g_i + n_i - 1] \ln [g_i + n_i - 1] - n_i \ln n_i - [g_i - 1] \ln [g_i - 1] \\ & - \alpha n_i - \beta \epsilon_i n_i) + \alpha N + \beta E \end{aligned} \quad (3.13)$$

When we form a set of derivatives, we get that

$$\frac{\partial G}{\partial n_i} = 0 \quad \text{and} \quad \frac{\partial G}{\partial \alpha} = \frac{\partial G}{\partial \beta} = 0 \quad (3.14)$$

Inserting for G gives

$$\frac{\partial G}{\partial n_i} = \sum_{i=1}^{\infty} (\ln [g_i + n_i - 1] + 1 - \ln n_i - 1 - \alpha - \beta \epsilon_i) \quad (3.15)$$

However, this is true for every i, and since these are by assumption independent of each other, we have the result

$$\frac{\partial G}{\partial n_i} = \ln\left[g_i + n_i - 1\right] - \ln n_i - \alpha - \beta\epsilon_i = 0 \tag{3.16}$$

Observe that since $g_i \gg 1$ and $n_i \gg 1$, these terms will dominate the logarithmic term, and we are allowed to drop the term of order unity. Solving for n_i, we find that

$$n_i = \frac{g_i}{e^{\alpha+\beta\epsilon_i} - 1} \tag{3.17}$$

On the other hand, the Fermi-Dirac distribution is found by maximizing the entropy as given by the statistical weight $W_{\mathrm{FD}}\{n_i\}$. We have

$$\ln W_{\mathrm{FD}}\{n_i\} \approx \sum_{i=1}^{\infty}\left(g_i \ln g_i - n_i \ln n_i - \left[g_i - n_i\right]\ln\left[g_i - n_i\right]\right) \tag{3.18}$$

and consequently we find that

$$\begin{aligned} G = & \sum_{i=1}^{\infty}\left(g_i \ln g_i - n_i \ln n_i - \left[g_i - n_i\right]\ln\left[g_i - n_i\right] - \alpha n_i - \beta\epsilon_i n_i\right) \\ & + \alpha N + \beta E \end{aligned} \tag{3.19}$$

The derivative is

$$\frac{\partial G}{\partial n_i} = -\ln n_i - 1 + \ln\left[g_i - n_i\right] + 1 - \alpha - \beta\epsilon_i = 0 \tag{3.20}$$

Solving for n_i this gives

$$n_i = \frac{g_i}{e^{\alpha+\beta\epsilon_i} + 1} \tag{3.21}$$

The Lagrange multipliers α and β may be determined by appealing to thermodynamical results. Such a procedure gives $\alpha = \frac{\mu}{k_B T}$ and $\beta = \frac{1}{k_B T}$.

3.2.4.1 The Grand Canonical Approach

It is worth pointing out that the same distributions can be derived using the grand canonical ensemble. In A.1 we show that the grand canonical partition function takes the form

$$\Xi = \begin{cases} \prod_i \frac{1}{1 - z e^{-\beta\epsilon_i}} & \text{for bosons} \\ \prod_i \left(1 + z e^{-\beta\epsilon_i}\right) & \text{for fermions} \end{cases} \tag{3.22}$$

See the appendix for details, and in particular the relation to the distribution functions.

3.3 Asymmetries in Two-Dimensional Quantum Gases

As a prelude to the virial expansion of an ideal quantum gas, we intend to investigate certain properties of the two-dimensional quantum gas. There are some striking mathematical similarities in the grand canonical partition functions between bosons and fermions. Using a power series expansion of these function, we will explore a unified formalism and take a closer look at certain thermodynamical results. It is a matter of necessity to first work out the density of states for an ideal quantum gas. In the spirit of generalization, we will carry this out in an arbitrary D-dimensional setting. At the end of the calculation, we will investigate how different choices for the spatial dimension D give rise to differencies among the density of states. Then, in sections (3.3.2), (3.3.3), and (3.3.3), the advertised exploration will be carried out.

3.3.1 D-Dimensional Density of States

In a D dimensional space, the possible energies of a free particle are

$$E = \frac{\hbar^2}{2m}\left[\sum_{i=1}^{D} k_i^2\right] \tag{3.23}$$

$$= \frac{\hbar^2\pi^2}{2m}\left[\sum_{i=1}^{D}\left(\frac{n_i}{l_i}\right)^2\right] \tag{3.24}$$

where l_i is the spatial length of the system in the ith direction and n_i is $n_i = 1, 2, 3, \ldots$. Here, we have used that

$$k_i = \frac{\pi}{l_i} n_i \tag{3.25}$$

which is due to the boundary conditions of the system. Since k_i are integral multiples of π/l_i, each state occupies a volume

$$V_k = \left(\frac{\pi}{l_i}\right)^D \tag{3.26}$$

in k-space, where $V = l_i^D$ is the physical volume of the system[5]. Moreover, we have

$$k = \sqrt{\sum_{i=1}^{D} k_i^2} \tag{3.27}$$

[5]The fact that we are simultaneously working in different spaces is an obvious source of confusion. Whenever there is room for any doubt, we will use a subscript k to denote if a volume or surface is in k-space or not.

so the energy is entirely a function of the magnitude $k = |\mathbf{k}|$ where $\mathbf{k} = (k_1, k_2, \cdots, k_D)$. The surface area of a D-dimensional hypersurface of radius R is given by

$$S_D(R) = \frac{2\pi^{D/2}}{\Gamma(D/2)} R^{D-1} \tag{3.28}$$

Using this, we find that the volume of a shell of thickness dk at the radius R is

$$dV_k = \frac{1}{2^D} \frac{2\pi^{D/2}}{\Gamma(D/2)} R^{D-1}\, dk \tag{3.29}$$

The pre-factor $1/2^D$ is included to compensate for the fact that we only wish to study the first "hyper-octant". The number of states that fit into this volume is simply

$$\frac{dV_k}{V_k} = \frac{1}{2^{D-1}\Gamma(D/2)} \frac{V}{\pi^{D/2}} k^{D-1}\, dk \tag{3.30}$$

since there is one state per volume V_k. We have used that the radius of such a hyper-surface is $R = k = |\mathbf{k}|$. In terms of energy, we use (3.23) and (3.27) to find

$$k = \sqrt{\frac{2mE}{\hbar^2}} \tag{3.31}$$

It follows that

$$\frac{dk}{dE} = \sqrt{\frac{2m}{\hbar^2}} \frac{1}{2} E^{-1/2} \tag{3.32}$$

or

$$dk = \sqrt{\frac{m}{2\hbar^2 E}}\, dE \tag{3.33}$$

By insertion, we find that

$$\frac{1}{2^{D-1}\Gamma(D/2)} \frac{V}{\pi^{D/2}} k^{D-1}\, dk \tag{3.34}$$

$$= \frac{V}{2^D \Gamma(D/2)} \left(\frac{2m}{\pi\hbar^2}\right)^{\frac{D}{2}} E^{\frac{D}{2}-1}\, dE \tag{3.35}$$

$$= g(E)\, dE \tag{3.36}$$

For $D = 2$ we see that

$$g(E) = \frac{2\pi m}{h^2} V \tag{3.37}$$

and $D = 3$ we have

$$g(E) = \frac{1}{8}\frac{1}{\Gamma(3/2)}\frac{V}{\pi^{3/2}}\left(\frac{2m}{\hbar^2}\right)^{3/2} E^{1/2} \tag{3.38}$$

$$= \frac{4\pi m}{h^3} V (2mE)^{1/2} \tag{3.39}$$

In addition, we need to tack on a factor g_s to account for internal degrees of freedom, e.g. spin.

Dimensional Induced Discrepancies

This is an opportune moment to discuss the dimensional implications of the density of states. We see that in the two-dimensional case (3.37), there is no dependence on energy at all in the expression for $g(E)$. The density of states is a constant, only dictated by the volume of the system, the mass of the constituent particles and fundamental constants of nature. In the three-dimensional counterpart (3.39), there is indeed an energy dependence. In fact, for all cases $D \neq 2$, the density of states is a function of energy. Although the following derivations are tractable for $D \neq 2$, they are particularly easy to carry out in the two-dimensional case.

3.3.2 The Fugacity Expansion

As noted earlier, the grand canonical partition function is derived in section (A.1). Despite it's elegant form, it is even more convenient and suggestive to consider the logarithm of these functions. Combined into a single expression, this becomes

$$\ln \Xi = a \sum_i \ln\left(1 + aze^{-\beta\epsilon_i}\right) \tag{3.40}$$

where $a = -1$ for bosons and $a = +1$ for fermions.

As long as $|x| \leq 1$, any logarithm $\ln(1+x)$ can be expanded into the power series as

$$\ln(1+x) = \sum_{n=1}^{\infty} \frac{(-1)^{n-1}}{n} x^n. \tag{3.41}$$

If we require $ze^{-\beta\epsilon} \leq 1$, we get the expression

$$\ln \Xi = a \sum_i \ln\left(1 + aze^{-\beta\epsilon_i}\right) \tag{3.42}$$

$$= \sum_{n=1}^{\infty} \frac{(-a)^{n-1}}{n} z^n Z_1(\beta n) \tag{3.43}$$

where $Z_1(\beta) = \sum_i e^{-\beta\epsilon_i}$ is the classical single-particle partition function.

The partition function $Z_1(\nu)$ (where we simply substitute $\nu = n\beta$) may be approximated by the integral

$$Z_1(\nu) = \int_0^\infty g(\epsilon)\, e^{-\nu\epsilon}\, d\epsilon. \tag{3.44}$$

The two-dimensional density of states was found in section (3.3.1) to be $g(\epsilon) = g_s \frac{2\pi m A}{h^2}$. As pointed out, it is independent of the energy, and may thus be pulled out of the integral over ϵ. We get

$$Z_1(\nu) = g_s \frac{2\pi A}{h^2} \int_0^\infty p e^{-\nu \frac{p^2}{2m}}\, dp \tag{3.45}$$

where we have used $m\, d\epsilon = p\, dp$. Being a Gaussian integral, which in general is solved by

$$\int_0^\infty e^{-\xi x^2} x^j\, dx = \frac{1}{2}\xi^{-\frac{k+1}{2}} \Gamma\left(\frac{j+1}{2}\right) \tag{3.46}$$

with $j > -1$ and $\xi > 0$, we see that

$$Z_1(\nu) = g_s \frac{2\pi m A}{h^2 \nu}. \tag{3.47}$$

Inserting this back into (3.43), we see that

$$\ln \Xi = \sum_{n=1}^\infty \frac{(-a)^{n-1}}{n} z^n Z_1(n\beta) \tag{3.48}$$

$$= -g_s \frac{A}{a h^2} \left(\frac{2\pi m}{\beta}\right) \mathrm{Li}(2, -az) \tag{3.49}$$

where we in the first step multiplied by a $-a/-a$ factor. $\mathrm{Li}(b, x)$ is the poly logarithmic function defined as

$$\mathrm{Li}(b, x) \equiv \sum_{n=1}^\infty \frac{x^n}{n^b} \tag{3.50}$$

with $x = -az$ and $b = 2$.

3.3.3 Thermodynamic Boson/Fermion Asymmetry

Finally, we wish to bridge statistical mechanics and thermodynamics.Starting with the pressure, we readily find

$$P = \frac{1}{A\beta} \ln \Xi \tag{3.51}$$

$$= -\frac{g_s}{a 2\pi m h^2} \left(\frac{2\pi m}{\beta}\right)^2 \mathrm{Li}(2, -az). \tag{3.52}$$

Now, once the connection is established, we may express other thermodynamic quantities through this result. In particular, we find the number density of particles and entropy as

$$\begin{aligned} n &= \left.\frac{\partial P}{\partial \mu}\right|_T && (3.53)\\ &= \left.\frac{\partial z}{\partial \mu}\right|_T \left.\frac{\partial P}{\partial z}\right|_T && (3.54)\\ &= -\frac{g_s}{ah^2}\left(\frac{2\pi m}{\beta}\right)\mathrm{Li}\,(1,-az)\,. && (3.55)\end{aligned}$$

To get to the last line, we used

$$\begin{aligned} z\frac{\partial}{\partial z}\mathrm{Li}\,(2,-az) &= z\frac{\partial}{\partial z}\left(\sum_{n=1}^{\infty}\frac{(-a)^n z^n}{n^2}\right) && (3.56)\\ &= \sum_{n=1}^{\infty} n\frac{(-a)^n z^n}{n^2} && (3.57)\\ &= \mathrm{Li}\,(1,-az) && (3.58)\end{aligned}$$

The entropy density is found as

$$\begin{aligned} s &= \left.\frac{\partial P}{\partial T}\right|_\mu && (3.59)\\ &= \left.\frac{\partial P}{\partial T}\right|_z + \left.\frac{\partial z}{\partial T}\right|_\mu \left.\frac{\partial P}{\partial z}\right|_\mu && (3.60)\\ &= \left.\frac{\partial P}{\partial T}\right|_z - \frac{\mu z}{k_B T^2}\left.\frac{\partial P}{\partial z}\right|_\mu && (3.61)\\ &= 2\frac{P}{T} - \frac{\mu n}{T}. && (3.62)\end{aligned}$$

In the last line we have used that

$$\begin{aligned} \frac{\partial P}{\partial T} &= -2k_B^2 T\frac{g_s}{a2\pi m h^2}(2\pi m)^2\,\mathrm{Li}\,(2,-az) && (3.63)\\ &= 2\frac{P}{T} && (3.64)\end{aligned}$$

and

$$\begin{aligned} \frac{\mu z}{k_B T^2}\frac{\partial P}{\partial z} &= \frac{\mu}{T}\beta z\frac{\partial P}{\partial z} && (3.65)\\ &= \frac{\mu n}{T} && (3.66)\end{aligned}$$

Finally, the energy density is found from $P = -\epsilon + \mu n + Ts$ to be

$$\begin{aligned} \epsilon &= -P + \mu n + Ts && (3.67)\\ &= P && (3.68)\end{aligned}$$

which follows from inserting for s.

Asymmetric Behavior

As a summary, we explicitly state the following results

$$P = -\frac{g_s}{a2\pi mh^2}\left(\frac{2\pi m}{\beta}\right)^2 \mathrm{Li}\,(2,-az) \tag{3.69}$$

$$n = -\frac{g_s}{ah^2}\left(\frac{2\pi m}{\beta}\right)\mathrm{Li}\,(1,-az) \tag{3.70}$$

$$s = 2\frac{P}{T} - \frac{\mu n}{T} \tag{3.71}$$

$$\epsilon = P \tag{3.72}$$

The expressions derived are general in the sense that both fermion and boson cases may be found by inserting the correct value for a (where $a = -1$ for bosons and $a = +1$ for fermions). We see that the bosonic case is asymmetric with respect to the thermodynamic results with the fermionic case. By this we mean that the bosonic system may be considered as a fermionic system with negative pressure, number density, entropy density, and energy. We must draw the conclusion that *the asymmetries*, which was first observed by Myrheim [27] in three dimensions, *equally well holds in two dimensions.*

3.4 Virial Expansion of a Generalized BE/FD Gas

The standard approach when investigating the thermodynamic properties of and ideal Bose or Fermi gas is to employ the so-called virial expansion. The virial expansion is a power series expansion of the equation of state. Recall how the ideal gas law is given as

$$\frac{PV}{Nk_BT} = 1 \tag{3.73}$$

Though the ideal gas law is a good approximation to real, classical gases at low densities, it is not perfect. For real gases, the ratio $PV/\left(k_BTN\right)$ is not exactly unity - it has a (dimensionless) temperature- and density-dependent behaviour. The deviation from unity may be encoded by the virial expansion

$$\frac{PV}{Nk_BT} = \sum_{i=0}^{\infty}\left(\rho\lambda^2\right)^{i-1}a_i \tag{3.74}$$

where a_i is known as the ith virial coefficient. If $a_1 = 1$ and $a_i = 0$ for $i > 1$ we have reproduced the ideal gas law. The goal of this section is to develop a unified expression that captures both the bosonic and fermionic particle statistics.

The derivation is not complicated in its individual steps. However, there are quite a number of them. If some seem unmotivated, we appeal to the consideration of the three results

$$\frac{PA}{k_BT} = \ln \Xi(z, A, T) \tag{3.75}$$

$$N = z\frac{\partial \ln \Xi(z, A, t)}{\partial z} \tag{3.76}$$

$$\frac{PA}{Nk_BT} = \sum_{i=0}^{\infty} \left(\rho\lambda^2\right)^{i-1} a_i. \tag{3.77}$$

It should be clear that if we are in a position to evaluate the two first expressions, the third will follow. The derivation is essentially the same in two- as in three-dimensional setups.

3.4.0.1 The Equation of State

The grand canonical partition function is related to the pressure P and the volume (or in two dimensions, the area A) as

$$\frac{PA}{k_BT} = \ln \Xi(z, A, T) \tag{3.78}$$

and the total number of particles as

$$N = z\frac{\partial \ln \Xi(z, A, t)}{\partial z} \tag{3.79}$$

The grand partition function was in section (A.1) found to be

$$\Xi(z, A, T) = \begin{cases} \prod_{\epsilon_i} \frac{1}{\left(1 - ze^{-\beta\epsilon_i}\right)} & \text{in the BE case} \\ \prod_{\epsilon_i} \left(1 + ze^{-\beta\epsilon_i}\right) & \text{in the FD case} \end{cases} \tag{3.80}$$

By insertion, we find for bosons that

$$\left(\frac{PA}{k_BT}\right)_{\text{BE}} = -\sum_{\epsilon_i} \ln\left(1 - ze^{-\beta\epsilon_i}\right) \tag{3.81}$$

and

$$(N)_{\text{BE}} = \sum_{\epsilon} \frac{1}{z^{-1}e^{\beta\epsilon_i} - 1} \tag{3.82}$$

while for fermions

$$\left(\frac{PA}{k_BT}\right)_{\text{FD}} = \sum_{\epsilon_i} \ln\left(1 + ze^{-\beta\epsilon_i}\right) \tag{3.83}$$

and

$$(N)_{\mathrm{FD}} = \sum_{\epsilon_i} \frac{1}{z^{-1}e^{\beta\epsilon_i}+1}. \tag{3.84}$$

Unfortunately, the two expressions (3.81) and (3.82) are divergent in the limit where $z \to 1$.[6] How do we work around this? By omitting the lowest energy levels from the rest of the sum, we get that

$$\left(\frac{P}{k_BT}\right)_{\mathrm{BE}} \tag{3.88}$$

$$\approx -\frac{1}{A}\ln(1-z) - \frac{1}{A}\left(\frac{mA}{2\pi\hbar^2}\right)\int_0^\infty \ln\left(1-ze^{-\beta\epsilon}\right)\,d\epsilon \tag{3.89}$$

$$= -\frac{1}{\lambda^2}\int_0^\infty \ln\left(1-ze^{-x}\right)\,dx - \frac{1}{A}\ln(1-z) \tag{3.90}$$

and

$$\left(\frac{N}{A}\right)_{\mathrm{BE}} \approx \frac{z}{A(1-z)} + \frac{1}{A}\left(\frac{mA}{2\pi\hbar^2}\right)\int_0^\infty \frac{1}{z^{-1}e^{\beta\epsilon}-1}\,d\epsilon \tag{3.91}$$

$$= \frac{1}{\lambda^2}\int_0^\infty \frac{1}{z^{-1}e^{x}-1}\,dx + \frac{z}{A(1-z)} \tag{3.92}$$

where $x = \beta\epsilon$ so that $dx = \beta\,d\epsilon$ and $\lambda = \left(\frac{2\pi\hbar^2}{mk_BT}\right)^{1/2}$. At this point, we could safely replace the sums by integrals[7], since the possible divergence is completely contained in the isolated terms. In addition, we wish to get a more suggestive relationship between the two results. Integration by parts gives

$$\left(\frac{P}{k_BT}\right)_{\mathrm{BE}} = -\frac{1}{\lambda^2}\left[x\ln\left(1-ze^{-x}\right)\big|_{x=0}^\infty - \int_0^\infty \frac{xze^{-x}}{1-ze^{-x}}\,dx\right] - \frac{1}{A}\ln(1-z) \tag{3.93}$$

$$= \frac{1}{\lambda^2}\int_0^\infty \frac{x}{z^{-1}e^{x}-1}\,dx - \frac{1}{A}\ln(1-z)\,. \tag{3.94}$$

[6] This is easily seen from the terms

$$\sum_\epsilon \ln\left(1-ze^{-\beta\epsilon}\right) = \ln(1-z) + \ln\left(1-ze^{-\beta\epsilon_1}\right) + \ln\left(1-ze^{-\beta\epsilon_2}\right) + \cdots \tag{3.85}$$

where we have used that $\epsilon_0 = 0$. Since $\ln(1-z) = \ln(x) \to -\infty$ as $x \to 0$, the first term in this series blows up. The corresponding expansion of the particle number is

$$\sum_\epsilon \frac{1}{z^{-1}e^{\beta\epsilon}-1} = \frac{1}{z^{-1}-1} + \frac{1}{z^{-1}e^{\beta\epsilon_1}-1} + \frac{1}{z^{-1}e^{\beta\epsilon_2}-1} + \cdots \tag{3.86}$$

$$= \frac{z}{1-z} + \frac{z}{e^{\beta\epsilon_1}-z} + \frac{z}{e^{\beta\epsilon_2}-z} + \cdots \tag{3.87}$$

which also blows up in the first term when $z \to 1$.

[7] Here, we have used the prescription $\sum_\epsilon \to \int g(\epsilon)\,f(\epsilon)\,d\epsilon$.

By looking at the integrals (3.92) and (3.94), we find the formal relationship striking. The term $-(1/A)\ln(1-z)$ can be shown to be negligble in the $z \to 1$ limit, and is consequently removed. See e.g. [30].

In the fermion case we are not faced with such delicacies, and we find that

$$\left(\frac{P}{k_B T}\right)_{\text{FD}} \approx \frac{m}{2\pi\hbar^2}\int_0^\infty \ln\left(1+ze^{-\beta\epsilon}\right)\,d\epsilon \tag{3.95}$$

$$= \frac{1}{\lambda^2}\int_0^\infty \ln\left(1+ze^{-x}\right)\,dx \tag{3.96}$$

with the replacement $x = \beta\epsilon$ so that $dx = \beta\,d\epsilon$ and as usual we have the mean thermal wavelength $\lambda = \left(\frac{2\pi\hbar^2}{mk_BT}\right)^{1/2}$. Just as for the bosons, we wish to cast the integral into a slightly different form. Once again, integration by parts gives

$$\left(\frac{P}{k_B T}\right)_{\text{FD}} = \frac{1}{\lambda^2}\left[x\ln\left(1+ze^{-x}\right)\big|_{x=0}^\infty + \int_0^\infty \frac{zxe^{-x}}{1+ze^{-x}}\,dx\right] \tag{3.97}$$

$$= \frac{1}{\lambda^2}\int_0^\infty \frac{x}{z^{-1}e^x+1}\,dx \tag{3.98}$$

The number of particles becomes

$$\left(\frac{N}{A}\right)_{\text{FD}} \approx \frac{m}{2\pi\hbar^2}\int_0^\infty \frac{1}{z^{-1}e^{\beta\epsilon}+1}\,d\epsilon \tag{3.99}$$

$$= \frac{1}{\lambda^2}\int_0^\infty \frac{1}{z^{-1}e^x+1}\,dx \tag{3.100}$$

which, once again, reveals a close resemblance between the expression for pressure (3.98) and density (3.100).

3.4.0.2 Introducing the BEFD function

As was pointed out above, there is a strong formal relationship between the various expressions for the pressure and density in both particle species. The Fermi-Dirac function is given by

$$f_n(z) = \frac{1}{\Gamma(n)}\int_0^\infty \frac{x^{n-1}}{z^{-1}e^x+1}\,dx \tag{3.101}$$

whilst the similar function

$$g_n(z) = \frac{1}{\Gamma(n)}\int_0^\infty \frac{x^{n-1}}{z^{-1}e^x-1}\,dx \tag{3.102}$$

is known as the Bose-Einstein function. These names derive from the fact that both functions appear frequently in problems involving the FD and BE

distributions respectively. With a generalization as the goal in mind, we define the combined function[8]

$$\tilde{f}_n(a,z) = \frac{1}{\Gamma(n)}\int_0^\infty \frac{x^{n-1}}{z^{-1}e^x + a}\,dx \tag{3.103}$$

which we will dub the Bose-Einstein/Fermi-Dirac function, or BEFD for short. As is easily seen, it produces the correct result for the bosonic case with $a = -1$ and the fermionic case with $a = +1$. It follows that this is valid for all n. For our needs, it suffices to find the solutions of $\tilde{f}_1(z)$ and $\tilde{f}_2(z)$.First we solve for $n = 1$. We find that

$$\tilde{f}_1(a,z) = \int_0^\infty \frac{ze^{-x}}{1 + aze^{-x}}\,dx. \tag{3.104}$$

We see that by using $u = ze^{-x}$ this may be written as

$$\tilde{f}_1(a,z) = -\int_z^0 \frac{1}{1+au}\,du \tag{3.105}$$

$$= -\frac{1}{a}\ln(1) + \frac{1}{a}\ln(1+az) \tag{3.106}$$

$$= \frac{1}{a}\ln(1+az) \tag{3.107}$$

This result coincides with well-established results for both the BE and FD function (by letting $a = -1$ and $a = +1$ respectively).[9]

3.4.0.3 The Recurrence Relation

In the standard derivation of the virial expansion of an ideal BE or FD gas, it is customary to utilize the recurrence relation

$$z\frac{\partial}{\partial z}f_n(z) = f_{n-1}(z) \quad \text{or} \quad z\frac{\partial}{\partial z}g_n(z) = g_{n-1}(z) \tag{3.108}$$

This suggests that we should be able to establish the similar result

$$z\frac{\partial}{\partial z}\tilde{f}_n(a,z) = \tilde{f}_{n-1}(a,z) \tag{3.109}$$

We insert for $\tilde{f}_n$ in $z\frac{\partial}{\partial z}\tilde{f}_n(a,z)$ and find

$$z\frac{\partial}{\partial z}\frac{1}{\Gamma(n)}\int_0^\infty \frac{x^{n-1}}{z^{-1}e^x + a}\,dx = \frac{1}{\Gamma(n)}\int_0^\infty \frac{x^{n-1}z^{-1}e^x}{(z^{-1}e^x + a)^2}\,dx \tag{3.110}$$

[8] Combined (or generalized) in a sense that, when $a = -1$ we get the correct function for the bosonic case, whilst when $a = +1$ we get the correct fermionic function. Using this notation, we may combine the two functions into a generalized expression.

[9] The results are $g_1(z) = -\ln(1-z)$ for the BE function and $f_1(z) = \ln(1+z)$ for the FD function.

Integration by parts gives

$$\frac{1}{(n-1)!}\int_0^\infty \frac{x^{n-1}z^{-1}e^x}{\left(z^{-1}e^x+a\right)^2}\,dx \tag{3.111}$$

$$= \frac{1}{(n-1)!}\left(-x^{n-1}\frac{1}{z^{-1}e^x+a}\bigg|_{x=0}^{\infty} + (n-1)\int_0^\infty \frac{x^{n-2}}{z^{-1}e^x+a}\,dx\right) \tag{3.112}$$

$$= \frac{1}{\Gamma(n-1)}\int_0^\infty \frac{x^{n-2}}{z^{-1}e^x+a}\,dx. \tag{3.113}$$

This is exactly what we wanted to show, and hence

$$z\frac{\partial}{\partial z}\tilde{f}_n(a,z) = \tilde{f}_{n-1}(a,z) \tag{3.114}$$

holds also in the generalized case.

3.4.0.4 Second Degree Solution by Recurrence

We have already found that $\tilde{f}_1(a,z) = \frac{1}{a}\ln(1+az)$. By the recurrence relation we get

$$\tilde{f}_2(a,z) = \int \frac{1}{z}\tilde{f}_1(a,z)\,dz \tag{3.115}$$

$$= \frac{1}{a}\int \frac{1}{z}\ln(1+az)\,dz \tag{3.116}$$

Substituting for $y = \ln(1+az)$ find that

$$\tilde{f}_2(a,z) = \frac{1}{a}\int \frac{ya}{e^y-1}\frac{e^y}{a}\,dy \tag{3.117}$$

$$= -\frac{1}{a}\int \frac{-y}{1-e^{-y}}\,dy \tag{3.118}$$

Substituting for $x = -y$ we find that

$$\tilde{f}_2(a,z) = \frac{1}{a}\int \frac{x}{1-e^x}\,dx \tag{3.119}$$

$$= -\frac{1}{a}\int \frac{x}{e^x-1}\,dx \tag{3.120}$$

The expression $\frac{x}{e^x-1}$ may be expanded by using the Bernoulli numbers. Using this, we find that

$$\tilde{f}_2(a,z) = -\frac{1}{a}\int\left(1-\frac{x}{2}+\sum_{n=1}^{\infty}\frac{x^{2n}}{(2n)!}B_{2n}\right)dx \tag{3.121}$$

$$= \frac{1}{a}\left[y+\frac{1}{4}y^2+\sum_{n=1}^{\infty}\frac{y^{2n+1}}{(2n+1)!}B_{2n}\right] \tag{3.122}$$

3.4.0.5 Combine Solutions to Determine Virial Coefficients

Inserting for $\tilde{f}_1(a,z)$ and $\tilde{f}_2(a,z)$ gives us the final result

$$\frac{PV}{Nk_BT} = \frac{\tilde{f}_2(a,z)}{\tilde{f}_1(a,z)} \tag{3.123}$$

$$= 1 + \frac{1}{4}y + \sum_{n=1}^{\infty} \frac{y^{2n}}{(2n+1)!} B_{2n} \tag{3.124}$$

Finally inserting for $y = a\rho\lambda^2$, we get

$$\frac{PV}{Nk_BT} = 1 + \frac{1}{4}a\rho\lambda^2 + \sum_{n=1}^{\infty} \frac{a^{2n}B_{2n}}{(2n+1)!} \left(\rho\lambda^2\right)^{2n} \tag{3.125}$$

We see that the a^{2n} term will always turn out to be unity, so the only place in our viral expansion where a a appears, is in the second virial coefficient

$$a_2 = \frac{1}{4}a \tag{3.126}$$

This reproduces the correct results in the fermionic and bosonic limits.

3.5 Summary

Although the physical properties of bosons and fermions in many respects are inverse to each other, the mathematical structure describing the bulk behavior of both particle classes are highly similar. This has enabled us to show that it is possible, in a combined expression, to derive the virial expansion of an ideal bosonic or fermionic gas in two dimensions.

Chapter 4

Fractional Exclusion Statistics

4.1 Introduction

Some of the motivation for this section is to give a short and (hopefully) straight forward explanation of the concept of fractional exclusion statistics. As will be clear in section 5, the statstical mechanics of an ideal anyon gas is well beyond our current abilities. With this perspective it is interesting to examine the simpler exclusion statistics. Most of the results are quite foreign to the standard literature, so we will approach the subject at a leisurely pace. Whenever methods from more familiar cases are employed, there will be some elaboration on the important similarities. Some thermodynamical results will be explored, in particular the virial expansion.

There are different notations in the relevant literature. As a heads up to the reader, we note that g_i and n_i are reserved for the number of energy levels in the ith cell and the corresponding occupation number respectively. The fractional exclusion statistics parameter is designated σ.

4.2 The Foundation of Fractional Exclusion Statistics

The foundation for the so-called Fractional Exclusion Statistics (FES) was the formulation of the generalized Pauli principle. Since we know how the original exclusion principle leads to rather pronounced quantum effects for a fermion and boson gas, one may ask what happens if we interpolate between the bosonic and fermionic case. This is to say: What happens if a particle isn't a boson or a fermion, but something in between? Although all elementary particles are classified either as fermions or bosons, considering such a situation isn't necessarily as artificial as it might appear.[1]

[1] In his original paper Haldane gives two examples of systems that may be described using a FES-approach, one of them being the fractional quantum Hall effect, which we met in section 2.4.1.

In 1991, when Haldane published his paper introducing the generalized Pauli principle, anyons where a hot topic among physicists. In fact, his paper starts out with a reference to anyons being particles obeying fractional statistics. The fractional statistics is explicitly stated by Haldane, whereas it is an implicit effect in the anyon case. It is pointed out that whatever the "particle" of fractional statistics is - it is not an elementary particle and that it is confined to the interior of a condensed matter region. This is much the same picture one has of anyonic "particles". Anyons are not elementary constituents of matter either.[2] The original exclusion principle dictates that states in the Hilbert space of the system are blocked out as fermions are added to the system. On the other hand, whenever bosons are added to the system, no states are blocked.

In the generalized exclusion principle, Haldane defines the statistical interaction σ through the relation[3]

$$\Delta d = -\sigma \Delta N \tag{4.1}$$

where Δd is the change in the dimensionality d of the Hilbert space, and ΔN is the number of particles added to (or subtracted from) the system. This is the generalized exclusion principle. It is evident that $\sigma = 0$ is identified as if bosons are added to the system, while $\sigma = 1$ is identified as fermions are added instead. Obviously, if $\sigma = 0$, no states are blocked out by adding new particles. This is what we would expect from adding bosons. If $\sigma = 1$ on the other hand, the number of states blocked out $-\Delta d$ by adding a number of particles ΔN particles are equal, i.e. $-\Delta d = \Delta N$. This is consistent with fermions being added to the system. All in all this seems to coincide with known physics.

4.3 The Distribution Function

As shown in section (3.2) and (A.1), there are different ways of deriving the Bose-Einstein and Fermi-Dirac distribution functions. By counting the number of possible ways to distribute bosons or fermions among energy levels

[2] This is a half truth. It has been argued that every theory is merely an *effective theory*, which means that we ignore physical effects that are either too large or too small to contribute to the dynamics in question. In this sense, anyons are just as elementary as electrons. See also section 2.4.3 for a short discussion.

[3] Haldane's original paper gives a more detailed description than we are prepared to do here. In his original treatise, the statistical interaction is given as

$$\Delta d_i = -\sum_j \sigma_{ij} \Delta N_j$$

which allows for the system to consist of particles of different species i and j. The bosonic case is given by $\sigma_{ij} = 0$ while the fermionic case by $\sigma_{ij} = \delta_{ij}$. We will limit ourselves to consider single-component (-species) systems.

in a cell spanning a certain interval of the energy spectrum, we found the number of microstates subject to the restrictions of conserved total energy and particle number. Having found this, we used Boltzmann's equation for entropy, and determined the equilibrium situation by maximizing the entropy using Lagrange multipliers. In essence, this is the same procedure we will follow here in order to establish the distribution function for the ideal FES-gas.

We will base our treatment on the three seminal papers on the foundations of FES thermodynamics, namely [15, 39] in which the distribution function is found, and [14] which developed the derivation of the thermodynamical results we are going to explore.

4.3.1 The Statistical Weight

Both [15] and [39] start out with considering the generalized exclusion principle of Haldane. As we saw in the previous section, there is a blocking of states in the Hilbert space of the system according to eq. (4.1). In a quantum mechanical formulation, a microstate of the system is usually simply referred to as a *state*. Such a state is the most detailed description of the physical state of the system that one can hope to give.[4] Mathematically, the state is said to correspond to a (unit) vector $|\psi(t)\rangle$ which is an element of a Hilbert space $\mathcal{H}$. Herein lies the connection to the statistical mechanics of the system. Since each independent state must be represented by orthogonal vectors in Hilbert space, the dimensionality of $\mathcal{H}$ reflects the number of possible (micro)states available to the system, which in turn is known as the statistical weight.

The subsequent derivation ideas are analogous to that of the microcanonical treatment of the Bose- and Fermi gases - for a reminder, see section 3.2. Isakov's discussion is based on the statistical weight

$$W_{\text{Isakov}} = \prod_i \frac{[g_i + n_i(1-\sigma) - 1]!}{(n_i)!\,[g_i - \sigma n_i - 1]!} \tag{4.2}$$

which can be seen to be identical with the Hilbert space as defined in [9]. On the other hand, Wu ask us to consider the statistical weights

$$W_{\text{B}} = \frac{[g_i + n_i - 1]!}{(n_i)!\,[g_i - 1]!} \tag{4.3}$$

and

$$W_{\text{F}} = \frac{(g_i)!}{(n_i)!\,[g_i - n_i]!} \tag{4.4}$$

[4] Unlike in the classical regime, when one operates on a quantum scale, there is no such thing as a precise point in phase space determining the microstate of the system to an arbitrary degree. As position and momentum are subject to Heisenberg's uncertainty relation, the formulation of quantum statistical mechanics must be based on other principles.

which is valid for n_i identical bosons or fermions respectively, occupying a group of g_i states. He goes on to suggest the interpolating expression

$$W_{\mathrm{Wu}} = \frac{[g_i + (n_i - 1)(1-\sigma)]!}{(n_i)![g_i - \sigma n_i - (1-\sigma)]!} \tag{4.5}$$

which reproduces W_{B} and W_{F} in the bosonic $\sigma = 0$ and fermionic $\sigma = 1$ limits. But are these expressions of Isakov and Wu equivalent by physical terms? Most certainly, they are *not* identical. This is, however, not necessarily a problem. As long as the two expressions yield the same predictions, we need to treat them on an equal footing (or perhaps pick our favorite based on some subjective criteria). After all, at this point we still have not encountered any physics of significance.

In order to explore the physical predictions that may be derived from the above result, we start out with Boltzmann's expression for entropy. This non-equilibrium entropy is given as

$$S = k_B \ln W. \tag{4.6}$$

From the second law of thermodynamics, we know that the system (left alone) will tend towards a maximum entropy state. But, we can not simply take the system to a maximum S while letting all the other state variables grow with it. Such a variation of the entropy will never reach a maximum, and hence no equilibrium state will be obtained.

As we saw in section 3.2, the standard prescription to solve such extremum problems is to constrain the system in some variables, while investigating the behavior with respect to variation of another variable. In particular, we wish to keep the total energy

$$\sum_i \epsilon_i n_i = E \tag{4.7}$$

and total particle number

$$\sum_i n_i = N \tag{4.8}$$

fixed, while seeking the maximum value for S.

4.3.1.1 The Isakov Weight

As the technical details in the subsequent derivations are almost identical, we will give a thorough calculation in the first case only. Beginning with Isakov's weight, we insert for W_{Isakov} into eq. (4.6) as follows

$$\frac{S_{\mathrm{Isakov}}}{k_B} = \sum_i \ln \frac{[g_i + n_i(1-\sigma) - 1]!}{(n_i)![g_i - \sigma n_i - 1]!}. \tag{4.9}$$

Using Stirling's approximation $\ln N! \approx N \ln N - N$, we find that

$$\begin{aligned}\frac{S_{\text{Isakov}}}{k_B} &\approx \sum_i \left([g_i + n_i (1-\sigma) - 1] \ln [g_i + n_i (1-\sigma) - 1] \right. \\ &\quad \left. - n_i \ln n_i - [g_i - \sigma n_i - 1] \ln [g_i - \sigma n_i - 1] \right) . \end{aligned} \tag{4.10}$$

This last line may be simplified as follows. Since we are assuming that $g_i \gg 1$ and $n_i \gg 1$, terms like $1/g_i$, $1/n_i$, σ/g_i, and σ/n_i will be negligible. We define the average "occupation number" $\langle n_i \rangle \equiv n_i/g_i$ so that, by pulling g_i outside, we get

$$\begin{aligned}\frac{S_{\text{Isakov}}}{k_B} &\approx \sum_i g_i \left([1 + \langle n_i \rangle (1-\sigma) - \langle n_i \rangle - [1 - \sigma \langle n_i \rangle]] \ln g_i \right. \\ &\quad + [1 + \langle n_i \rangle (1-\sigma)] \ln [1 + \langle n_i \rangle (1-\sigma)] \\ &\quad \left. - \langle n_i \rangle \ln \langle n_i \rangle - [1 - \sigma \langle n_i \rangle] \ln [1 - \sigma \langle n_i \rangle] \right) . \end{aligned} \tag{4.11}$$

Cancelling terms gives the final result

$$\begin{aligned}\frac{S_{\text{Isakov}}}{k_B} &= \sum_i g_i \left([1 + \langle n_i \rangle - \sigma \langle n_i \rangle] \ln [1 + \langle n_i \rangle - \sigma \langle n_i \rangle] \right. \\ &\quad \left. - \langle n_i \rangle \ln \langle n_i \rangle - [1 - \sigma \langle n_i \rangle] \ln [1 - \sigma \langle n_i \rangle] \right) \end{aligned} \tag{4.12}$$

which will be compared to that of Wu.

4.3.1.2 The Wu Weight

Analogously, we find by inserting for W_{Wu} and by using Stirling's approximation, that

$$\frac{S_{\text{Wu}}}{k_B} \tag{4.13}$$

$$\begin{aligned}&\approx \sum_i \left([g_i + (n_i - 1)(1-\sigma)] \ln [g_i + (n_i - 1)(1-\sigma)] \right. \\ &\quad \left. - n_i \ln n_i - [g_i - \sigma n_i - (1-\sigma)] \ln [g_i - \sigma n_i - (1-\sigma)] \right) . \end{aligned} \tag{4.14}$$

As in the Isakov-case, we may neglect $1/g_i$, σ/g_i etc. Thus, by pulling g_i outside and using $\langle n_i \rangle = n_i/g_i$, we get

$$\begin{aligned}\frac{S_{\text{Wu}}}{k_B} &= \sum_i g_i \left([1 + \langle n_i \rangle - \sigma \langle n_i \rangle] \ln [1 + \langle n_i \rangle - \sigma \langle n_i \rangle] \right. \\ &\quad \left. - \langle n_i \rangle \ln \langle n_i \rangle - [1 - \sigma \langle n_i \rangle] \ln [1 - \sigma \langle n_i \rangle] \right) . \end{aligned} \tag{4.15}$$

This is exactly the same expression as obtained by using the Isakov weight. All thermodynamical results derived hereof must necessarily coincide, regardless of the choice of weight. As we are free to choose whatever weight

we may seem fit, the Wu weight has the attractive property that, whenever we set $\sigma = 0$ for bosons or $\sigma = 1$ for fermions, the weight reproduce the corresponding weights for the bosonic and fermionic case. Thus, from a purely aesthetical point of view, we prefer the Wu weight. Once again, this does not really matter, since S is the same in both cases.

4.3.2 Maximizing Entropy and Deriving the Distribution Function

Just like in section 3.2.4, we wish to maximize the entropy in order to determine the equilibrium of the system. We have that the non-equilibrium entropy is given as eq. (4.12), or equivalently, eq. (4.15). In the notation of section 3.2.4, we have that $F = S/k_B$, and subject this function to the constraints $N - \sum_i g_i \langle n_i \rangle = 0$ with multiplier $-\beta\mu$ and $E - \sum_i \epsilon_i g_i \langle n_i \rangle = 0$ with multiplier β. It follows that

$$\begin{aligned} G &= \sum_i g_i \left([1 + \langle n_i \rangle - \sigma \langle n_i \rangle] \ln [1 + \langle n_i \rangle - \sigma \langle n_i \rangle] \right. \\ &\quad - \langle n_i \rangle \ln \langle n_i \rangle - [1 - \sigma \langle n_i \rangle] \ln [1 - \sigma \langle n_i \rangle] \\ &\quad \left. + \beta \langle n_i \rangle [\mu - \epsilon_i] \right) - \beta\mu N + \beta E. \end{aligned} \tag{4.16}$$

Varying this with respect to n_i, we find that

$$\begin{aligned} \frac{\partial G}{\partial \langle n_i \rangle} &= \sum_i g_i \left([1 - \sigma] \ln [1 + \langle n_i \rangle - \sigma \langle n_i \rangle] + [1 - \sigma] \right. \\ &\quad \left. - \ln \langle n_i \rangle - 1 + \sigma \ln [1 - \sigma \langle n_i \rangle] + \sigma + \beta [\mu - \epsilon_i] \right) \\ &= 0 \end{aligned} \tag{4.17}$$

where we have used $\partial G / \partial \lambda_i = 0$.

However, since all the terms in this sum are assumed independent, this relationship must be true term by term, i.e. all the terms in the sum are zero. We know that $g_i \neq 0$, and so it follows that

$$\begin{aligned} 0 &= [1 - \sigma] \ln [1 + \langle n_i \rangle - \sigma \langle n_i \rangle] - \ln \langle n_i \rangle \\ &\quad + \sigma \ln [1 - \sigma \langle n_i \rangle] + \beta [\mu - \epsilon_i] . \end{aligned} \tag{4.18}$$

Finding $\langle n_i \rangle$ is achieved in a couple of steps. Re-arranging and simplifying gives

$$\beta [\epsilon_i - \mu] \tag{4.19}$$

$$= [1 - \sigma] \ln [1 + (1 - \sigma) \langle n_i \rangle] - \ln \langle n_i \rangle + \sigma \ln [1 - \sigma \langle n_i \rangle] \tag{4.20}$$

which in turn may be written

$$\ln \left[\frac{1 + (1 - \sigma) \langle n_i \rangle}{\langle n_i \rangle} \right] + \sigma \ln \left[\frac{1 - \sigma \langle n_i \rangle}{1 + (1 - \sigma) \langle n_i \rangle} \right] = \beta [\epsilon_i - \mu] . \tag{4.21}$$

By introducing

$$w = \frac{\langle n_i \rangle}{1 + (1-\sigma)\langle n_i \rangle}$$

we get that

$$\begin{aligned} \beta[\epsilon_i - \mu] &= \sigma \ln\left[\frac{1 + (1-\sigma)\langle n_i \rangle}{1 + (1-\sigma)\langle n_i \rangle} - \frac{\langle n_i \rangle}{1 + (1-\sigma)\langle n_i \rangle}\right] \\ &\quad - \ln\left[\frac{\langle n_i \rangle}{1 + (1-\sigma)\langle n_i \rangle}\right] \end{aligned} \tag{4.22}$$

or simply

$$\sigma \ln[1 - w(\zeta)] - \ln[w(\zeta)] = \beta[\epsilon_i - \mu] \tag{4.23}$$

where we have defined $\zeta \equiv e^{\beta(\epsilon_i - \mu)}$. Eq. (4.23) is an example of a so-called functional equation. These are inherently hard to solve, and we will only look into three values for σ for which a solution is easily found. Also note that, given w as above, the distribution function is easily found to be

$$\langle n_i \rangle = \frac{w}{1 + (\sigma - 1)w} \tag{4.24}$$

in analogy with the Bose-Einstein and Fermi-Dirac distributions.

We wish to verify that our calculations are coinciding with the known limits, namely the Bose-Einstein and Fermi-Dirac distributions. Indeed they must, due to the way we have defined FES. Observe that the functional equation eq. (4.23) may be written as

$$[1 - w(\zeta)]^{\sigma} [w(\zeta)]^{-1} = e^{\beta(\epsilon_i - \mu)}. \tag{4.25}$$

For $\sigma = 0$ we expect to see the Bose-Einstein distribution reproduced. By inserting for $\sigma = 0$ in the functional equation, we find $w(\zeta)$ to be

$$w(\zeta) = e^{-\beta(\epsilon_i - \mu)}. \tag{4.26}$$

Inserting for $\sigma = 0$ and $w(\zeta) = e^{-\beta(\epsilon_i - \mu)}$, we see that eq. (4.24) becomes

$$\begin{aligned} \langle n_i \rangle_{\sigma=0} &= \frac{e^{-\beta(\epsilon_i - \mu)}}{1 - e^{-\beta(\epsilon_i - \mu)}} \\ &= \frac{1}{e^{\beta(\epsilon_i - \mu)} - 1} \end{aligned} \tag{4.27}$$

which is exactly the Bose-Einstein distribution as expected. The analogous calculation for the fermion case $\sigma = 1$ gives

$$w(\zeta) = \frac{1}{e^{\beta(\epsilon_i - \mu)} + 1} \tag{4.28}$$

and

$$\langle n_i \rangle_{\sigma=1} = \frac{1}{e^{\beta(\epsilon_i-\mu)}+1} \tag{4.29}$$

which is coinciding with the Fermi-Dirac distribution.

We promised to look into a few of the σ which yield a solution of eq. (4.23). Having verified the two important end points, the natural next candidate for inspection is the given by $\sigma = 1/2$. The value $\sigma = 1/2$ is best known as the semion point. It is not a boson nor a fermion, but precisely half way between the two, hence the term semion[5]. To find this, we solve for $w(\zeta)$ first. This gives

$$[1-w(\zeta)]^{\frac{1}{2}}[w(\zeta)]^{-1} = e^{\beta(\epsilon_i-\mu)} \tag{4.30}$$

or

$$-e^{2\beta(\epsilon_i-\mu)}w^2 - w + 1 = 0. \tag{4.31}$$

Solving for w, we have

$$w = -\frac{1 \pm \sqrt{4e^{2\beta(\epsilon_i-\mu)}+1}}{2e^{2\beta(\epsilon_i-\mu)}} \tag{4.32}$$

As a matter of convenience, we define $K \equiv \sqrt{4e^{2\beta(\epsilon_i-\mu)}+1}$ so that $\left(K^2-1\right)/2 = 2e^{2\beta(\epsilon_i-\mu)}$. Inserting into eq. (4.23) gives

$$\begin{aligned}\langle n_i \rangle_{\sigma=1/2} &= \frac{w}{1-\frac{1}{2}w} \\ &= \left(-\frac{2(1\pm K)}{K^2-1}\right) / \left(\frac{K^2-1+1\pm K}{K^2-1}\right) \\ &= \frac{2(1\pm K)}{K(\mp 1-K)}\end{aligned} \tag{4.33}$$

Choosing the negative root, we get

$$\begin{aligned}\langle n_i \rangle_{\sigma=1/2} &= \frac{2(1-K)}{K(1-K)} \\ &= \frac{2}{\sqrt{4e^{2\beta(\epsilon_i-\mu)}+1}}\end{aligned} \tag{4.34}$$

known as the semion distribution.

[5]One meaning of the word "semi" is "half of" some quantity.

4.3.3 Concluding Remarks

At this point, it may be interesting to make a comparison with another famous distriubtion, that is, the Maxwell-Boltzmann distribution. In the literature, e.g. [28], it is customary to combine the Bose-Einstein and Fermi-Dirac distributions into a single expression

$$\langle n_i \rangle = \frac{1}{e^{\beta(\epsilon_i - \mu)} + a} \tag{4.35}$$

where $a = -1$ for the bosonic and $a = +1$ for the fermionic case. These ideal distributions are valid for temperatures down to $T \to 0$. By setting $a = 0$, however, on finds the Maxwell-Boltzmann distribution. Both the Bose-Einstein and Fermi-Dirac case coincide with the Maxwell-Boltzmann distribution in the high temperature limit. On the other hand, in the low temperature limit, there is no (ordinary) ideal quantum gas that obeys the Maxwell-Boltzmann distribution. Inspired by the fact that $-1 \leq a \leq 1$, and that the mid-point in this range, $a = 0$, gives the Maxwell-Boltzmann, it is tempting to compare this to the FES distribution. On could naively ask, is $a = 0$ equivalent to $\sigma = 1/2$?

Before we go into the differences among the different distributions, we may note that they all converge in the $x \to \infty$ limit, where $x = \beta(\epsilon_i - \mu)$. This is so, because the exponential term will completely dominate the denominator, and hence all the distributions behave essentially as the Maxwell-Boltzmann distribution in this end of the spectrum. For values around $x = 1/2$, the semion and Maxwell-Boltzmann distributions seems to be far closer to each other than the two end point distributions are. They follow each other closely for a while, although at $x = -1/2$ it is obvious that they have different agendas, see figure 4.1 for a plot.

Clearly, the semion distribution at $\sigma = 1/2$ is not a Maxwell-Boltzmann distribution, as can be seen from the fact that eq. (4.34) can not be written as $\langle n_i \rangle = 1/e^{\beta(\epsilon_i - \mu)}$. The discrepancy between $a = 0$ and $\sigma = 1/2$ is simply a statement that the relationship between a and σ is non-linear. Having established that the semion distribution is not the same as the Maxwell-Boltzmann distribution, it is instructive to get a feeling of how far removed they are from each other. There are some important qualitative features we would like to address in this regard. The Bose-Einstein and Fermi-Dirac are the qualitative reciprocal of each other, in the sense that their average occupation numbers are strongly divergent (boson) and strongly convergent (fermion) respectively. It is customary to portray the Maxwell-Boltzmann distribution as kind of cross between these two cases, a picture that is justified by eq. (4.35), with $a = 0$.

On the other hand, in a FES setting, it is natural to consider the semion distribution as the hybrid distribution. However, from an inspection of figure 4.1, we see that there is a big difference between the Maxwell-Boltzmann and

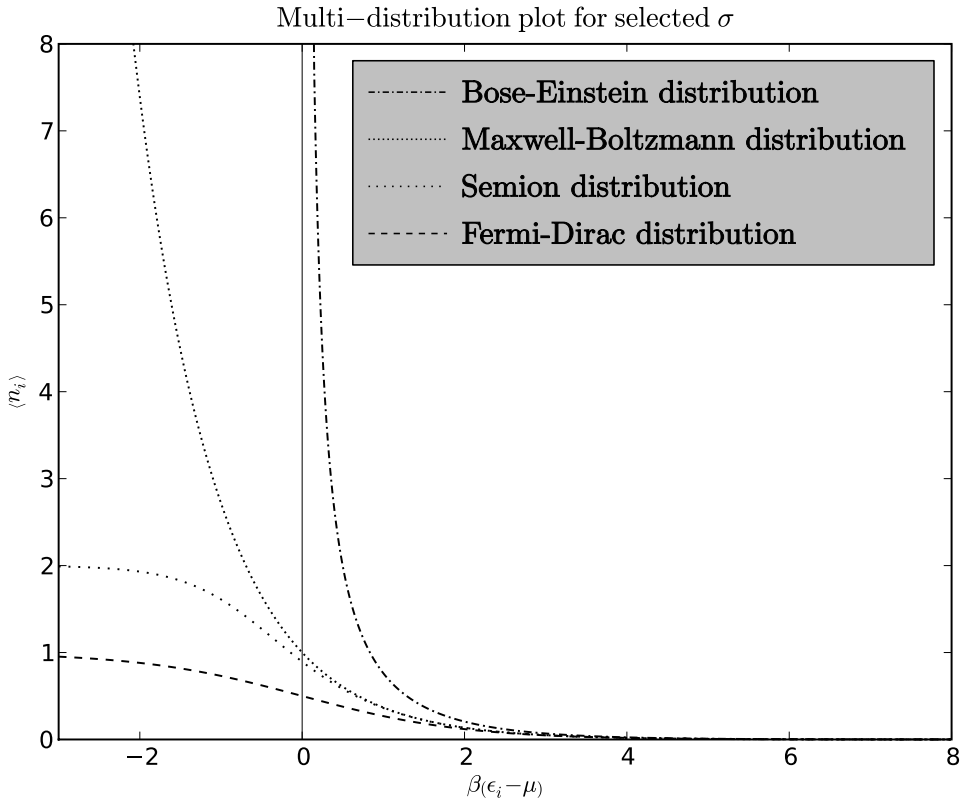

Figure 4.1: The standard distribution plot as presented in e.g. [28] reveals the reciprocal nature of the Bose-Einstein and Fermi-Dirac distributions. For the bosonic gas, we have $\mu < \epsilon$ for all ϵ. When $\mu \to \epsilon_0$, where ϵ_0 is the ground state energy, the occupation number becomes infinitely high, which is a signal of Bose-Einstein condensation. For the fermionic gas, the occupancy can not become greater than $\langle n_i \rangle_{\mathrm{f}} = 1$. This is due to the Pauli exclusion principle. The Maxwell-Boltzmann distribution is on the verge between convergence and divergence, making it a very special case. The semion distribution has an asymptote of 2.

semion distributions. The semion distribution is clearly convergent for $x = \beta(\epsilon_i - \mu)$ in the $x \to -\infty$ limit, with asymptote 2 , whereas the Maxwell-Boltzmann distribution is divergent in $x \to -\infty$.[6] However, had there been, in addition to the $e^{\beta(\epsilon_i - \mu)}$, a positive term in the denominator (no matter how small), the expression would have had a horizontal asymptote. Thus, we see that the Maxwell-Boltzmann distribution is almost in a state of limbo. It is on the verge of becoming convergent at any time.

What does the asymptote of 2 in the semion case tell us? It is a signal that at most 2 particles may occupy any state. This is the generalized exclusion principle at work. The possible distributions in the zone "in between" the Maxwell-Boltzmann distribution and the Bose-Einstein distribution, represent a physical limbo. A zone where there are no asymptotes - neither vertical nor horizontal. Thus, there is no upper bound on how many particles that may be in a single quantum state. On the other hand, if we extrapolate the interpretation of the Bose-Einstein distribution, we conclude (based on this diagram alone)[7] that there will be no Bose-Einstein-like condensation either.

4.4 Thermodynamics of an Ideal FES Gas

In this section we will follow [14] in order to derive some thermodynamical results for the ideal FES gas.

4.4.1 The D-Dimensional Ideal FES Gas

It can be shown that the pressure for an ideal FES gas is given by

$$P = \Delta \int_0^\infty n(\epsilon_i)\, \epsilon_i^{D/\eta}\, d\epsilon_i \tag{4.36}$$

where $\Delta = b^{-D/\eta} / \left[(2\sqrt{\pi}\hbar)^D \Gamma\left(1 + \frac{1}{2}D\right) \right]$ and b and η are determined via the dispersion relation $\epsilon(p) = bp^\eta$. Likewise, the density is found by evaluation of the integral

$$\rho = N/V = \frac{D\Delta}{\eta} \int_0^\infty n(\epsilon_i)\, \epsilon_i^{(D/\eta - 1)}\, d\epsilon_i. \tag{4.37}$$

See [18] and references therein for details. As pointed out in [14], it is sometimes advantageous to rewrite an integral of the form

$$I(f) = \int_0^\infty n(\epsilon_i)\, f(\epsilon_i)\, d\epsilon_i \tag{4.38}$$

[6] Divergent, in a sense that $\langle n_i \rangle \to \infty$ as $x \to -\infty$. In terms of asymptotes, on the other hand, we say that the distribution has a vertical asymptote at $x = 0$. This is because as $x \to -\infty$, we see that $1/(e^x - 1) \to \infty$.

[7] This is not a proof that no condensation can occur in this zone. However, from purely convergence considerations, this seems plausible.

as an integral over $w(\zeta)$ with $n(\epsilon_i) = w(\zeta)/[1+(\sigma-1)w(\zeta)]$.

In the previous section, we found (see eq. (4.23))

$$\sigma \ln[1-w(\zeta)] - \ln[w(\zeta)] = \beta[\epsilon_i - \mu]. \tag{4.39}$$

When solved for ϵ_i, this expression takes the form

$$\epsilon_i = \mu + \frac{1}{\beta}[\sigma \ln(1-w(\zeta)) - \ln w(\zeta)]. \tag{4.40}$$

We insert for $n(\epsilon_i)$ and ϵ_i, while using that

$$\begin{aligned} \frac{d\epsilon_i}{dw(\zeta)} &= \frac{1}{\beta}\frac{d}{dw(\zeta)}[\sigma \ln(1-w(\zeta)) - \ln w(\zeta)] \\ &= \frac{1}{\beta}\left[-\sigma\frac{1}{1-w(\zeta)} - \frac{1}{w(\zeta)}\right] \end{aligned} \tag{4.41}$$

from which it follows that $d\epsilon_i = -\frac{1}{\beta}\left[\sigma\frac{1}{1-w(\zeta)} + \frac{1}{w(\zeta)}\right] dw(\zeta)$. Hence, we find

$$\begin{aligned} I(f) &= \int_0^\infty n(\epsilon_i) f(\epsilon_i)\, d\epsilon_i \\ &= -\frac{1}{\beta}\int_{w(0)}^0 \left(\frac{w(\zeta)}{1+(\sigma-1)w(\zeta)}\right)\left[\sigma\frac{1}{1-w(\zeta)} + \frac{1}{w(\zeta)}\right] \\ &\quad \times f\left(\mu + \frac{1}{\beta}[\sigma\ln(1-w(\zeta)) - \ln w(\zeta)]\right) dw. \end{aligned} \tag{4.42}$$

Here, we have used that the limits of integrations follow from eq. (4.40). For $\epsilon_i \to +\infty$ we use that

$$\epsilon_i \sim \sigma\ln(1-w(\zeta)) - \ln w(\zeta). \tag{4.43}$$

When $w(\zeta) \to 0$, we see that this is equivalent to $\epsilon_i \to +\infty$ (since $\ln 1 = 0$ and $-\ln 0 = +\infty$). The limit of integration where $\epsilon_i \to 0$ is designated as $w(0)$. Furthermore, we simplify the integrand as

$$\begin{aligned} &\frac{w(\zeta)}{1+(\sigma-1)w(\zeta)}\left[\sigma\frac{1}{1-w(\zeta)} + \frac{1}{w(\zeta)}\right] \\ &= \frac{w(\zeta)}{1+(\sigma-1)w(\zeta)}\left[\frac{1+(\sigma-1)w(\zeta)}{(1-w(\zeta))w(\zeta)}\right] \\ &= \frac{1}{1-w(\zeta)}. \end{aligned} \tag{4.44}$$

Thus, we see that

$$I(f) = \frac{1}{\beta}\int_0^{w(0)} \frac{f\left(\mu + \frac{1}{\beta}[\sigma\ln(1-w) - \ln w]\right)}{1-w}\, dw \tag{4.45}$$

where we have reversed the limits of integrations on the expense of a negative sign.

This whole derivation may seem a little unmotivated at first. Yet, when we compare the expression

$$n(\epsilon_i)\, d\epsilon_i = -\frac{1}{\beta}\left(\frac{1}{1-w}\right) dw \tag{4.46}$$

to that of pressure eq. (4.36) and density eq. (4.37), we realize that they may be rewritten as integrals over w. Why is this good? Well, almost as if by magic, the cumbersome distribution function (which requires closed form expressions for w as a function of ϵ in order to be evaluated) has now disappeared from our integral. So what appeared to add complexity to our integral, in fact has removed the most troubling characteristic in a simple and elegant way.

4.4.2 The Two-Dimensional, Non-Relativistic FES Gas

As both the pressure and density are expressed in quite general terms, it would be possible to investiagte these relations under different conditions. Nevertheless, we will restrict ourselves to the two-dimensional, non-relativistic regime. In that case, we have $D = \eta = 2$ so that the dispersion relation reads $\epsilon(p) = \frac{1}{2m}p^2$ and the prefactor Δ is

$$\Delta = \frac{m}{2\pi\hbar^2}. \tag{4.47}$$

By inserting for D and η together with the expression for $n(\epsilon)\, d\epsilon$ into eq. (4.36), we get that

$$\begin{aligned} P &= \Delta \int_0^\infty n(\epsilon)\, \epsilon\, d\epsilon \\ &= \frac{\Delta}{\beta} \int_0^{w(0)} \left(\frac{1}{1-w}\right) \left(\frac{1}{\beta}\left[\sigma \ln(1-w) - \ln w\right] + \mu\right) dw \end{aligned} \tag{4.48}$$

Similarly, the density is found by inserting into eq. (4.37)

$$\begin{aligned} \rho &= \Delta \int_0^{w(0)} n(\epsilon)\, d\epsilon \\ &= \frac{\Delta}{\beta} \int_0^{w(0)} \left(\frac{1}{1-w}\right) dw. \end{aligned} \tag{4.49}$$

This is readily determined to be

$$\begin{aligned} \rho &= \frac{\Delta}{\beta} \int_0^{w(0)} \left(\frac{1}{1-w}\right) dw \\ &= -\frac{\Delta}{\beta} \ln(1 - w(0)). \end{aligned} \tag{4.50}$$

Solving for $w(0)$ this becomes

$$1 - w(0) = e^{-\frac{\beta\rho}{\Delta}} \tag{4.51}$$

or simply

$$w(0) = 1 - e^{-\frac{\beta\rho}{\Delta}}. \tag{4.52}$$

Having found the density, it is time to evaluate the pressure. This is given by the expression in eq. (4.48)

$$P = \frac{\Delta}{\beta}\left(\underbrace{\frac{\sigma}{\beta}\int_0^{w(0)}\frac{\ln(1-w)}{1-w}\,dw}_{I_1} - \underbrace{\frac{1}{\beta}\int_0^{w(0)}\frac{\ln w}{1-w}\,dw}_{I_2} + \underbrace{\int_0^{w(0)}\frac{\mu}{1-w}\,dw}_{I_3}\right) \tag{4.53}$$

which have been conveniently split up in the three separate integrals I_1, I_2, and I_3. The three integrals are found as follows. First, we have I_1 which is solved as

$$\begin{aligned} I_1 &= \frac{\sigma}{\beta}\int_0^{w(0)}\frac{\ln(1-w)}{1-w}\,dw \\ &= -\frac{1}{2}\frac{\sigma}{\beta}\left[\ln(1-w(0))\right]^2 \end{aligned} \tag{4.54}$$

where we have used the substitution $u = \ln(1-w)$ and $du = -1/(1-w)\,dw$, together with $u = 0$ for $w = 0$ and $u = \ln(1-w(0))$ for $w = w(0)$ as limits of integration. To further simplify this, we rewrite eq. (4.50) as

$$\ln(1-w(0)) = -\frac{\rho\beta}{\Delta} \tag{4.55}$$

and so we have

$$\begin{aligned} I_1 &= -\frac{1}{2}\frac{\sigma}{\beta}\left(-\frac{\rho\beta}{\Delta}\right)^2 \\ &= -\frac{1}{2}\frac{\sigma\rho^2\beta}{\Delta^2}. \end{aligned} \tag{4.56}$$

Postponing I_2 for a moment, we determine I_3 through

$$\begin{aligned} I_3 &= \mu\int_0^{w(0)}\frac{1}{1-w}\,dw \\ &= -\mu\ln\left(e^{-\rho\beta/\Delta}\right) \\ &= \mu\frac{\rho\beta}{\Delta}. \end{aligned} \tag{4.57}$$

Once again, the functional equation comes in handy. Solved for μ, while $\epsilon_i = 0$ and inserting for $w(0) = 1 - e^{-\frac{\beta\rho}{\Delta}}$, eq. (4.40) reads

$$\begin{aligned} \mu &= -\frac{1}{\beta}\left[\sigma \ln\left(1 - w\left(0\right)\right) - \ln w\left(0\right)\right] \\ &= \frac{\sigma\rho}{\Delta} + \frac{1}{\beta}\ln\left(1 - e^{-\rho\beta/\Delta}\right) \end{aligned} \tag{4.58}$$

Inserting for μ in eq. (4.57), we find that

$$I_3 = \frac{\sigma\rho^2\beta}{\Delta^2} + \frac{\rho}{\Delta}\ln\left(1 - e^{-\rho\beta/\Delta}\right) \tag{4.59}$$

Finally, we solve the slightly more cumbersome I_2 integral as follows. We have

$$I_2 = \frac{1}{\beta}\int_0^{w(0)} \frac{\ln w}{1-w}\, dw \tag{4.60}$$

If we, by using integration by parts, identify $u = \ln w$ so that $du = \frac{1}{w}\, dw$ and $dv = \frac{1}{1-w}\, dw$ so that $v = -\ln\left(1-w\right)$, we see that

$$\begin{aligned} I_2 &= \frac{1}{\beta}\int_0^{w(0)} \frac{\ln w}{1-w}\, dw \\ &= \frac{1}{\beta}\left(-\ln w \ln\left(1-w\right)\big|_0^{w(0)} + \int_0^{w(0)} \frac{\ln\left(1-w\right)}{w}\, dw\right) \\ &= \frac{1}{\beta}\left(-\ln w\left(0\right)\ln\left(1 - w\left(0\right)\right) + \int_0^{w(0)} \frac{\ln\left(1-w\right)}{w}\, dw\right) \end{aligned} \tag{4.61}$$

where we have used that

$$\begin{aligned} \lim_{x\to 0^+} \frac{\ln\left(1-x\right)}{1/\ln x} &\overset{d/dx}{=} \lim_{x\to 0^+} \frac{-\frac{1}{1-x}}{-\frac{1}{x}/\left(\ln x\right)^2} \\ &\overset{d/dx}{=} \lim_{x\to 0^+} \frac{2\left(\ln x\right)\frac{1}{x}}{-1/x^2} \\ &\overset{d/dx}{=} 2\lim_{x\to 0^+} \frac{1/x}{1/x^2} \\ &= 2\lim_{x\to 0^+} x \\ &= 0. \end{aligned} \tag{4.62}$$

This means that the term $\ln w \ln\left(1-w\right)$ where $w \to 0$ in eq. (4.61) may be dropped.

As suggested in [18], we are going to make the substitution

$$w = 1 - e^{-\rho'\beta/\Delta} \tag{4.63}$$

which implies that

$$dw = \frac{\beta}{\Delta} e^{-\rho'\beta/\Delta}\, d\rho'. \tag{4.64}$$

The lower limit of integration is found through $0 = 1 - e^{-\rho'\beta/\Delta}$ such that $-\rho'\frac{\beta}{\Delta} = 0$. Because β and Δ are non-zero constants it follows that $\rho' = 0$. The upper limit of integration is determined by $w(0) = 1 - e^{-\rho'\beta/\Delta}$ or $1 - e^{-\rho\beta/\Delta} = 1 - e^{-\rho'\beta/\Delta}$. In other words, this implies $\rho' = \rho$. Inserting for $w = 1 - e^{-\rho'\beta/\Delta}$ we find that

$$\begin{aligned} I_2 &= \frac{1}{\beta}\left(-\ln w(0)\ln(1-w(0)) + \int_0^{w(0)} \frac{\ln(1-w)}{w}\, dw\right) \\ &= \frac{1}{\beta}\left(-\ln\left(1-e^{-\rho\beta/\Delta}\right)\ln\left(e^{-\rho\beta/\Delta}\right) + \right. \\ &\quad \left. \frac{\beta}{\Delta}\int_0^{\rho} \frac{\ln\left(1-\left(1-e^{-\rho'\beta/\Delta}\right)\right)}{1-e^{-\rho'\beta/\Delta}} e^{-\rho'\beta/\Delta}\, d\rho'\right) \\ &= \frac{1}{\Delta}\left(\rho\ln\left(1-e^{-\rho\beta/\Delta}\right) - \frac{\beta}{\Delta}\int_0^{\rho}\frac{\rho'}{e^{\rho'\beta/\Delta}-1}\, d\rho'\right). \end{aligned} \tag{4.65}$$

Inserting I_1, I_2, and I_3 back into eq. (4.53), we find that

$$\begin{aligned} P &= \frac{\Delta}{\beta}\left(\underbrace{\frac{\sigma}{\beta}\int_0^{w(0)}\frac{\ln(1-w)}{1-w}\, dw}_{I_1} - \underbrace{\frac{1}{\beta}\int_0^{w(0)}\frac{\ln w}{1-w}\, dw}_{I_2} + \underbrace{\int_0^{w(0)}\frac{\mu}{1-w}\, dw}_{I_3}\right) \\ &= \frac{\Delta}{\beta}\left(\frac{\sigma\rho^2\beta}{\Delta^2} - \frac{1}{2}\frac{\sigma\rho^2\beta}{\Delta^2} + \frac{\rho}{\Delta}\ln\left(1-e^{-\rho\beta/\Delta}\right)\right. \\ &\quad \left. -\frac{\rho}{\Delta}\ln\left(1-e^{-\rho\beta/\Delta}\right) + \frac{\beta}{\Delta^2}\int_0^{\rho}\frac{\rho'}{e^{\rho'\beta/\Delta}-1}\, d\rho'\right) \\ &= \frac{1}{2}\frac{\sigma\rho^2}{\Delta} + \frac{1}{\Delta}\int_0^{\rho}\frac{\rho'}{e^{\rho'\beta/\Delta}-1}\, d\rho' \end{aligned} \tag{4.66}$$

So what about the remaining integral? What was originally an integral over all possible energies has now been reduced to an integral over density ρ' with a cut-off $\rho' = \rho$. Recall from section (3.4) how we used the generating function of the Bernoulli numbers

$$\frac{x}{e^x - 1} = \sum_{n=0}^{\infty} B_n \frac{x^n}{n!} \tag{4.67}$$

to evaluate integrals on the form

$$\int \tfrac{x}{e^x-1}\, dx. \tag{4.68}$$

The same technique applies here. The remaining integral is found to be

$$\begin{aligned}\frac{1}{\Delta}\int_0^{\rho}\frac{\rho'}{e^{\rho'\beta/\Delta}-1}\,d\rho' &= \frac{\Delta}{\beta^2}\int_0^{\rho\beta/\Delta}\frac{x}{e^x-1}\,dx \\ &= \frac{\Delta}{\beta^2}\int_0^{\rho\beta/\Delta}\sum_{n=0}^{\infty}B_n\frac{x^n}{n!}\,dx \end{aligned} \tag{4.69}$$

where we have used $x = \rho'\beta/\Delta$ and $dx = \beta/\Delta\, d\rho'$. This is easily evaluated as

$$\frac{\Delta}{\beta^2}\sum_{n=0}^{\infty}\frac{B_n}{n!}\int_0^{\rho\beta/\Delta}x^n\,dx = \frac{\Delta}{\beta^2}\sum_{n=0}^{\infty}\frac{B_n}{(n+1)!}\left(\frac{\rho\beta}{\Delta}\right)^{n+1} \tag{4.70}$$

or in other words

$$P = \frac{1}{2}\frac{\sigma\rho^2}{\Delta}+\frac{\Delta}{\beta^2}\sum_{n=0}^{\infty}\frac{B_n}{(n+1)!}\left(\frac{\rho\beta}{\Delta}\right)^{n+1}. \tag{4.71}$$

So much for the pressure. We know that in order to find the equation of state (which has been our objective all along), we need an expression containing three independent thermodynamic variables. Just as in section 3.4, we wish to express the equation of state through its virial expansion

$$\frac{PV}{Nk_BT} = \sum_{l=1}^{\infty}\left(\rho\lambda^2\right)^{l-1}a_l \tag{4.72}$$

where a_l (once more) are the virial coefficients. We have already found the pressure in eq. (4.71). The density may be written as

$$\frac{V}{Nk_BT} = \frac{\beta}{\rho}. \tag{4.73}$$

Thus, we see that by multiplying them together, we get

$$\begin{aligned}\frac{PV}{Nk_BT} &= \frac{\beta}{\rho}\left(\frac{1}{2}\frac{\sigma\rho^2}{\Delta}+\frac{\Delta}{\beta^2}\sum_{n=0}^{\infty}\frac{B_n}{(n+1)!}\left(\frac{\rho\beta}{\Delta}\right)^{n+1}\right) \\ &= B_0+B_1\frac{1}{2}\frac{\rho\beta}{\Delta}+\frac{1}{2}\frac{\sigma\rho\beta}{\Delta}+\sum_{n=2}^{\infty}\frac{B_n}{(n+1)!}\left(\frac{\rho\beta}{\Delta}\right)^{n}\end{aligned} \tag{4.74}$$

In the last step, we canceled a factor $\frac{\rho\beta}{\Delta}$ from the sum against the factor $\frac{\Delta}{\rho\beta}$ outside the sum, thus decreasing the power-term from $\left(\frac{\rho\beta}{\Delta}\right)^{n+1}$ to $\left(\frac{\rho\beta}{\Delta}\right)^{n}$. Furthermore, we pulled out the two first term of the sum and expressed them explicitly.

The first Bernoulli numbers are known to be $B_0 = 1$, $B_1 = -\frac{1}{2}$, $B_2 = \frac{1}{6}$, $B_4 = -\frac{1}{30}$, $B_6 = \frac{1}{42}$ and so forth. This is in agreement with the findings in [14]. The notation may be even further simplified. Due to the fact that every odd Bernoulli number greater than two is zero, the sum in the above result may be expressed as starting from $n = 1$, while neglecting every odd term. By inserting for B_0 and B_1, collecting terms, and re-writing the sum over n we end up with the final result

$$\frac{PV}{Nk_BT} = 1 + \frac{1}{4}\lambda^2(2\sigma - 1) + \sum_{n=1}^{\infty} \frac{B_{2n}}{(2n+1)!} \left(\rho\lambda^2\right)^{2n}. \qquad (4.75)$$

where we have combined $\Delta = m/2\pi\hbar^2$ with β to find $\lambda^2 \equiv \left(2\pi\hbar^2\right)/\left(mk_BT\right) = \beta/\Delta$. This is the virial expansion of the non-relativistic, two-dimensional FES gas.

4.4.3 Comments

The result eq. (4.75) is easily interpreted in terms of σ. The only σ-dependence in this expansion resides in the second virial coefficient. Should we expect this? We certainly expect the virial expansion to reproduce the known results for a Bose-Einstein and Fermi-Dirac gas. Indeed it does - setting $\sigma = 0$ gives the second virial coefficient to be $a_2 = -1/4$, setting $\sigma = 1$ gives $a_2 = +1/4$. The virial expansion found in section 3.4 was

$$\frac{PV}{Nk_BT} = 1 + \frac{1}{4}a\rho\lambda^2 + \sum_{n=1}^{\infty} \frac{B_{2n}}{(2n+1)!} \left(\rho\lambda^2\right)^{2n} \qquad (4.76)$$

where $a = -1$ reflects bosonic and $a = +1$ the fermionic case. The point is this. In this case too, the entire difference between the two particle species is found in the second virial coefficient. There could of course have been a σ-dependence in the higher order coefficients. It would, however, have to be of the form $f(\sigma)$ so that $f(\sigma = 0) = 1$ and $f(\sigma = 1) = 1$ for all higher order virial coefficients (because we expect the FES gas to reproduce the known endpoints in the virial expansion as well as any other regards). Thus, the fact that there is no σ-dependence in higher order terms is perhaps not *that* surprising after all.

Chapter 5

The Anyon Gas

Introduction

The solution to the two-anyon problem has been known from the beginning of the field of fractional statistics [24]. Still, the full three-anyon problem remains unresolved, not to mention higher-anyon problems. So is this the last word regarding many-anyon physics? Not at all. Most real physical systems are (far) removed from the idealized systems treated in elementary text books. Usually the numbers of particles in the system, or the complexity of the interaction (as in the anyon case), demand a statistical treatment. With such a perspective in mind, we realize that a quantum statistical approach to anyons may be quite fruitful - and even a goal in itself. This is the focus of the current section.

5.1 Interacting Systems and Cluster Expansions

Intuitively, we think of the anyon problem in terms of a non-interacting system. However, by recalling how an ideal anyon gas may be considered an interacting Bose (or Fermi) gas, we find it natural to review the standard approach to interacting quantum gases. After all, the Bose and Fermi gases have been known since the conception of quantum mechanics, and their interacting variants have been studied extensively.

Not surprisingly, these systems are inherently much harder to solve than their non-interacting counterparts. The reason for this is that the statistical mechanics of ideal quantum gases fundamentally relies on the solution of ideal quantum systems. These are in turn solved by separation of variables. For interacting quantum systems, the wave function does not (generally) separate this easily.

This is where the method of cluster expansions enters. In this method, the grand partition functions are written as a series expansion, with the leading terms giving the ideal system and higher order terms accounting for the interactions. The method is especially suited for dilute systems.

Formally, it is only valid in the infinite volume limit, a subtlety which will be addressed in due course. See e.g. [28] for a detailed treatment.

Much research has been devoted to the virial expansion of an anyon gas. The second virial coefficient, as we will demonstrate, is quite easily found. Historically, it was first found in [3], although we will use a different method [5]. It is worth pointing out that we will follow an even more recent variant of this regularization, as exposed in [18, 25]. The cluster expansion share some mathematical features with the virial expansion. We will start out by establishing their connection, and in the continuation of that discussion determine the second virial coefficient of an ideal anyon gas. Finally, some results relating to the third virial coefficient will be explored.

5.1.1 The Virial Expansion and the Cluster Integrals

The grand canonical partition function can be expressed using the so-called cluster integrals b_l as

$$\frac{1}{V}\ln\Xi = \sum_{l=1}^{\infty} b_l z^l \tag{5.1}$$

where $z = e^{\beta\mu}$ is the fugacity. As previously mentioned, this is only really valid in the $V \to \infty$ limit. In the following, we will write $A = V$ for the two-dimensional volume (i.e. area) of the system. It is worth pointing out that this expression does not coincide with the usual way of defining the cluster integrals b_l. The expansion of the grand canonical partition function, as found in [28] amongst others, is usually written

$$\frac{1}{V}\ln\Xi = \frac{1}{\lambda^3}\sum_{l=1}^{\infty} b_l z^l \tag{5.2}$$

or correspondingly

$$\frac{1}{A}\ln\Xi = \frac{1}{\lambda^2}\sum_{l=1}^{\infty} b_l z^l \tag{5.3}$$

for a two-dimensional system. Through these expressions, the cluster integrals b_l are defined to be dimension-less. In order for this definition of b_l to make sense (and conform with established literature), we have to absorb a factor of $1/\lambda^2$ in every cluster integral b_l. The $l = 1$ coefficient is usually defined so that it evaluates to $b_l = 1$. Thus, with our modified definition, we establish that

$$b_1 \equiv \frac{1}{\lambda^2}. \tag{5.4}$$

The reason we choose this slightly unorthodox definition is to comply with two prominent sources on anyon theory [25, 18].

Recall, that the equation of state may be expanded by the virial expansion (see eq. (3.74)) as

$$\frac{PA}{Nk_BT} = \sum_{i=1}^{\infty} \left(\rho\lambda^2\right)^{i-1} a_i. \tag{5.5}$$

Using (eq. (3.78) and eq. (3.79))

$$\frac{PA}{k_BT} = \ln \Xi\left(z, A, T\right) \quad \text{and} \quad N = z\frac{\partial \ln \Xi\left(z, A, t\right)}{\partial z} \tag{5.6}$$

in combination with eq. (5.1), it follows that

$$\frac{P}{k_BT} = \sum_{l=1}^{\infty} b_l z^l \tag{5.7}$$

and

$$\rho = \sum_{l=1}^{\infty} l b_l z^l. \tag{5.8}$$

Rewriting the virial expansion and inserting for the pressure and density in terms of cluster integrals, we get

$$\sum_{l=1}^{\infty} b_l z^l = \sum_{l=1}^{\infty} l b_l z^l \left(\sum_{i=1}^{\infty} \left(\lambda^2\right)^{i-1} \left(\sum_{l=1}^{\infty} l b_l z^l \right)^{i-1} a_i \right). \tag{5.9}$$

By expanding both sides and equating coefficients, we find that

$$b_2 = 2b_2 + a_2\lambda^2 b_1^2, \qquad b_3 = 3b_3 + 4a_2\lambda^2 b_1 b_2 + a_3\lambda^4 b_1^3, \quad \cdots. \tag{5.10}$$

Solving these relations for a_i, we find the two first virial coefficients in terms of b_l to be

$$a_2\lambda^2 = -\frac{b_2}{b_1^2} \tag{5.11}$$

and

$$a_3\lambda^4 = 4a_2^2\lambda^2 - \frac{2b_3}{b_1^3}. \tag{5.12}$$

At this point, the reader might recall how we encountered the fugacity expansion of the grand canonical partition function in section (3.3.2). We will now use the similar results

$$\Xi = \sum_{n=0}^{\infty} z^n Z_N \tag{5.13}$$

and

$$\ln(1+x) = \sum_{k=1}^{\infty} \frac{(-1)^{k+1}}{k} x^k. \tag{5.14}$$

Combining these expressions, it follows that

$$\ln \Xi \tag{5.15}$$

$$= \ln\left(\sum_{n=0}^{\infty} z^n Z_N\right)$$

$$= \left(\sum_{n=1}^{\infty} z^n Z_N\right) - \frac{1}{2}\left(\sum_{n=1}^{\infty} z^n Z_N\right)^2 + \frac{1}{3}\left(\sum_{n=1}^{\infty} z^n Z_N\right)^3 - \cdots \tag{5.16}$$

which in turn begs to be related to

$$\frac{1}{A}\ln \Xi = \sum_{l=1}^{\infty} b_l z^l. \tag{5.17}$$

Equating eq. (5.16) with eq. (5.17), we see that

$$A\sum_{l=1}^{\infty} b_l z^l \tag{5.18}$$

$$= \left(\sum_{n=1}^{\infty} z^n Z_N\right) - \frac{1}{2}\left(\sum_{n=1}^{\infty} z^n Z_N\right)^2 + \frac{1}{3}\left(\sum_{n=1}^{\infty} z^n Z_N\right)^3 - \cdots . \tag{5.19}$$

By equating coefficients it follows that

$$b_1 = \frac{Z_1}{A} \tag{5.20}$$

$$b_2 = \frac{2Z_2 - Z_1^2}{2A} \tag{5.21}$$

$$b_3 = \frac{3Z_3 - 3Z_1 Z_2 + Z_1^3}{3A}. \tag{5.22}$$

It is now trivial to relate the virial coefficients to the partition functions. We find that

$$a_2\lambda^2 = -\frac{A\left(2Z_2 - Z_1^2\right)}{2Z_1^2} \tag{5.23}$$

and

$$a_3\lambda^4 = 4a_2^2\lambda^2 - 2\left(\frac{A}{Z_1}\right)^3\left(\frac{3Z_3 - 3Z_1Z_2 + Z_1^3}{3A}\right). \tag{5.24}$$

This concludes the relations between the cluster integrals and the virial coefficients. We are now ready to calculate the second virial coefficient using the partition functions Z_1 and Z_2.

5.2 The Virial Coefficients

5.2.1 Second Virial Coefficient by Harmonic Regulator

It is clear that there is a profound difference in the physics of an ideal boson (or fermion) gas and an ideal anyon gas. Only the two-anyon problem has been solved so far, and any solution of the three-anyon problem is expected to be highly non-trivial. However, since the two-anyon problem *has* been solved, we know that we should in principle be able to work out the two-anyon partition function. From this, the second virial coefficient will follow[1]. One problem we are immediatly exposed to is the fact that the N-body partition function Z_N of a system of free particles is divergent. This follows from the fact that the energy degeneracies are infinite, and that the partition function is given as

$$Z = \sum_i g_i e^{-\beta E_i} \tag{5.25}$$

where g_i is the degeneracy of the ith energy level. To resolve this, we will have to break this infinite degeneracy somehow.

We will break this degeneracy by using a so-called harmonic oscillator regulator. What this means is that we take the free system and confine it to a harmonic oscillator potential. In the end, when the desired relations are established, we will release the system from the regulator. Hopefully, at that point, we will have a sensible answer to our question, i.e. a non-divergent form of the second virial coefficient. The motivation for using a harmonic regulator is more easily appreciated once we have determined the single-particle partition function of such a regulated system.

The two-dimensional harmonic oscillator for a single particle has the energy

$$E = (n+1)\,\hbar\omega \tag{5.26}$$

where $n = n_x + n_y$ with $n = 0, 1, 2, \ldots$. Since $n_x = 0, 1, 2, \ldots$ and $n_y = 0, 1, 2, \ldots$, the degeneracy of such a system is $g_n = n + 1$. This follows from the fact that there is no degeneracy on the quantum numbers n_x and n_y. From this, we see that

$$Z_1 = \sum_{n=0}^{\infty} (n+1)\, e^{-\beta(n+1)\hbar\omega}. \tag{5.27}$$

To evaluate this, we used

$$(n+1)\, e^{-\beta(n+1)\hbar\omega} = \frac{\partial}{\partial x} e^{x(n+1)} \tag{5.28}$$

[1] This statement is expressed in hindsight. It is not given that the partition functions will yield a non-divergent result upon calculation.

where $x = -\beta\hbar\omega$. It follows that

$$\begin{aligned} Z_1 &= \frac{\partial}{\partial x} e^x \sum_{n=0}^{\infty} e^{xn} \\ &= \frac{\partial}{\partial x}\left[e^x \frac{1}{1-e^x}\right] \\ &= \frac{1}{2\left[\left(\frac{e^x+e^{-x}}{2}\right)-1\right]} \end{aligned} \tag{5.29}$$

It can be shown by elementary algebra that this is equivalent to $4\sinh^2\left(\frac{x}{2}\right)$ using $\cosh x = \frac{e^x+e^{-x}}{2}$ and $\cosh(x) - 1 = 2\sinh^2\left(\frac{x}{2}\right)$. In other words, we have

$$Z_1 = \frac{1}{4\sinh^2\left(\frac{\beta\hbar\omega}{2}\right)}. \tag{5.30}$$

Note that this partition function is valid for all particle species, as statistical effects will only emerge once we have a system consisting of two or more particles.

Now, let's have closer look at eq. (5.4) and eq. (5.20). By equating these, we realize that

$$\frac{1}{\lambda^2} = \frac{Z_1}{A}. \tag{5.31}$$

Inserting for Z_1 it follows that

$$\frac{mk_BT}{2\pi\hbar^2} = \frac{1}{A}\frac{1}{4\sinh^2\left(\frac{\beta\hbar\omega}{2}\right)}. \tag{5.32}$$

In the high-temperature limit, i.e. $\beta \to 0$, $\sinh x$ goes approximately as $\sinh x \approx x$, which in turn reveals that

$$\omega^2 \sim \frac{1}{A}\frac{2\pi}{m\beta}. \tag{5.33}$$

In other words, the frequency of the harmonic oscillator squared ω^2 is the proportional inverse of the area A. In physical terms, we can intuitively understand this as follows. Imposing a harmonic oscillator potential is effectively the same as confining a particle to a finite region of space. When the potential is turned off, we are at the same time releasing the particle to move in the entire plane. This is the motivation for using a harmonic oscillator.

We found in the previous section that the second virial coefficient is related to the single- and two-anyon partition function as

$$a_2\lambda^2 = \frac{A\left(Z_1^2 - 2Z_2\right)}{2Z_1^2}. \tag{5.34}$$

Recall how the cluster integrals are only truly valid in the infinite area limit. Thus, in terms of ω, we get

$$\begin{aligned} a_2(\alpha) &= \lim_{A\to\infty} \frac{A}{2}\frac{1}{\lambda^2}\left(1-\frac{2Z_2}{Z_1^2}\right) && (5.35)\\ &= \frac{1}{2}\lim_{\omega\to 0}\left(Z_1-\frac{2Z_2}{Z_1}\right) && (5.36)\end{aligned}$$

where have used eq. (5.33) to rewrite the limit from $A\to\infty$ to $\omega\to 0$. Note that

$$\begin{aligned} b_2 &= \frac{2Z_2-Z_1^2}{2A}\\ &= \frac{\lambda^2}{2}\left(\frac{2Z_2-Z_1^2}{Z_1}\right)\\ &= -\frac{\lambda^2}{2}\left(Z_1-\frac{2Z_2}{Z_1}\right) && (5.37)\end{aligned}$$

so that $a_2(\alpha)$ is now proportional to b_2, i.e.

$$a_2(\alpha) = -\lim_{\omega\to 0}\frac{1}{\lambda^2}b_2.$$

At this point, we touch upon a delicate point. The way it is written, the second virial coefficient won't evaluate to the correct result when the limit is calculated. The reason for this is that for two particles, the harmonic potential is

$$\begin{aligned} \omega^2\left(\mathbf{r}_1^2+\mathbf{r}_2^2\right) &= \omega^2\left(\frac{1}{2}(\mathbf{r}_1+\mathbf{r}_2)^2+\frac{1}{2}(\mathbf{r}_1-\mathbf{r}_2)^2\right)\\ &= 2\omega^2\mathbf{R}^2+\frac{1}{2}\omega^2\mathbf{r}^2 && (5.38)\end{aligned}$$

where the relative coordinate is given by $\mathbf{r}=\mathbf{r}_1-\mathbf{r}_2$ and $\mathbf{R}=\frac{1}{2}(\mathbf{r}_1+\mathbf{r}_2)$ is the COM coordinate. As such, we identify $\omega_{\text{COM}}^2=2\omega^2$ and $\omega_{\text{rel}}^2=\frac{1}{2}\omega^2$, and in general (for the l-particle system) we have $\omega_{\text{COM}}^2=l\omega^2$. Now, it is the COM that determines the relationship between ω and A, and so we have to multiply the lth cluster integral b_l by l. In effect, this increase our expression for the second virial coefficient by a constant factor of 2, and hence we have

$$a_2(\alpha) = \lim_{\omega\to 0}\left(Z_1-\frac{2Z_2}{Z_1}\right). \quad (5.39)$$

In order to calculate this limit, we need to know an explicit expression of Z_2.

To determine Z_2, we take the interesting part of the free two-anyon system and subject it to a harmonic oscillator potential - the interesting

part being the relative two-anyon motion. Given the resulting energy spectrum with accompanying finite degeneracies, finding the partition function is pretty straightforward. Upon evaluation of the relevant limit we will encounter a divergency. This is luckily easy to dispose of, and in fact we will find that the ω-dependence disappears before we take the $\omega \to 0$ limit.

Our system can be split into a COM and relative degree of freedom. In other words, we may express the two particle partition function as

$$\begin{aligned} Z_2 &= Z_2^{\mathrm{com}} Z_2^{\mathrm{rel}} && (5.40) \\ &= Z_1 Z_2^{\mathrm{rel}}. && (5.41) \end{aligned}$$

The reason we have $Z_2^{\mathrm{com}} = Z_1$ is that the COM behaves as if it is a single particle. In the harmonic oscillator potential, the two-anyon energy spectrum is given by

$$E_n(\alpha, \omega) = (2n + 1 + \alpha)\hbar\omega \quad (5.42)$$

with degeneracy $n + 1$ or

$$E_n(\alpha, \omega) = (2n + 1 - \alpha)\hbar\omega \quad (5.43)$$

with degeneracy n, corresponding to negative and positive angular momentum respectively. The principal quantum number is given by $n = 0, 1, 2, \ldots$. For a detailed calculation, see [18]. Using this, we get

$$Z_2^{\mathrm{rel}}(\alpha, \omega) = \sum_{n=0}^{\infty} \left[(n+1)\, e^{-\beta(2n+1+\alpha)\hbar\omega} + n e^{-\beta(2n+1-\alpha)\hbar\omega} \right] \quad (5.44)$$

or

$$Z_2^{\mathrm{rel}}(\alpha, \omega) = \frac{\cosh\left([1-\alpha]\,\hbar\beta\omega\right)}{2\sinh^2\left(\hbar\beta\omega\right)}. \quad (5.45)$$

However, in order to utilize these results, we need to make a slight modification of eq. (5.39). We have effectively split the $a_2(\alpha)$ into two parts - one term due to the ideal Bose gas, and a second part due to the interaction. Thus, from

$$a_2(\alpha) = a_2(0) - \lim_{A\to\infty} \frac{A}{\lambda^2 Z_1^2} \left[Z_2(\alpha) - Z_2(0) \right] \quad (5.46)$$

it follows that

$$a_2(\alpha) = -\frac{1}{4} - 2 \lim_{\omega\to 0} \left[\frac{Z_2(\alpha, \omega) - Z_2(0, \omega)}{Z_1} \right] \quad (5.47)$$

By using the above result, we find that

$$\begin{aligned} a_2(\alpha) &= -\frac{1}{4} - 2\lim_{\omega\to 0}\left[Z_2^{\mathrm{rel}}(\alpha,\omega) - Z_2^{\mathrm{rel}}(0,\omega)\right] \\ &= -\frac{1}{4} - 2\lim_{\omega\to 0}\left[\frac{\cosh\left([1-\alpha]\,\hbar\beta\omega\right)}{2\sinh^2(\hbar\beta\omega)} - \frac{\cosh(\hbar\beta\omega)}{2\sinh^2(\hbar\beta\omega)}\right]. \end{aligned} \tag{5.48}$$

A direct evaluation of this limit yields two divergent terms. To work around this problem, we use the definitions of the hyperbolic functions. This gives

$$a_2(\alpha) \tag{5.49}$$

$$= -\frac{1}{4} - 2\lim_{\omega\to 0}\left[\frac{e^{(1-\alpha)\hbar\beta\omega} + e^{-(1-\alpha)\hbar\beta\omega}}{e^{2\hbar\beta\omega} + e^{-2\hbar\beta\omega} - 2} - \frac{e^{\hbar\beta\omega} + e^{-\hbar\beta\omega}}{e^{2\hbar\beta\omega} + e^{-2\hbar\beta\omega} - 2}\right] \tag{5.50}$$

Inserting the series expansion of the exponential function to the second order $e^x \approx 1 + x + \frac{1}{2}x^2 + \mathcal{O}\left(x^3\right)$, we get that

$$\begin{aligned} a_2(\alpha) &= -\frac{1}{4} - 2\lim_{\omega\to 0}\left[\frac{\left((1-\alpha)\,\hbar\beta\omega\right)^2}{(2\hbar\beta\omega)^2} - \frac{(\hbar\beta\omega)^2}{(2\hbar\beta\omega)^2}\right] \\ &= -\frac{1}{4} - 2\left[(1-\alpha)^2 - 1\right]\lim_{\omega\to 0}\left[\frac{(\hbar\beta\omega)^2}{4\left(\hbar\beta\omega\right)^2}\right] \\ &= -\frac{1}{4}\left(1 - 4\alpha + 2\alpha^2\right) \end{aligned} \tag{5.51}$$

or summarized, the second virial coefficient is found to be

$$a_2(\alpha) = -\frac{1}{4}\left(1 - 4\alpha + 2\alpha^2\right). \tag{5.52}$$

With $\alpha = 0$ for the bosonic end and $\alpha = 1$ for the fermionic end, this result is coinciding with the result from section 3.4. In particular, it was found that

$$\frac{PV}{Nk_BT} = 1 + \frac{1}{4}a\rho\lambda^2 + \sum_{n=1}^{\infty}\frac{a^{2n}\left(\rho\lambda^2\right)^{2n}}{(2n+1)!}B_{2n} \tag{5.53}$$

where the second virial coefficient is seen to be

$$a_2 = \frac{1}{4}a. \tag{5.54}$$

where $a = -1$ for the bosonic and $a = +1$ for the fermionic limits respectively.

5.2.2 The Linear N-Anyon Partition Function

We will now turn to a subset of the full N-anyon partition function which is important as a benchmark result, and which bears a particular relevance to the second virial coefficient. It can be shown that the N-anyon spectrum consists of levels which interpolate linear with α, and with levels that interpolate non-linear with α. It is the non-linear levels that are so difficult to determine. In fact, the linear part of the N-anyon problem has an energy spectrum that yields the partition function

$$Z_N^{\text{lin}}(\alpha) = \frac{\cosh\left[\frac{1}{2}N(N-1)(1-\alpha)\beta\hbar\omega\right]}{2^{2N-1}} \prod_{l=1}^{N} \frac{1}{\sinh^2\left(\frac{l\beta\hbar\omega}{2}\right)}. \quad (5.55)$$

as shown in e.g. [25]. The α-dependence enables us to interpolate between the bosonic ($\alpha = 0$) and fermionic ($\alpha = 1$) limits. Although this is generally not the entire N-anyon partition function, we have that in the $N = 2$ anyon case it *is* the entire partition function. In other words, we have

$$Z_2(\alpha) = \frac{\cosh\left[(1-\alpha)\beta\hbar\omega\right]}{8\sinh^2\left(\frac{\beta\hbar\omega}{2}\right)\sinh^2(\beta\hbar\omega)}. \quad (5.56)$$

The verification of this result is rather tedious - and essentially no new insight will be gained form its treatment. This is why we refer the interested reader to [25], and simply acknowledge that the results can be shown to coincide.

5.2.3 Third Virial Coefficient

Determining the third virial coefficient of the ideal anyon gas constitues to solving the three-anyon problem. Clearly, this is a very hard problem, and we will only deal with it in a highly cursory manner. It has been known for a while [18] that the energy spectrum of the three-anyon system consists of a set of levels which interpolate *linear* between the bosonic and fermionic limits, and a complimentary set which interpolate in a *non-linear* fashion between the known endpoints. For $N = 2$, the linear states account for the entire spectrum, and so eq. (5.55) captures the entire two-anyon partition function. In three or more particle systems, the linear partition function take into account only a part of the spectrum.

In particular, we find for $N = 3$ that

$$Z_3^{\text{linear}}(\alpha) = \frac{\cosh\left[3(1-\alpha)\beta\hbar\omega\right]}{32\sinh^2\left(\frac{\beta\hbar\omega}{2}\right)\sinh^2(\beta\hbar\omega)\sinh^2\left(\frac{3\beta\hbar\omega}{2}\right)} \quad (5.57)$$

which, as usual, interpolates between $\alpha = 0$ and $\alpha = 1$. At these endpoints, the *full* partition function is expected to coincide with part of the three-boson and three-fermion partition functions respectively. In fact, since the

interpolation is continuous (and the spectrum is expected to be continuous with α), we would be surprised if the difference between $Z_3^{\mathrm{b}} - Z_3^{\mathrm{lin}}(0)$ was different from $Z_3^{\mathrm{f}} - Z_3^{\mathrm{lin}}(1)$. In order to investigate this, we need an expression for Z_3^{b} and Z_3^{f}.

For the sake of brevity, we will simply echo the established results, and refer the interested reader to e.g. [25] for a more detailed calculation. It can be shown that

$$Z_3^{\mathrm{boson}} = \frac{\cosh(3\beta\hbar\omega) + 2\cosh^2\left(\frac{\beta\hbar\omega}{2}\right)}{32\sinh^2\left(\frac{\beta\hbar\omega}{2}\right)\sinh^2(\beta\hbar\omega)\sinh^2\left(\frac{3\beta\hbar\omega}{2}\right)} \tag{5.58}$$

to be the three-boson partition function. Similarly, the three-fermion partition function is found to be

$$Z_3^{\mathrm{fermion}} = \frac{1 + 2\cosh^2\left(\frac{\beta\hbar\omega}{2}\right)}{32\sinh^2\left(\frac{\beta\hbar\omega}{2}\right)\sinh^2(\beta\hbar\omega)\sinh^2\left(\frac{3\beta\hbar\omega}{2}\right)}. \tag{5.59}$$

As stated earlier, we wish to calculate the difference between these partition functions and the linear three anyon partition function.

We find, in particular, that

$$\begin{aligned} Z_3^{\mathrm{boson}} - Z_3^{\mathrm{linear}}(0) &= \frac{\cosh^2\left(\frac{\beta\hbar\omega}{2}\right)}{16\sinh^2\left(\frac{\beta\hbar\omega}{2}\right)\sinh^2(\beta\hbar\omega)\sinh^2\left(\frac{3\beta\hbar\omega}{2}\right)} \\ &= Z_3^{\mathrm{fermion}} - Z_3^{\mathrm{linear}}(1) \end{aligned} \tag{5.60}$$

which, as discussed above, is what we would expect. This difference must necessarily be equivalent to the endpoints of the non-linear part of the three-anyon partition function. To see this, let

$$Z_3(\alpha) = Z_3^{\mathrm{linear}}(\alpha) + Z_3^{\mathrm{non\text{-}linear}}(\alpha) \tag{5.61}$$

At $\alpha = 0$ we would expect $Z_3(0) = Z_3^{\mathrm{boson}}$, while at $\alpha = 1$ we would expect$Z_3(1) = Z_3^{\mathrm{fermion}}$. Now, if this is correct, it follows that

$$Z_3^{\mathrm{non\text{-}linear}}(0) = Z_3^{\mathrm{boson}} - Z_3^{\mathrm{linear}}(0) \tag{5.62}$$

and

$$Z_3^{\mathrm{non\text{-}linear}}(1) = Z_3^{\mathrm{fermion}} - Z_3^{\mathrm{linear}}(1). \tag{5.63}$$

So, if this is right, it follows that

$$\begin{aligned} Z_3^{\mathrm{non\text{-}linear}}(0) &= Z_3^{\mathrm{non\text{-}linear}}(1) \\ &= \frac{\cosh^2\left(\frac{\beta\hbar\omega}{2}\right)}{16\sinh^2\left(\frac{\beta\hbar\omega}{2}\right)\sinh^2(\beta\hbar\omega)\sinh^2\left(\frac{3\beta\hbar\omega}{2}\right)}. \end{aligned} \tag{5.64}$$

This is only a constant proportionallity factor. There will be a non-trivial α-dependence as well. This suggest that there might be some symmetry in the way $Z_3^{\text{non-linear}}(\alpha)$ interpolates between $0 \leq \alpha \leq 1$.

Finally, for the sake of completeness, we wish to make some concluding remarks. Without proving these, the following facts may guide further investigation of the third virial coefficient. It can be shown that contribution to $a_3(\alpha)$ from the linear states is divergent, however, the divergence is independent of α. From this, it can be shown that

$$a_3(\alpha) - a_3(\alpha') = 0 \tag{5.65}$$

that is - the divergences cancel in the difference. Even more importantly, it has been shown that

$$a_3(\alpha) = a_3(1-\alpha) \tag{5.66}$$

which implies that the third virial coefficient only has to be calculated for half of the interval $0 \leq \alpha \leq 1$, say $0 \leq \alpha \leq 1/2$. It is important, still, to note that this mirror symmetry does not hold for higher virial coefficients.

In addition to this, to the second order in α, the third virial coefficient $a_3(\alpha)$ is known to be

$$a_3(\alpha) = \frac{1}{36} + \frac{\alpha^2}{12} + \mathcal{O}(\alpha^3) \tag{5.67}$$

about the bosonic and fermionic limits[18]. What's more, it has been deduced using numerical calculations of the three-anyon spectrum, that the third virial coefficient is finite for all α. The result obtained in [26] even suggest that the third virial coefficient is given by

$$a_3(\alpha) = \frac{1}{36} + \frac{1}{12\pi^2}\sin^2(\pi\alpha) + c\sin^4(\pi\alpha) \tag{5.68}$$

where $c = -(1.652 \pm 0.012) \cdot 10^{-5}$. If this is true, the hope for an analytical result is reduced significantly.

As seen above, it seems that there is little hope for finding the third virial coefficient analytically. Is this a signal that the three-anyon problem will be even harder to solve than what was first expected? Not necessarily. The queer form of the suggested third virial coefficient may arise as an artifact of taking the limit of the expression

$$a_3(\alpha) = 4a_2^2(\alpha) - \lim_{x\to 0} x^2\left(3Z_3 - 3Z_2Z_1 + Z_1^3\right)$$

where we have used $x \equiv \beta\hbar\omega$, $\lambda^2/A = (\beta\hbar\omega)^2$ and $a_3\lambda^4 = 4a_2^2\lambda^4 - 2b_3/b_1^3$ with $b_1 = Z_1/A$ and $b_3 = \left(3Z_3 - 3Z_1Z_2 + Z_1^3\right)/3A$. Perhaps even more likely, there may be intractable problems finding a closed form expression for Z_3 even *if* an analytical expression for the non-linear three-anyon spectrum is known. From other areas of statistical mechanics it is not uncommon to face serious mathematical difficulties when one is to calculate partition functions.

	$\mathcal{O}(\alpha^0)$	$\mathcal{O}(\alpha^1)$	$\mathcal{O}(\alpha^2)$
a_2	$\mp\frac{1}{4}$	$\frac{1}{2}\pm\frac{1}{2}$	$-\frac{1}{2}$
a_3	$\frac{1}{36}$	0	$\frac{1}{12}$
a_4	0	0	$\frac{1}{16\sqrt{3}}\ln\frac{\sqrt{3}+1}{\sqrt{3}-1}\pm\frac{1}{16}$
a_5	$-\frac{1}{3600}$	0	$\frac{1}{36}\pm\left(\frac{1}{6\sqrt{6}}\ln\frac{3+\sqrt{6}}{3-\sqrt{6}}-\frac{1}{6\sqrt{3}}\ln\frac{\sqrt{3}+1}{\sqrt{3}-1}\right)$
a_6	0	0	$\pm\frac{5}{576}+\left(\frac{5}{864\sqrt{2}}\ln\frac{\sqrt{2}-1}{\sqrt{2}+1}+\frac{65}{288\sqrt{3}}\ln\frac{\sqrt{3}+1}{\sqrt{3}-1}\right.$ $\left.+\frac{8}{27\sqrt{5}}\ln\frac{\sqrt{5}+1}{\sqrt{5}-1}-\frac{25}{48\sqrt{6}}\ln\frac{3+\sqrt{6}}{3-\sqrt{6}}+\frac{9}{32\sqrt{10}}\ln\frac{4+\sqrt{10}}{4-\sqrt{10}}\right)$

Table 5.1: The exact results of $a_2(\alpha)$ to $a_6(\alpha)$ up to order α^2 around the bosonic and fermionic points. The results are plotted in ... The table shows the result in both the bosonic and fermionic basis. The upper sign is identified as the bosonic basis, while the lower sign is identified as the fermionic basis. From [18].

5.3 Higher Virial Coefficients and Discussion

For the sake of completeness, we will finally look at the higher virial coefficients. The results are merely echoed here - for detailed derivations see references in [18]. As was seen in the previous section, the three-anyon problem is still unresolved. In addition, we have seen how the free N-boson and free N-fermion systems are exactly solvable (had they not, we wouldn't be able to derive their partition functions). This follows from the fact that their wave functions are symmetric and anti symmetric products of the single-particle wave functions. So shouldn't the free three-anyon problem be solvable this way too? Unfortunately no - the three-anyon wave function is far more complex, and have not yet been found analytically.

Consequently, the N-anyon problem is even harder to solve. However, since it is known that the system should interpolate between the bosonic and fermionic limits, it is possible to exploit these known solutions and treat the anyonic contribution as perturbations around these endpoints. Using this approach, the contributions in orders α^0, α^1, and α^2 to the six lowest virial coefficients has been calculated, as shown in table 5.1. The table incorporate both the bosonic and fermionic ends, where the upper sign is associated with the bosonic and the lower sign is associated with the fermionic end. This table, although only correct around the bosonic and fermionic ends, reveals some important properties of the higher virial coefficients. The properties we will examine has been shown rigorously; the table only serve as an illustration in this respect. For references, see [18].

First of all, we would like to point out that the mirror symmetry, i.e.

$$a_3(\alpha) = a_3(1-\alpha), \tag{5.69}$$

is only valid for the third virial coefficient. This can be deduced from the

fact that only the third virial coefficient has identical endpoint contributions, that is,

$$a_3(\alpha) = \frac{1}{36} + \frac{1}{12}\alpha^2 \tag{5.70}$$

around the endpoints. This can be seen to coincide with the numerical result from section 5.2.3. There, we found that the contribution in $\mathcal{O}(\alpha^2)$ was $\sin^2(\pi\alpha)/(12\pi^2)$. Using the small angle formula, $\sin x \approx x$ for small x and that $\sin\pi = -1$, together with $\alpha \approx 0$ or $\alpha \approx 1$, we get

$$\frac{1}{12\pi^2}\sin^2(\pi\alpha) \approx \frac{1}{12}\alpha^2 \tag{5.71}$$

around the end points. Thus, the perturbed result confirm the numerical calculations (although, historically, it was the other way around). Note that all the other virial coefficients has different contributions around the respective ends, which consequently terminate any hope of similar symmetries.

In addition, we would like to turn our attention to the contribution in the order of α^1. As can be clearly seen from the table, the only virial coefficient with a contribution of order α^1 is the second virial coefficient. This, in turn, implies that there are no cusps about either the bosonic or fermionic ends in the higher virial coefficients. For the second virial coefficient, however, this is not the case. As a plot of the second virial coefficient reveals, see figure 5.1, there are cusps in the bosonic endpoints. This is due to the α^1 contribution $\frac{1}{2} \pm \frac{1}{2}$, and does not appear at higher coefficients.

The fourth virial coefficient has, just like the third, been calculated numerically. We are not prepared to go into the technical details, for these see the original paper [20]. It was found that the numerical simulation of the fourth virial coefficient, when fitted to the known perturbed results, could be expressed as

$$a_4(\alpha) \tag{5.72}$$

$$= \frac{\sin^2\pi\alpha}{16\pi^2}\left(\frac{1}{\sqrt{3}}\ln\left(\sqrt{3}+2\right) + \cos\pi\alpha\right) \tag{5.73}$$

$$+ (c_4 + d_4\cos\pi\alpha)\sin^4\pi\alpha + \cdots \tag{5.74}$$

where $c_4 = -0.0053 \pm 0.0003$ and $d_4 = -0.0048 \pm 0.0009$. We immediately notice that there are no contributions of the order α^0 or α^1, a result which is in agreement with the perturbed calculations. Furthermore, we see that for $\alpha \sim 0$ we have

$$\frac{\sin^2\pi\alpha}{16\pi^2}\left(\frac{1}{\sqrt{3}}\ln\left(\sqrt{3}+2\right) + \cos\pi\alpha\right)$$

$$\approx \frac{1}{16}\left(\frac{1}{\sqrt{3}}\ln\left(\frac{\sqrt{3}+1}{\sqrt{3}-1}\right) + 1\right)\alpha^2 \tag{5.75}$$

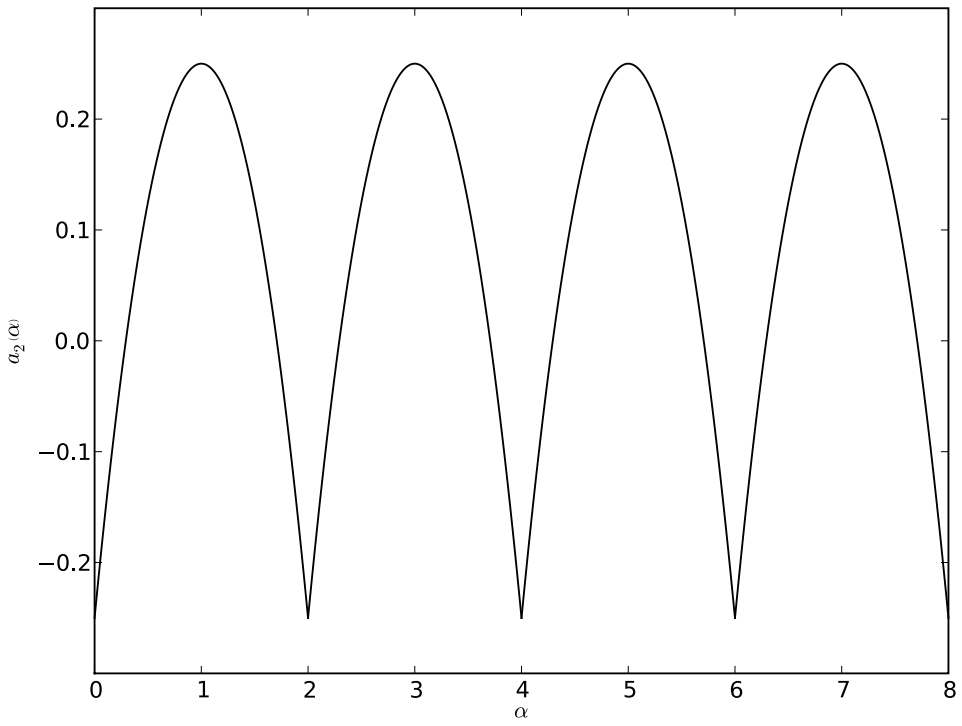

Figure 5.1: The second virial coefficient for an ideal anyon gas as a function of α. Bose-points are located at $0, 2, 4, \ldots$ and Fermi-points at $1, 3, 5, \ldots$. Clearly, there are cusps at the bosonic ends, yet no cusps in the fermionic ends.

and for $\alpha \sim 1$ we find

$$\begin{aligned} & \frac{\sin^2 \pi\alpha}{16\pi^2}\left(\frac{1}{\sqrt{3}}\ln\left(\sqrt{3}+2\right)+\cos\pi\alpha\right) \\ \approx\ & \frac{1}{16}\left(\frac{1}{\sqrt{3}}\ln\left(\frac{\sqrt{3}+1}{\sqrt{3}-1}\right)-1\right)\alpha^2 \end{aligned} \tag{5.76}$$

where we have used that $\ln\left(\sqrt{3}+2\right) = \ln\left(\frac{\sqrt{3}+1}{\sqrt{3}-1}\right)$. This is coincident[2] with the perturbed $\mathcal{O}\left(\alpha^2\right)$ contribution, which goes as

$$\tfrac{1}{16\sqrt{3}}\ln\tfrac{\sqrt{3}+1}{\sqrt{3}-1} \pm \tfrac{1}{16}. \tag{5.77}$$

We have no partitive result for comparison for the $\mathcal{O}\left(\alpha^4\right)$ contribution.

According to [18], using arguments from "regular" statistical mechanics, the virial expansion should not exist. However, it seems that the non-trivial braiding effects disqualifies theorems from regular statistical mechanics, and that the hope is that the virial expansion exists. In fact, in the above mentioned paper [20], it is stated that "We work out here a path integral representation for the cluster coefficients of anyons, which shows that they are finite.". We are not in a position to verify this assertion (or analyze it in depth) here, however, this further strengthens the beliefe of the existence of virial coefficients to arbitrary order. Anyhow, from the perturbation method referred to earlier, the existence is verified at least to order $\mathcal{O}\left(\alpha^2\right)$.

[2] This should hardly come as a surprise. The numerical calculations are, after all, *fitted* to the perturbed results.

Chapter 6

Conclusions

6.1 Recent Activities

Where does the three-anyon problem stand today? From a slow start in the earliest days of anyonic physics the field was blessed with increasing activity during the 80s. With the discovery of the fractional quantum Hall effect and the subsequent understanding of anyons being a vital ingredient in its description, some of the finest minds of condensed matter physicis have devoted much attention to anyons. Additional proposals that anyons could be used in theoretical models of high temperature superconductivity, further increased the interest of anyons in the community. All in all, the anyonic system was studied extensively in the eighties and early nineties. However, closer to the millennium, it seems that the interest for these weird creatures had declined. Specifically, it seems to have been made little progress in the three-anyon problem since the mid 90s.

About the same time (1997), Alexander Kitaev proposed that a certain kind of anyons could be used in quantum computing. One of the inherently hard challenges in order to build a quantum computer, is to protect the so-called qubits from a phenomena known as decoherence. Avoiding decoherence is critical to build a successful quantum computer. The scientific, economical, and military impact of the advent of quantum computing will be enormous. Obviously, we are not anywhere close to a situation where quantum computers are available to the public. But it is not unreasonable to compare the invention of quantum computers to other major technological advances - like the cellular phone or the laser.[1] This is mainly why there has been an increasing interest in anyons in recent years.

[1] It could be tempting to compare the invention of quantum computers with that of classical computers. However, the impact of classical computing has transformed our world to such an extent that it is hard to imagine quantum computing ever surpassing this. On the other hand, attempts of for-telling the future are usually quite futile, so all bets are off.

Detached from these quantum computational considerations, Johan Engquist seems to have made progress towards a solution of certain parts of the non-linear states of the three-anyon problem, see figure 6.1 for an illustration. The three-anyon problem is so hard to solve due to the non-trivial braiding effects. Still a work in progress, and without going too much into the details, he has found coordinates that simplify the problem. However, the simplifications comes at a price. As he says: "The problem is to find a set of differential equations that are as simple as possible, while keeping the permutations equally simple. It is a delicate balancing act."

The observation that certain non-linear interpolations may be constructed in a manner similar to the harmonic oscillator, simplifies the problem further. He has found an operator $\mathcal{O}$ which commutes with the angular momentum operator L.[2] For a given angular momentum, the ground state with minimal energy must be annihilated by this operator $\mathcal{O}$. The whole problem reduces to the Laplace equation, with anyonic boundary conditions[3]. Effectively, this is equivalent to solving a non-trivial Poisson equation. Luckily, not the entire equation has to be solved - it is sufficient to solve it for certain points. At the time of writing, the problem is to determine these points. If these are found, the rest of the problem follows. If this method turns out successful, the next natural step will be to examine other non-linear interpolations using the same scheme. At this point we can only speculate, but hopefully there are some kind of connection amongst the different classes of non-linear interpolations, and perhaps between the three-anyon and the general N-anyon problem.

6.2 Further Developments

If the current work on the three-anyon problem will turn out fruitful, there will certainly be a revival in the interest of solving the third virial coefficient. As mentioned above, in the most optimistic scenario this work will lead to new insight and possibly enable the systematic treatment of the N-anyon system. Yet, for this to occur, there are quite a number of events that has to take place. First of all, the lowest non-linear state has to be found. If this is found, one must establish a relation to other non-linear states. If this is impossible, we will find ourselves in need of solving an infinitude of similar non-linear classes of states. This will shatter our hope of finding a closed form for the entire three anyon spectrum using this method.

However, if we know a great deal about the lower part of the three-anyon spectrum, there might be some way to calculate the major contributions to

[2] The operator in question is the four-dimensional Laplacian Δ_ψ.

[3] Conditions which incorporates the permutations of the problem.

Figure 6.1: A qualitative picture of a certain class of the non-linear interpolations in the three-anyon problem. When interpolating from the bosonic end (at $\alpha = 0$) to the fermionic end (at $\alpha = 1$), it can be shown that the change in angular momentum is $\Delta L = 3$. The level spacing ΔE between consecutive levels in the class is constant. Thus, by determining the ground state, one can construct *any* state in this class by annihilation and creation operators. In the original paper, which is merely included for referential purposes, the statistical parameter θ is related to α as $\alpha = \theta/\pi$. From [32]. The class of non-linear interpolations considered by Engquist is represented by the lowest-lying non-linear state in this spectrum.

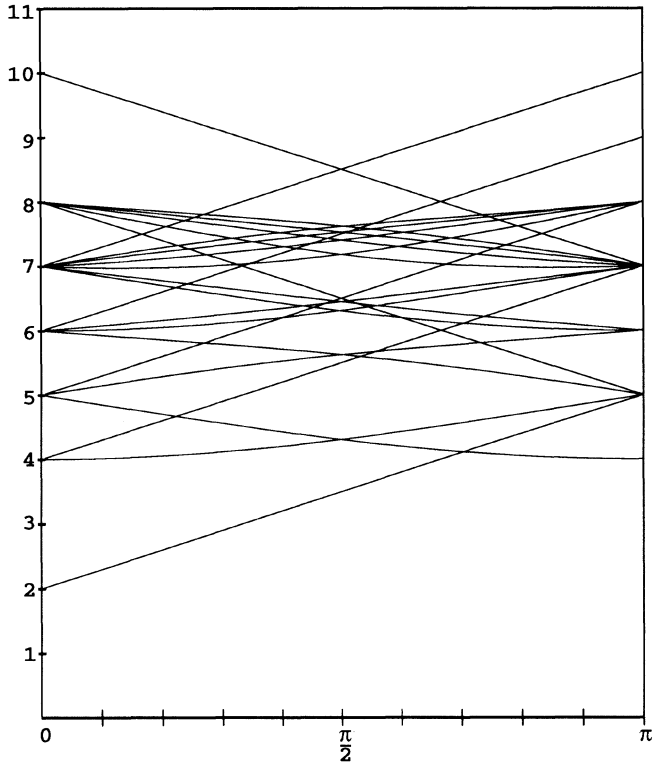

FIG. 1. The energy spectrum of three anyons interacting via harmonic forces vs the statistical flux θ. The energies are given in units of the harmonic frequency.

the third virial coefficient. After all, the partition function is defined as

$$Z = \sum_i g_i e^{-\beta E_i} \tag{6.1}$$

which reveals that higher energies contribute less to the entire partition function. With a reasonable cut-off, there might be some hope to establish the three-anyon partition function with great accuracy. If the degeneracy g_i can be determined on closed form, this might be feasible. On the other hand, there is an apparent problem due to the divergences of the linear partition function in the harmonic regulator (briefly mentioned in section 5.2.3). As was seen in the calculation of the second virial coefficient, it is through their difference that divergences cancel. This might be the case for the three-anyon partition function as well. Thus, it is not inconceivable that in order for the divergences to cancel, we will need the entire non-linear three-anyon partition function on closed form.

On a personal note, I have been captivated by the simple, yet subtle nature of the fractional exclusion statistics (FES). Simple, because it is a concept easily grasped, e.g. quite a lot easier than the more sophisticated anyons. Subtle, because it enables the possibility of interpolating between bosonic and fermionic statistics, a subject which I believe still keeps some interesting secrets from us. It compels us to contemplate the nature of quantum statistical mechanics, and indeed Pauli's exclusion principle, which is so vital to the world as we know it. In a more practical manner, I think we could benefit from a systematic analysis of the arbitrary σ-dependent distribution function of the FES gas for different σ (besides the $\sigma = 0, 1/2, 1$ cases which was investigated here). Moreover, it would come as little surprise if FES finds applications in other phenomena in the field of condensed-matter physics, which is an unbelievable rich and diverse field.

6.3 Concluding Remarks

There should be little doubt that the full story of the nature of anyons is far from being told. In this thesis, we have merely scratched the surface. We started out with a thorough (but far from exhaustive) introduction to anyons, and we firmly established the appropriate anyon Lagrangian. Then, a short section on the quantum Hall effect in general, and the fractional quantum Hall effect in particular, displayed the assumed existence of anyons in such FQHE systems.

Our project has, in a broad sense, been to investigate two-dimensional quantum gases. Not only are the two-dimensional Bose-Einstein and Fermi-Dirac systems highly rewarding to calculate due to their amenability. It also serve as important endpoint results in the more complex problems of determining the FES and N-anyon system. Despite their physical differences, it

was shown that their development can easily be captured by a single formulation combining their independent expressions. The mathematical methods are practically identical in the Bose-Einstein and Fermi-Dirac cases, and the combined derivation is carried out using elementary calculus. We also confirmed certain thermodynamical asymmetries between the two particle classes.

The FES system was introduced by appealing to the generalized exclusion principle. The equilibrium distribution is conveniently derived along the same lines as in the ideal bosonic and fermionic case. A short analysis of the diverse nature of the Bose-Einstein, Maxwell-Boltzmann, semion and Fermi-Dirac distributions was given. With the general distribution established through a complicated functional equation, the virial expansion of an ideal FES gas in two dimensions was carried out. The appropriate endpoints where found to coincide with the FES result.

Finally, we examined the problem of determining the virial coefficients of an ideal anyon gas. Apparently, there has not been much progress regarding these issues since the numerical calculations of the third and fourth virial coefficients in 1995 - 1997. More than a decade later, the technological advances in computer power has been significant. Motivated by this alone, we could hope to see a re-run of the calculations found in the 90's - or perhaps initiate refined models which where out of reach for earlier technologies. This could prove particulary fruitful in conjuction with carrying out the perturbative results to higher orders in $\mathcal{O}(\alpha)$.

No matter what such calculations will hold, the conclusion is clear: there are still much to learn about the anyonic system.

Appendix A

Standard Material

A.1 The Grand Canonical Approach

We will essentially follow [28] in the current derivation of the Bose-Einstein and Fermi-Dirac distributions using the grand canonical method. The canonical partition function is given as

$$Z_N(V,T) = \sum_E e^{-\beta E} \tag{A.1}$$

where E is the energy eigenvalue of the system. β is as always defined to be $\beta = 1/k_B T$, i.e. the temperature. The total energy may be expressed as a sum over single-particle energies

$$E = \sum_i \epsilon_i n_i \tag{A.2}$$

where n_i is the occupation number of the ith (single-particle) state with energy ϵ_i. The total number of particles available to the system is

$$N = \sum_i n_i. \tag{A.3}$$

By introducing the statistical weight factor $g\{n_i\}$, the partition function may be written

$$Z_N(V,T) = {\sum_{\{n_i\}}}' g\{n_i\} e^{-\beta \sum_i \epsilon_i n_i} \tag{A.4}$$

where the sum ${\sum_{\{n_i\}}}'$ runs over all permissible distribution sets $\{n_i\}$. These weight factors are

$$g_{\mathrm{BE}}\{n_i\} = 1 \tag{A.5}$$

for the Bose-Einstein system and

$$g_{\mathrm{FD}}\left\{n_i\right\} = \begin{cases} 1 & \text{if all } n_i = 0 \text{ or } 1 \\ 0 & \text{otherwise} \end{cases}. \tag{A.6}$$

This is just a sophisticated way of saying that bosons can have unlimited occupation numbers, while fermions are limited to the exclusion principle.

The canonical partition function and the grand canonical partition function are related by

$$\Xi\left(z,V,T\right) = \sum_{N=0}^{\infty} z^N Z_N\left(V,T\right). \tag{A.7}$$

By substituting into this equation, we find that

$$\Xi\left(z,V,T\right) = \sum_{N=0}^{\infty} z^N {\sum_{\{n_i\}}}' e^{-\beta\sum_i \epsilon_i n_i} \tag{A.8}$$

$$= \sum_{N=0}^{\infty} \left[{\sum_{\{n_i\}}}' \prod_i \left(ze^{-\beta\epsilon_i}\right)^{n_i} \right] \tag{A.9}$$

where we have used that $N = \sum_i n_i$ and we have incorporated the statistical weight factor $g\left\{n_i\right\}$. This imposes boundaries on the possible distribution sets $\left\{n_i\right\}$ in the sum ${\sum_{\{n_i\}}}'$. The clue is now to realize that this may be written as a sum over all the possible numbers n_i independently of each other. This means that we can write

$$\Xi\left(z,V,T\right) = \sum_{n_0,n_1,\cdots} \left[\left(ze^{-\beta\epsilon_0}\right)^{n_0} \left(ze^{-\beta\epsilon_1}\right)^{n_1} \cdots \right] \tag{A.10}$$

$$= \left[\sum_{n_0} \left(ze^{-\beta\epsilon_0}\right)^{n_0}\right] \left[\sum_{n_1} \left(ze^{-\beta\epsilon_1}\right)^{n_1}\right] \cdots . \tag{A.11}$$

In the Bose-Einstein system, the n_i must be summed from $n_i = 0$ to $n_i = \infty$, thus yielding an infinite product of geometric series $\sum_{n_i} \left(ze^{-\beta\epsilon_i}\right)^{n_i} = \frac{1}{1-ze^{-\beta\epsilon_i}}$. In the Fermi-Dirac system, on the other hand, the occupation number can only be $n_i = 0$, which evaluates $\left(ze^{-\beta\epsilon_i}\right)^{n_i} = 1$ or $n_i = 1$ which gives $\left(ze^{-\beta\epsilon_i}\right)^{n_i} = ze^{-\beta\epsilon_i}$. Thus, we have that the grand canonical partition function takes the form

$$\Xi = \begin{cases} \prod_i \frac{1}{1-ze^{-\beta\epsilon_i}} & \text{for bosons} \\ \prod_i \left(1+ze^{-\beta\epsilon_i}\right) & \text{for fermions} \end{cases}. \tag{A.12}$$

This may be compactly written as

$$\ln\Xi = a\sum_i \ln\left(1+aze^{-\beta\epsilon_i}\right) \tag{A.13}$$

where $a = -1$ and $a = +1$ in the bosonic and fermionic case respectively. The distribution function is given by

$$\begin{aligned} \langle n_i \rangle &= -\frac{1}{\beta}\left(\frac{\partial \ln \Xi}{\partial \epsilon}\right)_{z,T,\text{all other } \epsilon} \\ &= \frac{1}{z^{-1}e^{\beta\epsilon} + a} \end{aligned} \tag{A.14}$$

where, once again $a = \pm 1$.

Bibliography

[1] P. W. Anderson. More is different. *Science*, 177:393–396, 1972.

[2] Matsumoto Y. Uemura Y. Ando, T. Theory of hall effect in a two-dimensional electron system. *Journal of the Physical Society of Japan*, 39(2):279–288, 1975.

[3] Schrieffer R. Wilczek F. Zee A. Arovas, D. P. Statistical mechanics of anyons. *Nuclear Physics B*, 251:117 – 126, 1985.

[4] Zhou W. Goldman V. J. Camino, F. E. Realization of a laughlin quasiparticle interferometer: Observation of fractional statistics. *Physical Review B*, 72(7):075342, Aug 2005.

[5] Georgelin Y. Ouvry S. Comtet, A. Statistical aspects of the anyon model. *Journal of Physics*, A22:3917–3926, 1989.

[6] Störmer H. L. Eisenstein, J. P. The fractional quantum hall effect. *Science*, 248:1510–1516, 1990.

[7] S. Forte. Quantum mechanics and field theory with fractional spin and statistics. *Review of Modern Physics*, 64:193–236, 1992.

[8] T. Frankel. *The Geometry of Physics, An Introduction, 2nd ed.* Cambridge University Press, 2004.

[9] F. D. M. Haldane. "fractional statistics" in arbitrary dimensions: a generalization of the pauli principle. *Physical Review Letters*, 67(8):937–940, Aug 1991.

[10] B. I. Halperin. Quantized hall conductance, current-carrying edge states, and the existence of extended states in a two-dimensional disordered potential. *Physical Review B*, 25(4):2185–2190, Feb 1982.

[11] B. I. Halperin. Statistics of quasiparticles and the hierarchy of fractional quantized hall states. *Physical Review Letters*, 52(18):1583–1586, Apr 1984.

[12] B. I. Halperin. Statistics of quasiparticles and the hierarchy of fractional quantized hall states. *Physical Review Letters*, 52(26):2390, Jun 1984.

[13] M. Horsdal. *The $\nu = 1$ quantum Hall effect and its one-dimensional representation.* PhD thesis, University of Oslo, 2008.

[14] Arovas D. P. Myrheim J. Polychronakos A. P. Isakov, S. B. Thermodynamics for fractional exclusion statistics. *Physics Letters A*, 212:299 – 303, 1996.

[15] B. Isakov. Generalization of statistics for several speceis of identical particles. *Modern Physics Letters B*, 8:319–327, 1994.

[16] H. F. Jones. *Groups, Representations and Physics.* Taylor & Francis, 1998.

[17] Turaev V. Kassel, C. *Braid Groups.* Graduate Texts in Mathematics. Springer, 2008.

[18] Avinash Khare. *Fractional Statistics and Quantum Theory, 2nd ed.* World Scientific, 2005.

[19] Dorda G. Pepper M. Klitzing, K. v. New method for high-accuracy determination of the fine-structure constant based on quantized hall resistance. *Physical Review Letters*, 45(6):494–497, Aug 1980.

[20] Mashkevich S. Myrheim J. Olaussen K. Kristoffersen, A. The fourth virial coefficient of anyons. *International Journal of Modern Physics A*, 13:3723– 3747, 1998.

[21] Michael G. G. Laidlaw and C'ecile Morette DeWitt. Feynman functional integrals for systems of indistinguishable particles. *Physical Review D*, 3(6):1375–1378, Mar 1971.

[22] R. B. Laughlin. Quantized hall conductivity in two dimensions. *Physical Review B*, 23(10):5632–5633, May 1981.

[23] R. B. Laughlin. Anomalous quantum hall effect: An incompressible quantum fluid with fractionally charged excitations. *Physical Review Letters*, 50:1395–1398, 1983.

[24] Myrheim J. Leinaas, J. M. On the theory of identical particles. *Nuovo Cimento*, 37:1–23, 1977.

[25] Alberto Lerda. *Anyons: Quantum Mechanics of Particles with Fractional Statistics.* Lecture Notes in Physics. Springer, 1992.

[26] Myrheim J. Olaussen K. Mashkevich, S. The third virial coefficient of anyons revisited. *Physics Letters B*, 382(1-2):124 – 130, 1996.

[27] J. Myrheim. Statistical physics: A very brief introduction. (Unpublished).

[28] R. K. Pathria. *Statistical Mechanics, 2nd ed.* Elsevier, 1996.

[29] Girvin S. M. et al. Prange, R. E. *The Quantum Hall Effect.* Graduate Texts in Contemporary Physics. Springer, 1987.

[30] L. E. Reichl. *A Modern Course in Statistical Physics, 2nd ed.* John Wiley & Sons, Inc., 1998.

[31] Hobson M. Bence S. Riley, K. *Mathematical Methods for Physics and Engineering, 2nd ed.* Cambridge University Press, 2002.

[32] Verbaarschot J. J. M. Zahed I. Sporre, M. Numerical solution of the three-anyon problem. *Physical Review Letters*, 67(14):1813–1816, Sep 1991.

[33] A. Stern. Anyons and the quantum hall effect - a pedagogical review. *Annals of Physics*, 323(1):204 – 249, 2008. January Special Issue 2008.

[34] Tsui D. C. Gossard A. C. Störmer, H. L. The fractional quantum hall effect. *Review of Modern Physics*, 71:298–305, 1999.

[35] Stormer H. L. Gossard A. C. Tsui, D. C. Two-dimensional magnetotransport in the extreme quantum limit. *Physical Review Letters*, 48(22):1559–1562, May 1982.

[36] F. Wilczek. Magnetic flux, angular momentum, and statistics. *Physical Review Letters*, 48(17):1144–1146, Apr 1982.

[37] F. Wilczek. Quantum mechanics of fractional-spin particles. *Physical Review Letters*, 49(14):957–959, Oct 1982.

[38] Y. Wu. General theory for quantum statistics in two dimensions. *Physical Review Letters*, 52(24):2103–2106, Jun 1984.

[39] Y. Wu. Statistical distribution for generalized ideal gas of fractional-statistics particles. *Physical Review Letters*, 73(7):922–925, Aug 1994.